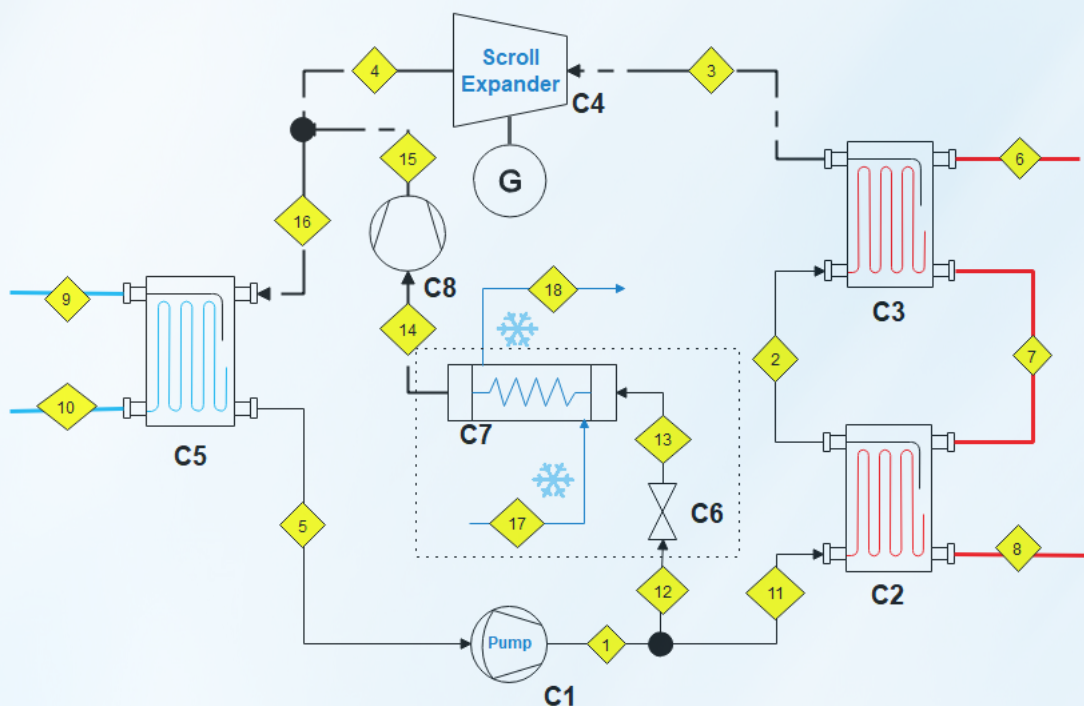


Thermoeconomic Optimization of Organic Rankine Cycle (ORC) for Low Grade Heat Recovery at temperatures below 100°C

Senthil Kumar Arumugam

Master of Science Thesis Report
Delft University of Technology



Thermoeconomic Optimization of Organic Rankine Cycle (ORC) for low grade heat recovery at temperatures below 100°C

by

Senthil Kumar Arumugam

in partial fulfillment of the requirements for the degree of

Master of Science
in Sustainable Energy Technology

at the Delft University of Technology,
to be defended publicly on Tuesday October 17, 2017 at 12:30 PM.

Supervisor:	Dr. Kas Hemmes,	TU Delft
Thesis committee:	Prof. Dr. Kornelis Blok,	TU Delft
	Dr. P. V. Aravind,	TU Delft
	Dr. Lydia Stougie,	TU Delft
	Theo Woudstra,	TU Delft

This thesis is confidential and cannot be made public

An electronic version of this thesis is available at <http://repository.tudelft.nl/>.

Executive Summary

Low-grade heat sources are abundant on earth but are majorly untapped due to lower thermodynamic efficiency at low temperatures and cost considerations. In the recent years, significant research has been done to convert this energy resource into useful forms of energy. This work aims at optimizing Organic Rankine Cycle (ORC) based heat engine and a cogeneration system developed to generate electricity and cooling from heat sources below 100°C from both thermodynamic and economic point of view. This requires thermodynamic and economic modelling of the systems. Due to lack of enough information and time to build mathematical models based on thermodynamics and economics, flow sheet modelling was considered the best option. Cycle Tempo software was used to model the prototypes of the basic ORC system and cogeneration system based on the patent owned by Heat Source Energy (HSE). The basic ORC model developed was simulated for 40 kW and the cogeneration model was simulated for 25 kW of electricity and 3 Refrigeration Tonnes (RT) of cooling based on the capacity of the prototypes the company has developed already.

Based on the critical study of El Sayed (1989) and Gaggioli (1989) on various thermoeconomic methodologies, exergoeconomics was chosen to be used for analysis and optimization of the system. It is an algebraic thermoeconomic method that aims at providing information that is crucial to the cost effective design and operation of the system. Its major advantage is that it can be used to evaluate and optimize system design even if input data and functions for thermodynamic and economic model development are not available or not in required form. Thus, exergoeconomics is the most compatible method to use when flow sheet modelling software is used for model development. It comprises of exergy analysis, economic analysis, exergy costing and exergoeconomic evaluation. The systems are optimized for cost effectiveness based on the exergoeconomic evaluation.

Since exergoeconomics is applied at the component level, all the previous steps are performed at the same aggregation level. The exergy analysis of both the systems revealed that the exergy destruction at the expander is the most dominating thermodynamic loss in the system. Condenser also had a high exergy destruction but being a dissipative component most of the exergy destruction happening at the condenser is unavoidable. The other heat exchangers namely the evaporator and the preheater had relatively lower contribution to the total exergy destruction in both the systems.

The economic analysis is performed using the Total Revenue Requirement (TRR) method presented by Bejan et al. (1996). To calculate the product costs of the system only the purchase cost of the system equipment and other investment needed to build the system are considered. From a thermal system design point of view importance is given only to the production cost of the products of the system because they are directly dependent on the system design and capital investment for building the system. But the market price of the product can depend on the production cost, desired profit and factors like demand and supply, competition, subsidies and regulations by governments. Therefore, the cost rate values found in this study does not represent actual costs of the system. They are mainly indicative of the cost effectiveness of the system. The cost rate value for both investment and operation and maintenance of each component, is calculated by apportioning the levelized cost of capital investment and operation

and maintenance for the system to each component according to their contribution to the total equipment cost.

In exergoeconomic analysis, cost rates are assigned to each exergy streams which are solved based on the cost balance and auxiliary equations developed. While developing the cost balance equations for evaporator and preheater the specific cost of fuel exergy is assumed to be zero as this value practically varies widely depending on the application. Therefore, the cost balance equations when solved for specific applications will result in higher cost rates for the exergy streams. Solving the set of algebraic equations for unknown cost rates enables calculation of exergoeconomic variables based on which the exergoeconomic evaluation is performed.

Exergoeconomic evaluation revealed that in both the systems the expander ranked top in the value of total cost rate increase associated with a component which represents the total monetary expense to the operator while operating the component. This value includes the cost rate of investment, operation, maintenance and the cost of exergy destroyed in the component. Due to the high contribution of cost rate of exergy destruction to this value it was deduced that improving the exergetic efficiency of the expander should be the first priority during design optimization even at the expense of reducing the efficiency of other components especially the heat exchangers. This is the main trade-off outcome of the exergoeconomic design evaluation. In the same way other components were prioritized for optimization keeping in mind the overall cost effectiveness of the systems.

The total specific cost of the products is the objective function for optimization as the main target is to improve the cost effectiveness of the system. It is to be noted that the specific cost of the products generated during each iteration are average costs and not marginal costs as given by rigorous optimization procedures. However, the average cost values are a good approximation for marginal costs as significant improvement can be achieved even though exact optimum cannot be achieved. The exergoeconomic optimization procedure when applied to both the systems showed that increasing the expander efficiency at the expense of heat exchanger efficiency resulted in improved cost effectiveness of the systems although it was more significant only in the cogeneration system. A significant reduction in total exergy destruction and cost of exergy destruction was observed in both the systems.

Experimental testing was done on the prototype HSE18R of the cogeneration system. The maximum gross efficiency achieved by the power cycle of the system was 9.6%. The efficiency found from simulation based on similar process parameters was 9.43%. Although the value is lower it is relatively comparable and validates the system performance during the test run. The maximum isentropic efficiency achieved by the expander was 75% at a pressure ratio of 2.55. The refrigeration cycle of the system was tested but due to lack of standard testing conditions at the time of the experiment, the coefficient of performance achieved was lower than expected. But it was concluded that the refrigeration cycle was working in synergy with the power cycle of the system.

The cycle tempo model developed for transcritical CO₂ power cycle, a future objective for HSE systems, was simulated for 40 kW of power. It was observed that the cycle achieved a gross efficiency of 7.98% but the back work ratio of the pump was close to 50% when CO₂ was used. One potential application studied was the use of HSE systems as retrofitted equipments in ships for extracting power from the heat available in jacket cooling water stream that cools the ship engines. Although OTEC was considered initially as a potential application due to the theoretical possibility of using the technology, the practical issues in scaling up of scroll expander size for larger OTEC plants and running scroll expanders in parallel made it an economically non viable application for using HSE technology.

Contents

1. Introduction	1
1.1. Background Information	2
1.2. Patent Description	2
1.3. Objectives	2
1.4. Methodology of Research	3
2. Theory and Literature Study	5
2.1. HSE System Features	5
2.1.1. Scroll Expander	5
2.1.2. Diaphragm Pumps	10
2.1.3. Working fluid in HSE systems	12
2.2. Thermoeconomic Methodologies	13
2.2.1. Algebraic Methods:	14
2.2.2. Calculus methods:	15
2.3. Exergoeconomic Analysis & Optimization	16
2.3.1. Exergy Analysis	17
2.3.2. Economic Analysis	18
2.3.3. Exergy Costing and Cost balance	21
2.3.4. Exergoeconomic evaluation	23
2.3.5. Iterative Exergoeconomic Optimization Procedure	24
3. Modelling and Exergy Analysis	25
3.1. Modelling of HSE systems	26
3.2. Exergy Analysis	30
4. Economic Analysis	35
4.1. Conventional economic analysis	35
4.2. Use of TRR method in Exergoeconomics	36
4.3. Sensitivity Analysis	37
5. Exergoeconomic Evaluation	41
5.1. Basic Organic Rankine Cycle with R410A	41
5.2. Cogeneration System with R410A	44
6. Exergoeconomic Optimization	49
6.1. Basic ORC system with R410A	49
6.2. Cogeneration system with R410A	53
7. Experimental Results and Discussion	57
7.1. Performance of HSE18R prototype	57
7.2. Performance of the Scroll Expander:	59
7.3. Performance of the Refrigeration Cycle:	60
7.4. Comparison with Modelling results	62
8. Future of HSE systems	63
8.1. Transcritical CO ₂ power cycle	63

8.2. Potential Applications	65
9. Conclusions and Recommendations	69
9.1. Conclusions	69
9.2. Limitations of Research	70
9.3. Future Recommendations	70
References	76
Glossary	77
9.4. List of Acronyms	77
9.5. List of Symbols	79
Appendix	80
A. Modelling	81
B. Economic Analysis	85
C. Exergoeconomic Analysis	87
D. Exergoeconomic Optimization	91
E. Experimental Results	97

List of Figures

1.1. Methodology of Research	3
2.1. Expansion process of a scroll expander under different crank angles	6
2.2. Schematic of flank and radial leakage	7
2.3. PV diagram for Under/Over expansion loss	7
2.4. Solubility chart of R410A in POE oil	9
2.5. Diaphragm Pump	11
2.6. Summary of Phase down schedule for countries not under Article 5 of Montreal protocol	13
2.7. Exergy rates of fuel and product for selected components at steady state operation	18
2.8. Cost rates of fuel and product for selected components at steady state operation	22
2.9. Schematic to illustrate cost balance	22
3.1. Comparing T-S diagram of R410A with other type of fluids	25
3.2. ORC system with R410A as working fluid	27
3.3. Cogeneration system with R410A as working fluid	29
3.4. Exergy Destruction in components of basic ORC system	31
3.5. Exergy Destruction in components of cogeneration system	32
6.1. Changes in decision variables at each iteration	50
6.2. Contribution to Exergy Destruction by system components	52
6.3. Changes in decision variables at each iteration	54
6.4. Contribution to Exergy Destruction by system components	56
7.1. Gross and Net thermal efficiency Vs Power Output	58
7.2. Effect of heat input rate on the system performance	59
7.3. Performance of scroll expander under varying load	59
7.4. Isentropic Efficiency of Expander Vs Scroll Inlet Temperature	60
8.1. Temperature variation in heat exchangers for ORC and tCO ₂ systems	63
8.2. Schematic of the Transcritical CO ₂ cycle	64
8.3. Exergy Destruction in components of transcritical co ₂ system	65
8.4. Heat Balance for MAN Diesel engine operating at 100 SMCR rating	66

List of Tables

2.1. Physical Properties of R410A	12
2.2. Assumptions of various economic parameters	18
3.1. Mass flow and thermophysical properties of streams	27
3.2. Mass flow and Thermophysical properties of fluid in each stream	29
3.3. Fuel and Product exergy definitions for each component of basic ORC system	30
3.4. Exergy definition for components of cogeneration system	31
3.5. Exergy calculations for each component of basic ORC system	31
3.6. Exergy calculations for each component in the cogeneration system	32
4.1. Cost of basic ORC and cogeneration system	35
4.2. Cost rates associated with each component of basic ORC system	36
4.3. Cost rates associated with each system component	36
4.4. Different Scenarios considered for sensitivity analysis	37
4.5. Effect of different scenarios on TRR of basic ORC and cogeneration system	38
4.6. \dot{Z}_k values of each component in basic ORC system	39
4.7. \dot{Z}_k values of each component in cogeneration system	39
5.1. Components ranked according to $\dot{Z}_k + \dot{C}_{D,k}$ value	43
5.2. Components ranked based on $\dot{Z}_k + \dot{C}_{D,k}$ value	46
5.3. Effect of operation hours on the total cost rate of products in the cogeneration system	47
6.1. Results of 1st iteration	51
6.2. Results of 2nd iteration	51
6.3. Results of 3rd iteration	51
6.4. Results of 4th iteration	52
6.5. Exergy analysis of the basic ORC system without the preheater	53
6.6. Results of 1st iteration	54
6.7. Results of 2nd iteration	55
6.8. Results of 3rd iteration	55
6.9. Results of 4th iteration	55
8.1. Physical Properties of R744	64
8.2. Exergetic variables calculated for Transcritical CO ₂ cycle	65

Acknowledgement

I would like to first thank my thesis supervisor Dr Kas Hemmes for his unconditional support throughout this research work. His door was always open for me to approach whenever I ran into trouble or had questions regarding my work. I am especially thankful to him for giving me the space to explore and develop the research on my own. This helped me hone my research skills and develop myself as an individual.

I would also like to thank Mr Theo Woudstra for his support during the course of my thesis; and especially for his patience in helping me resolve the issues I had with Cycle Tempo software. The discussions with him that had sometimes continued for hours altogether taught me a lot about applied thermodynamics.

Special thanks goes to Mr Keith Johnson from Heat Source Energy for giving me the opportunity to work on his innovation and for his continued support throughout the work. The technical discussions that we had always helped to better understand his technology. I would also like to thank him for offering me a research position in his company after my graduation.

I would like to acknowledge my other committee members Prof Kornelis Blok, Dr PV Aravind and Dr Lydia Stougie for their critical review and comments which helped me improve the quality of my research output.

Away from work, I would like to acknowledge the support of my friends, both at Delft University and back home, for putting up with my idiosyncrasies and for being there during difficult times of my life. I don't think I could have faced the outside world the way I did, without their help from the time I left my home several years back to pursue my career.

Finally, I want to thank my family for their ever continuing support and love. And a special thanks to my hero, my father, Mr Arumugam Sivaraman for believing in me and for being my inspiration in life. I could not have done this without their encouragement and in particular the motivation given by my girlfriend Monisha at right times to keep pushing myself.

1. Introduction

Energy from external sources has been an integral part of human life ever since fire was used on a daily basis 300,000 years ago by early humans (Harari, 2014). Although energy was extracted from various sources like wood or oil over the history of humans, a paradigm shift in the energy scenario happened when fossil fuels were discovered during the 19th century at a time when industrial revolution was spreading to different parts of the world. Energy demand grew rapidly with industrialization and lifestyle changes among the modern humans. Fossil fuels due to their high energy density, availability and accessibility became an ideal source of energy and has ever since dominated the energy scenario around the globe.

The extensive use of non-renewable fossil fuels by a largely growing human population on earth has had a negative impact on its biosphere. Fossil fuel burning has been a major contributor to climate change, fuelling the debate on the future of our planet and the pathways to meet the energy demands of the ever growing population. Sustainability in meeting this ever growing energy demand and in all aspects of development has become global goals for all countries to achieve. Energy from renewable sources is not new and has gained a great momentum in the last couple of decades. Although renewable energy integration could greatly contribute to our fight against climate change, it is also necessary to give importance to energy efficiency measures as they are often easy and quick to implement, cost effective and already available to us with the present technology (Knoop & Lechtenböhmer, 2017).

In order to realize the decarbonization goals of the global energy system, renewables should work in synergy with energy efficiency and electrification. When both RE and EE are pursued together, they can help in faster reduction of energy intensity while increasing the share of renewable energy resulting in an overall reduction in the cost for energy system. This synergy would also have important environmental and societal benefits like reduction in air pollution levels (IRENA, 2017).

Low grade heat recovery has gained attention of researchers around the world as a means to increase the share of renewable energy and also to improve energy efficiency. This is because of the availability of the vast untapped potential of low temperature solar thermal and geothermal sources and industrial waste heat sources. In the literature for low grade heat recovery, the definition of the term 'low grade' differs among various studies (Parker & Kiessling, 2016). In this study of technology developed for low grade heat recovery, heat sources with temperature lower than 100°C are defined as the low grade heat.

A large amount of the low grade heat at temperatures lower than 100°C are being wasted due to lack of cost effective technology (Iqbal et al., 2017). In this thesis work, the concept developed by Heat Source Energy Corporation to produce electricity and other useful forms of energy from low grade heat using scroll expanders and refrigerant R410A as working fluid is studied with special focus on identifying the thermodynamic irreversibilities and improving the cost effectiveness of the system.

1.1. Background Information

Heat Source Energy Corporation (HSE Corp) is a technology provider and system manufacturer aiming mainly at producing useful energy from low grade thermal sources like geothermal and waste heat streams from industries. Mr. Keith Johnson from HSE Corp started working on the heat engine technology in 2009 and has filed numerous patents over the years two of which are described in Section 1.2 due to their relevance to the current study. The technology was developed not while trying to invent a new cycle for low grade heat or while researching for improvement of current technologies. However, the system developed is an intelligent assembly of commercially available equipments from the HVAC industry with modifications and careful sizing based on Organic Rankine cycle, a thermodynamic cycle proposed as the main candidate by the literature for low temperature applications. Several prototypes of the system has been built and tested over the years. The first successful testing of the HEDC (Heat engine Decompression Cycle) system in IJlst, Netherlands was done in 2013 under the supervision of Dr Kas Hemmes from Delft University of Technology. The most recent testing was done on the prototype (HSE18R) of a cogeneration system producing electricity and refrigeration in May, 2017 at Salt Lake City, Utah, United States of America under the supervision of Dr Kas Hemmes. The results of this testing performed during the course of this study was analyzed and discussed in Chapter 7 of this report.

1.2. Patent Description

The research work established in this report is based on the patents owned by Heat Source Energy Corporation namely US20150369086 A1 and WO2014124061 A1. The patent US20150369086 A1 (Johnson & Newman, 2015) describes an improved organic rankine cycle which uses an organic refrigerant with boiling point less than -35°C and a positive displacement decompressor that derives energy from the pressure differential between two pressure zones. The high pressure zone absorbs heat from a source at less than 82°C , a range which is abundant and largely untapped, to maintain the refrigerant at a high pressure vapor state. The low pressure zone transfers the heat from the refrigerant vapor to heat sinks like cold streams or ambient air. The decompressor maintains a pressure differential of 20 to 42 bar between the two pressure zones along with a positive displacement hydraulic pump. To prevent the effect of fluid hammer and cavitation an eccentrically shaped tank works as the holding tank for the refrigerant before the suction line of the pump. This tank acts as a pulsation dampener and gives a net positive suction head (NPSH) to the pump inlet. The refrigerants mainly proposed in the patent are R410A, R407C and R744.

The patent WO2014124061A1 describes about the subsystem designed to lubricate the expander. The bypass system takes a portion of the high pressure working fluid at the exit of the pump, mixes it with lubricant oil and then heated up to a certain temperature. This mixture is then atomized and mixed with the vapour entering the inlet of the expander. The advantages of lubricating the expander with POE oil dissolved in the working fluid has been discussed in section 2.1.1. The patent allows for addition of auxiliary circuits that can be added to the main system like a refrigeration cycle or pre-heating system.

1.3. Objectives

The research work reported here was undertaken with the following key research objectives:

1. To develop flow sheet models of HSE prototypes in cycle tempo for further study.
2. To understand and minimize the thermodynamic irreversibilities and improve the cost

effectiveness of the prototypes modelled in Cycle-Tempo using suitable thermoeconomic methods.

- To identify the trade-offs between investment cost and exergetic efficiency of system components.
 - To improve the cost effectiveness of the systems.
3. To analyze the experimental data to verify modelling results and obtain better understanding of the performance of the system.
 4. To investigate the use of CO₂ as working fluid for low temperature applications.
 5. To identify potential applications for HSE systems and study their economic and technological feasibility.

1.4. Methodology of Research

Based on literature study and the type of data available from the company, iterative exergo-economic optimization was considered as the suitable optimization technique and therefore the research methodology is based upon the objective of performing exergo-economic evaluation of the HSE systems and optimizing them to come up with a cost effective design. The methodology adapted in this work is described by Figure 1.1.

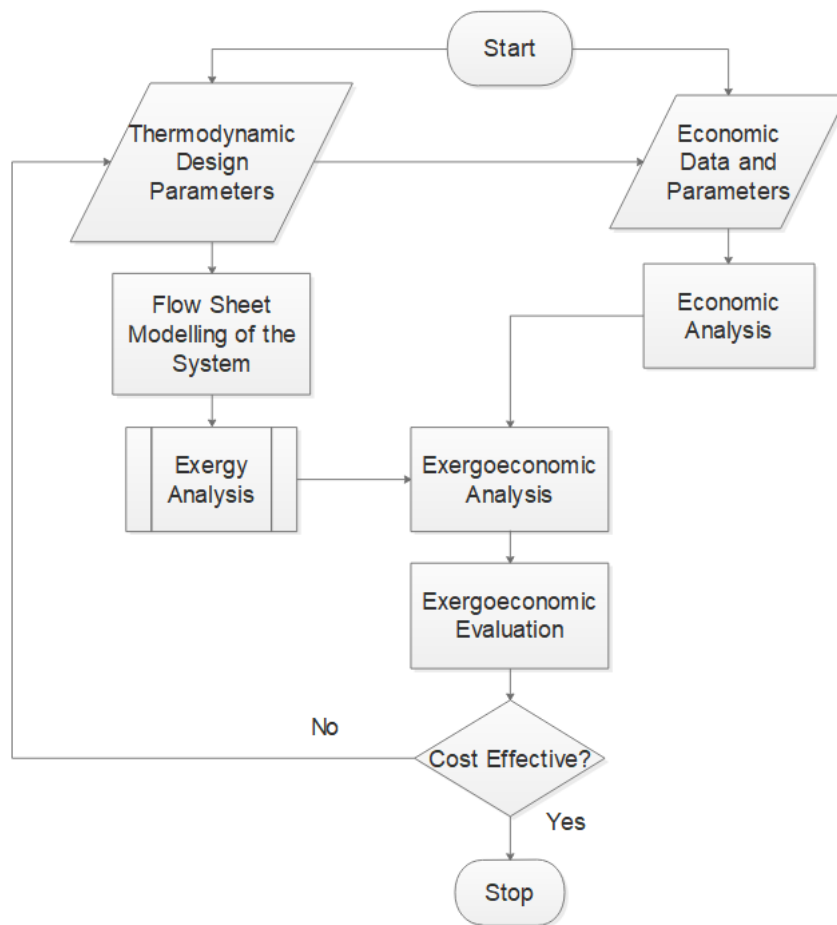


Figure 1.1.: Methodology of Research

2. Theory and Literature Study

2.1. HSE System Features

The small scale ORC system prototypes developed by Heat Source Energy Corporation has a Scroll expander (positive displacement decompressor) as the expansion machine, a Diaphragm pump (positive displacement pump) for pumping the refrigerant through the system, brazed plate type heat exchangers for evaporation and condensation process and use R410A as the working fluid. The working and key features of these components are explained in the following sections.

2.1.1. Scroll Expander

The expander in an ORC system has critical influence on the overall system performance. Volumetric expanders are suitable for small scale applications as they work with high pressure ratios, low mass flows and rotational speeds (Leontaritis et al., 2015). Scroll expanders are a good choice for such applications in spite of their complicated design due to their main advantages which are (Ma et al., 2017):

- Less moving parts than other reciprocating machines
- Ability to cope with two phase working fluids
- High isentropic efficiency
- High reliability and robustness due to mechanical simplicity
- Low rotational speed with less noise and vibration
- lower price and availability at broader power range

Scroll expanders are positive displacement machines which in principle are scroll compressors operating in reverse. Though the concept of scroll machines originated in early 20th century the casting technology at that time was not mature enough to make a prototype. Scroll compressor saw its first commercial use in air conditioners during 1980s. The idea of using scroll compressors as expanders in micro-ORCs has garnered interest during the last two decades (Garg, Karthik, Kumar, & Kumar, 2016). This has led to various experimental studies on scroll expanders, typically based on the methodology of modifying a scroll compressor to operate in reverse and achieve expander characteristics. Such an approach was first used by Zanelli et al.(1994) who used a modified scroll compressor to study the isentropic efficiency achieved in the expander mode.

Scroll expander consists of two intricate spiral shaped scrolls inter fitted into each other in a way that one scroll can move in an angular direction within the walls of the stationary scroll. This intricate design ensures that at any instant a certain number of gas chambers are formed between the scroll walls that trap the gas at different temperature and pressure. The number of gas chambers formed in this way determine the built-in volume ratio of the scroll expander, thus making them a key variable during the design process (Garg et al., 2016). When the high pressure intake gas comes in through the central region of the scrolls, the crescent shaped gas

pockets move towards the periphery of the scroll, thus rotating the orbiting scroll. Figure 2.1 visualizes this expansion process in a scroll expander at various crank angles at an increment of 90° (Lu et al., 2017). The number of rotations of the shaft during one cycle, when the gas moves from intake to discharge, depends on the scroll geometry, especially the rolling angle (Garg et al., 2016; Oralli, Tarique, Zamfirescu, & Dincer, 2011).

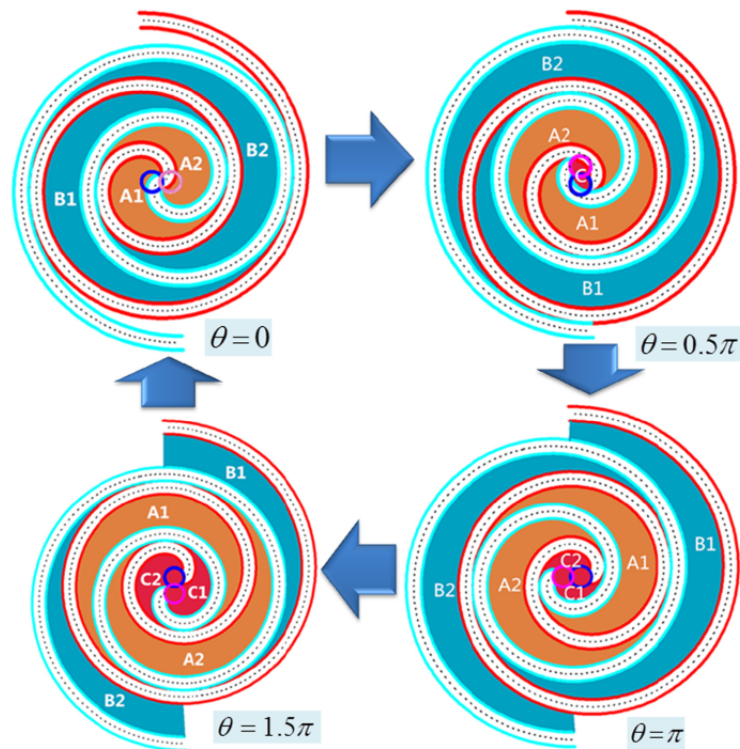


Figure 2.1.: Expansion process of a scroll expander under different crank angles (Lu et al., 2017)

Losses in a Scroll Expander

The isentropic efficiency of scroll expanders are generally higher than other available expanders but still there are losses due to various reasons which needs to be understood clearly to improve the performance of the expander through geometric and process modifications. The losses that occur during actual expansion in a scroll expander can be mainly categorized into thermodynamic and mechanical losses which are explained below:

Thermodynamic losses:

Supply pressure drop:

The suction process in a expander is theoretically isobaric but that is not achieved in reality as there are pressure drops witnessed during suction. This pressure loss affects the power capacity of the expander and the resulting pressure pulsation adversely affects the stability of the expander (Garg et al., 2016). Yaginasawa et al.(2001) mentions in their study that this supply pressure drop is an inherent characteristic of a scroll machine. However, the suction process can be improved by modifying the scroll wrap profile of the original scroll compressor from which the expander is developed and by optimizing the suction orifice(Song et al., 2015).

Flank and Radial leakage:

During expansion the fluid can leak from high pressure to the low pressure chamber along the flank walls of the scroll and also from the radial clearance between the moving and the fixed scroll at the top and bottom of the scrolls. The flank leakage depends on the scroll height and flank clearance between the fixed and moving scroll whereas the radial leakage depends on the scroll thickness and the radial clearance between the fixed and moving scroll (Garg et al., 2016). Using lubricants along with working fluid reduces flank leakages and also lubricates the bearings, thus reducing the frictional losses as well. On the other hand the radial leakage is best reduced by proper heat and wear resistant tip sealing (Song et al., 2015). Figure 2.2 gives a schematic for radial and flank leakages in a scroll expander (Garg et al., 2016).

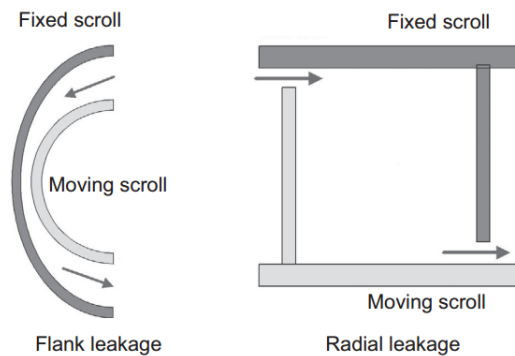


Figure 2.2.: Schematic of flank and radial leakage (Garg et al., 2016)

From the study on performance of an oil-free scroll expander by Yanagisawa et al. (2001) it was found that at lower rotational speed of the expander the leakage losses are more dominant than the mechanical losses.

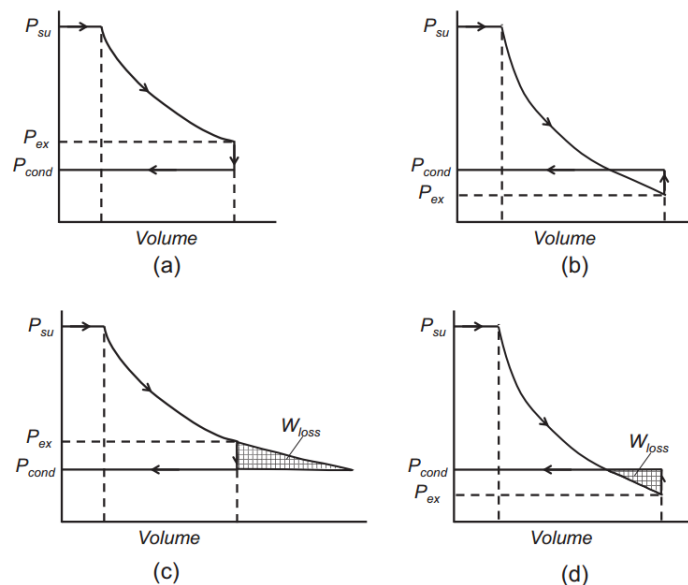


Figure 2.3.: PV diagram for Under/Over expansion loss (Garg et al., 2016)

Under or Over expansion:

In situations when under or over expansion happens the exhaust gas pressure is different from that of the condenser. In this case, the exhaust gas will undergo an isochoric compression or expansion at the end of the expansion within closed chambers thus reducing the isentropic work possible. Figure 2.3 represents the PV work lost during under or over expansion in the scroll expander. This loss is mainly due to the mismatch between the expander pressure ratio and the power cycle's operational pressure ratio. Over expansion affects the expander performance more than under expansion as it would cause losses by back flow and re-compression of the working fluid after the expansion process (Garg et al., 2016; Song et al., 2015).

Mechanical Losses:

In general, the mechanical torque loss due to the main bearing and the crank mechanisms that support the orbiting motion of the scroll lower the performance of the expander. Theoretically this would be equal to the loss due to friction between orbiting and fixed scroll (Yanagisawa et al., 2001). The mechanical losses that occur in a scroll expander are explained below:

Frictional loss at crank pin and journal bearing

Crank pin that rotates within the orbiting scroll bearing to give the required degree of freedom to convert orbiting motion into shaft rotation suffers torque loss due to frictional forces. The crank shaft that connects with the generator passes through a journal bearing which also has significant frictional loss (Garg et al., 2016).

Thrust bearing and coupling losses

The thrust bearing surface supports the orbiting scroll and prevents it from overturning due to the thrust force from the gas pressure inside the chamber against the constraint forces acting on it. Oldham coupling used in a typical scroll expander contributes to frictional losses when it slides between the moving scroll and the guide slot present on the casing of the expander (Garg et al., 2016).

Scroll Expander in HSE systems:

The HSE system uses a magnetic coupling to transmit power from the shafts of the scroll expander to the electric generator. This reduces the frictional and torque losses in the coupling of expander and generator shafts and reduces vibration and noise caused by misalignment of shafts. Also, employing magnetic coupling for power transmission prevents fluid leakage from seals as it allows for hermetic operation of both the components.

The other mechanical losses discussed in the previous section can be reduced by sufficient lubrication of the expander. As stated in the patent in Section 1.2, HSE system has a dedicated lubrication system that adds an atomized mixture of lubricant oil and the working fluid to the main flow of working fluid before the inlet of the expander. The mixture of working fluid and POE oil (Polyolester oil) is atomized using spray nozzles which converts the oil into very fine droplets that enable it to mix homogeneously with the working fluid. This atomized mixture prevents the oil from entering the expander in bulk form which may stall the expander and also increases the density of the refrigerant mixture which may help seal the expander to limit slippage of moving parts (Johnson, 2016). The oil present in the fluid at the exhaust of the expander is then filtered in an efficient oil separator to prevent the oil from disturbing the heat transfer processes in the system. Kane et al. (2003) in their study on mini-hybrid solar power plant integrated two scroll expanders with different volumetric displacements (53 cm^3 and 72 cm^3) to two superposed organic rankine cycles. It was found that the efficiency decreased due to under and over expansion. Also, the lubrication achieved by mixing oil with the working fluid resulted in deterioration of heat transfer process in heat exchangers due to presence of excess oil

in the mixture. This necessitates the need for effective oil filtering after the expansion process to prevent the lubricant oil from interfering with the other cycle processes especially heat transfer.

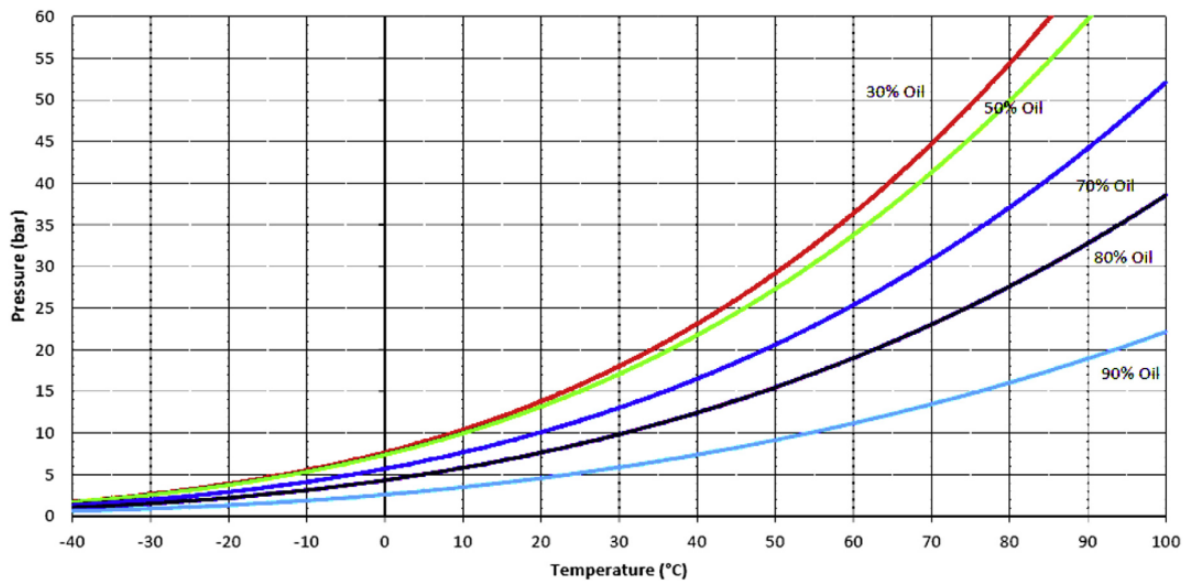


Figure 2.4.: Solubility chart of R410A in POE oil
(Ramaraj et al., 2014)

From Figure 2.4 it is evident that the solubility of the refrigerant in the POE oil is a function of the pressure and temperature. For a certain pressure, increase in temperature results in higher solubility of R410A in POE oil which might pose a problem for oil separation after the expansion process. It is easier to separate oil when the oil and refrigerant are present as a two phase mixture. The oil being heavier than refrigerant can be separated with the help of gravity and filtering manifolds designed for the purpose as explained in the patent (Johnson, 2016). Zanelli et al. (1994) investigated the performance of a scroll expander integrated into a small ORC test rig. The expander was modified from a hermetic scroll compressor and was tested with R134a as the working fluid. The maximum isentropic efficiency observed was 65% at a nominal speed of 3000 rpm. The efficiency dropped to a lower value and became unstable at higher rotational speed of 4200 rpm which the authors partly attribute to the poor lubrication.

Mathias et al. (2009) tested a refrigeration scroll compressor used in the reverse as an expander and observed a maximum isentropic efficiency of 83% with R123 as working fluid. They used this value to model the expansion process in their energetic and exergetic modelling of organic rankine cycle. In the experimental study of an ORC system with R245fa as working fluid by Bracco et al. (2013), a modified hermetic scroll compressor was used as expander. Their use of oil for lubrication and sealing was similar to that of Kane's study (2003) where a mixture of the working fluid and the oil was circulated in the system. They observed that the isentropic efficiency dropped from 0.75 to 0.6 due to under expansion with expansion ratio between 5 to 6.5 and rotational speed reducing from 4500 to 3000 rpm.

Lemort et al. (2012) studied the performance characteristics of a scroll expander in a heat pump and observed a maximum isentropic efficiency of 71.3% with R245fa as the working fluid. They also observed that the isentropic efficiency dropped due to over expansion and with decrease in lubrication oil at a pressure ratio of 4.22 and a temperature of 365K. Lemort et al. (2009) in their experimental testing of scroll expander prototype integrated into an organic rankine

cycle achieved a maximum isentropic efficiency of 68%. In this study, the experimental results were used to identify parameters for a semi-empirical simulation of the expander and When this validated model was used to quantify the losses occurring in a scroll expander, it pointed out that the internal leakage losses, supply pressure drop and mechanical losses are the main losses that affect the performance of a scroll expander.

For modelling the expansion process in Cycle Tempo software the isentropic efficiency of the expander must be specified. Although Heat Source Energy Corporation claims to achieve 90% isentropic efficiency while operating the modified scroll expander with the lubrication system, lack of experimental support to validate it necessitated the search in literature pool for reasonable value of isentropic efficiency to be used in the theoretical and simulation work. Among the experimental studies done on scroll expanders made from hermetic scroll compressors, an isentropic efficiency close to 80% or more were observed in some studies (Bracco et al., 2013; Mathias et al., 2009; Lemort et al., 2012). Therefore, an isentropic efficiency of 75% was assumed for the expander in the base case model. This assumption is also validated by the experimental results discussed in Section 7.2.

2.1.2. Diaphragm Pumps

Positive displacement pumps pressurize the liquid by compressing a specific volume of the working fluid. These kind of pumps are preferred when the volumetric flow is low but the required discharge head is high. The diaphragm pumps used in HSE (model name for Heat Source Energy Corp) systems are positive displacement pumps that uses the reciprocating action of rubber or teflon diaphragms along with suitable suction and discharge valves to pump a fluid to higher pressure. The main advantages of a diaphragm pump is that they greatly prevent leakage of liquid and allows to keep the discharge head constant even when the volumetric flow changes. This makes it an excellent choice for ORC systems as it can handle unstable heat sources by adjusting the flow rate without changing the discharge head, which in turn leads to constant evaporation temperature and high generation efficiency (Xu et al., 2017).

For modelling the pumping process in cycle tempo, the isentropic efficiency of the pump has to be specified. The pumping process in an organic rankine cycle is assumed as a non-isentropic process with constant isentropic efficiency in many of the theoretical investigations on ORC systems (Xu et al., 2017). The constant isentropic efficiency values used in those investigations were assumptions which varies from different studies. Delgado-Torres et al.(2010) in their work on theoretical analysis and optimization of solar organic Rankine cycle for low temperature applications assumed an isentropic efficiency of 75%. Tchanche et al. (2009) assumed a value of 80% in their study of working fluids for low-temperature solar organic cycle and Chen et al.(2011) assumed 85% as pump efficiency when they proposed a supercritical rankine cycle with zeotropic mixtures for low grade heat to power conversion.Garg et al.(2016) in their work on developing a framework on scroll expander design for ORC applications used a pump efficiency of 90%, a relatively high value compared to various other studies (Xu et al., 2017). Also, in some studies researchers use the mass flow and enthalpy difference to represent the power consumed by the pump (Chang et al., 2015; J. Wang et al., 2012). Although assumptions like these simplify the analysis of ORC cycle, it leads to over estimation of the performance of ORC systems and can create problems in practice. This is because the working fluid pump consumes a significant amount of power produced by the expander, defined as back work ratio in organic rankine cycles, and is important to study their performance for cycle optimization (Xu et al., 2017).

Back work ratio as found from various studies range from 15 - 25% of the total power produced by the expander. Desideri et al.(Desideri, Gusev, Van den Broek, Lemort, & Quoilin, 2016) in their experimental work to compare working fluids for low temperature ORC system derived a

back work ratio of 22.2% and Zhang et al.(2016) found a back work ratio of 20% approximately in their study on a 200 kW solar power plant based on organic rankine cycle. Peris et al.(2015) measured a value of 16.68% for back work ratio in their characterization of organic rankine cycle for power and CHP from low grade heat sources. Thus, the existing researches prove that the working fluid pump efficiency has significant influence on the performance and economic feasibility of ORC system and cannot be neglected or arbitrarily assumed.

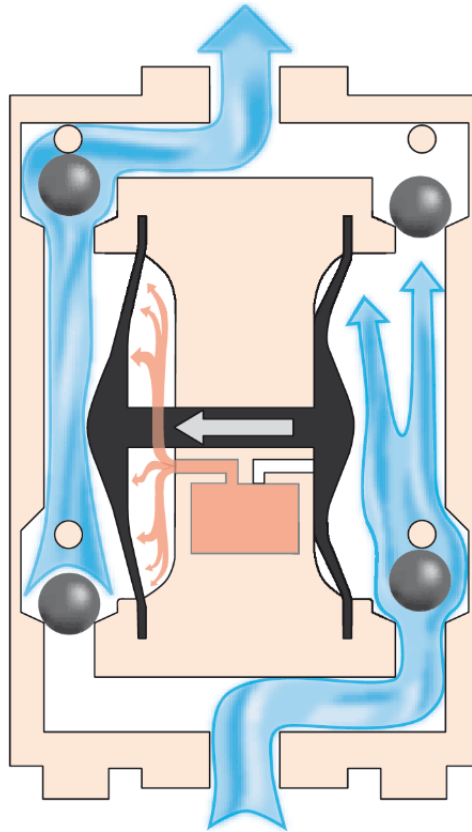


Figure 2.5.: Diaphragm Pump

Searching the literature pool showed that there are only a very few research papers that focus on the efficiency of working fluid pumps used for organic rankine cycle and waste heat recovery applications. Lei et al. (2016) found that the electrical efficiency of roto-jet pump was in the range of 11% to 23% when used in a small scale ORC system using R123 as working fluid. Meng et al. (2017) in their experimental study on a multi-stage centrifugal pump used in ORC based waste heat recovery applications observed that the electrical efficiency varied from 15% to 65.7%.

Xu et al. (2017) in their experimental research focusing on the pumping process of an ORC tested the performance of a diaphragm pump with 4 different working fluids under various working conditions. They aimed at finding the influence of working fluid physical properties on the isentropic efficiency of the diaphragm pump which would help future researchers to select reasonable value of isentropic efficiency for the pumping process in theoretical simulation work on ORC. The isentropic efficiency of the pump varied from 57.22% to 93.51% for compressing the working fluids tested. Also, they had proposed that the novel parameter $\alpha_V/\rho C_p$ of the working fluid at pump inlet conditions directly influences the isentropic efficiency of the pump. Based on experimental results, at constant volume flow rate and pressure difference, the isentropic efficiency was observed to be decreasing with increasing value of $\alpha_V/\rho C_p$. Also, the efficiency

increased with increase in pressure difference and volumetric flow rate. Therefore, the study emphasizes that the isentropic efficiency selected for pumping process in ORC simulation should not be a constant for all liquids but should be based on factors like pumping style, operation conditions and the fluid characteristics.

The factor $\alpha_V/\rho C_p$ found for R410A at the pump inlet conditions was lower compared to the values found for liquids in the study by Xu et al.(2017), implying that the isentropic efficiency would be higher. Also, the very low temperature difference in the working fluid at the inlet and the outlet of the pump, observed during the experiments mean that the diaphragm pumps have high isentropic efficiency (Refer Chapter 7. This is because the isentropic process of an in-compressible substance is an isothermal process:

$$\Delta s = c_v \ln \frac{T_2}{T_1} \quad (2.1)$$

$$\Delta s = 0 \text{ implies } T_1 = T_2$$

Thus, for the purpose of this study, an isentropic efficiency of 90% was assumed for the pumping process throughout all simulations.

2.1.3. Working fluid in HSE systems

R410A is a modern refrigerant used commonly in the HVAC industry as a replacement for R-22, a refrigerant that is being phased out for its ocean depletion potential. R410a has zero ocean depletion potential but has higher global warming potential. But this is expected to be compensated by the higher efficiency achieved with R410a systems due to their lower pressure ratio and higher cooling capacity.

The main advantage of using R410A as the working fluid for the ORC system is its compatibility with scroll expander and its high liquid thermal conductivity that improves the effectiveness of heat transfer process. Although R410A is a mixture, it exhibits near azeotropic behaviour and thus witnesses negligible temperature glide during heat transfer. Also, the frictional pressure drops in brazed plate type heat exchangers for R410A tends to be lower because of the smaller specific volume of the vapour resulting in lower vapour velocity (Subbiah, 2012). From pressure temperature charts of R410A it can be seen that the saturation pressure at low temperatures is high compared to other liquids. Scroll expander losses are reduced when operated at higher pressures that reduces super heating and enhances its performance (Quoilin, Lemort, & Lebrun, 2010).

Table 2.1 gives the physical properties of R410A fluid (Lemmon, 2003; Devotta et al., 2001).

Table 2.1.: Physical Properties of R410A

Properties of R410A	Values
Boiling Point at 1 atm	-51.44°C
Molecular Weight	72.59 kg/kmol
Critical Temperature	71.34°C
Critical Pressure	49.01 bar
Critical Density	459.03 kg/m ³
ASHRAE Safety Category	A1
Ozone Depletion Potential (ODP)	0
Global Warming Potential (GWP)	1730

R410A being a Hydro Fluoro Carbon (HFC) mixture has zero impact on ozone layer but is a powerful greenhouse gas with a high GWP potential of 1730 (refer Table 2.1). This is the major disadvantage of using it as the working fluid because it poses a potential problem for the continued use of R410A as working fluid for HSE systems due to environmental concerns. The Kigali amendment of the Montreal Protocol from October 2016 aims for phase-down of HFCs by reducing consumption and production. This amendment will come into force by January 2019 with the goal to achieve 80% reduction in consumption by 2047, given that at least 20 parties ratify the amendment. It is expected that the impact would reduce 0.5 °C of global warming by 2100 (Clark & Wagner, 2017).

Article 5 of the Montreal protocol takes into consideration the special situation in developing countries and all the countries that come under the article are given more time in implementing the various targets of the protocol including the Kigali Amendment. Figure 2.6 gives the summary of phase down schedule agreed in the Kigali Amendment for non - Article 5 countries that comprise of all developed countries and several other major economies of the world.

	Non- Article 5 (Main Group)		Non- Article 5: Belarus, the Russian Federation, Kazakhstan, Tajikistan & Uzbekistan	
Baseline Years	2011, 2012 & 2013		2011, 2012 & 2013	
Baseline Calculation	Average production/consumption of HFCs in 2011, 2012 & 2013 <i>plus 15% of HCFC baseline production/consumption</i>		Average production/consumption of HFCs in 2011, 2012 & 2013 <i>plus 25% of HCFC baseline production/consumption</i>	
Reduction steps				
Step 1	2019	10%	2020	5%
Step 2	2024	40%	2025	35%
Step 3	2029	70%	2029	70%
Step 4	2034	80%	2034	80%
Step 5	2036	85%	2036	85%

Figure 2.6.: Summary of Phase down schedule for countries not under Article 5 of Montreal protocol

(Clark & Wagner, 2017)

HSE considers United States of America (USA) to be its first major market. It is to be noted that as of 21st September 2017 United States of America, which has agreed to start freezing consumption of HFCs by 2019 during the Kigali agreement, is yet to ratify the amendment (UNEP, 2017). Provided that the USA ratifies the amendment, it is legally bound to reduce consumption by 2019 which could affect the use of R410A as working fluid in the country. This emphasizes the need to search for alternative working fluids suitable for low temperature applications and which have zero ODP and very low GWP values.

2.2. Thermoeconomic Methodologies

El-Sayed et al.(1989) and Gaggioli et al. (1989) in their critical review on various second law costing methods classify thermoeconomic methodologies into two broad categories: Algebraic methods and Calculus methods which will be discussed in detail in the following sections.

2.2.1. Algebraic Methods:

Conventional economic analysis and auxiliary cost equations derived for each component of a system are combined to give algebraic cost balance equations which are used by these methods to investigate the cost formation process of a system (Bejan et al., 1996).

The Theory of the Exergetic Cost (TEC)

This methodology was developed by Lozano et al.(1993) based on a set of propositions and introduces a new thermodynamic concept called the exergetic cost. Exergetic cost of a flow is defined as the amount of exergy needed to produce this flow. The first step in this methodology is to divide the system into units comprising of one or set of components and a single fuel and product has to be defined for each component. Then, a system of equations are built with cost balance equations of each unit (Proposition 1), cost equations for external flows into the system which are externally determined (Proposition 2) and losses which have zero cost (Proposition 3). However this procedure is hardly enough and a solution is possible only when the following propositions are considered: 1) if a stream included in the fuel of a component goes through another component and used in it, then the unit cost of the stream flowing into and out of the component is the same 2) if the product of a component has two or more streams then the unit cost of the stream are equal. The unit exergetic costs derived from the procedure can be used for optimization of the systems under consideration and is rather straightforward in its application.

The theory of exergetic cost - dis-aggregating methodology

This methodology was an improvement to the exergetic cost method as part of the structural theory standard proposed by Erlach et al. (1999) to use thermoeconomic methodologies with a common mathematical formulation. In this method, the exergetic cost determined for each component is distributed to other components according to the entropy changes happening within them.

Exergoeconomic analysis (EEA) methods

The exergoeconomic analysis (EEA) method with various approaches was proposed by Tsatsaronis and co-workers (Tsatsaronis, Lin, & Pisa, 1993; Bejan et al., 1996; Tsatsaronis & Moran, 1997; Tsatsaronis & Park, 2002). The two main variants in these methodologies are *Specific cost* and *Average Cost*. The concept of average cost is similar to the theory of exergetic cost whereas in the specific cost method, the cost of the exergy added to a stream is calculated and added to the component that makes use of that exergy. Thus, a component will obtain exergy from streams at different costs depending on the components which supplied the exergy to the streams. The cost of external irreversibilities is always added to the primary product of the system especially in co-generation plants where there would be two or more useful products from the system. Optimization procedure in exergoeconomics is quite different from the conventional optimization methods due to the fact that it is based on an iterative design improvement procedure that doesn't calculate a global optimum for a predefined objective function (Tsatsaronis, 1996). The iterative procedure rather tries to optimize the parameters of the overall system design and the process itself. The characteristic parameters of exergoeconomic evaluation are relative cost difference, exergoeconomic factor and exergetic efficiency. The EEA methods are broadly classified into three approaches:

1. Last-in-first-out (LIFO Principle)
2. Specific Exergy Costing/Average Cost approach
3. Modified Productive Structure analysis (MOPSA) approach

1. Last-in-first-out (LIFO Principle) LIFO principle of cost accounting was developed by Tsatsaronis et al. (1993) to calculate the cost of exergy supply to a stream/material using the exergy units spent. This improves the fairness of the costing process by eliminating the need for auxiliary assumptions. This principle is based on the idea that the exergy supplied last to the stream is used first and thus the cost associated with the exergy removed will be equal to the cost of exergy supplied to the stream which is calculated from previous step.

2. Specific Exergy Costing/Average Cost (SPECO/AVCO) approach SPECO/AVCO approach was first proposed by Lazzaretto and Tsatsaronis (1999, 2001) and was later improved by Tsatsaronis and co-workers (Cziesla & Tsatsaronis, 2002) to include fuzzy interference systems for more accurate exergoeconomic evaluation of system components and systematically improved SPECO methodology (Lazzaretto & Tsatsaronis, 2006). According to this approach the fuel and product exergy of a component are defined by considering exergy additions to and removals from material and energy streams. In the same way the cost additions to and removals from the same energy stream based on LIFO principle are then used to calculate the average costs of the component under consideration. The three main steps in this approach are 1) identifying the exergy streams through exergy analysis of the entire system, 2) defining the fuel and product exergy of each component in the system and 3) cost balance equations. This approach has been successfully applied by various researchers in thermoeconomics to analyze and optimize both simple and complex thermal systems.

3. Modified Productive Structure Analysis (MOPSA) approach MOPSA approach was first proposed by Kim et al. (1998) and is based on exergy costing method but without the flow stream cost calculations. Instead a cost balance equation is developed by assigning unit exergy cost to the exergy in a stream for each component. Then these set of equations are solved to find the production cost of useful products from the system and the monetary of various exergy costs. This approach has been compared with SPECO approach for exergoeconomic optimization of CHP plants (Kim et al., 1998; Kwak et al., 2003, 2004).

2.2.2. Calculus methods:

Calculus methods of thermoeconomic evaluation are built upon differential equations developed from cost flows in a system and optimization procedures based on Lagrange multipliers. The main disadvantage of using calculus methods for complex systems like CHP plants is that the Lagrange multiplier varies from iteration to iteration when a thermoeconomic isolation is not achieved in a component (R. B. Evans, 1980).

Thermoeconomic functional approach (TFA)

Thermoeconomic functional approach was first studied as Ph.D thesis by Frangopoulos (1983) and its application on CGAM problem was the method's first remarkable application (C. A. Frangopoulos, 1994). The approach is based on the Lagrangian method of mathematical optimization. The implementation of this approach requires accurate system simulation to obtain first order derivatives of the objective function and is based on the decomposition of the system to be optimized. The each sub unit of the system, not necessarily a single component, has cost balance equations which are solved to find the costs associated with the sub-components of the system. For optimization of systems, an optimization algorithm is directly used as it takes less effort while analyzing complex systems. The main disadvantage is that this approach does not give any information about the thermodynamic and economic relationships between various sub-components of the system. Frangopoulos later formulated and structured this approach in a way that artificial intelligence can be used for optimization of complex thermal systems and is called as the Intelligent Functional Approach (IFA) (C. Frangopoulos, 1991).

Engineering functional analysis (EFA)

The Engineering Functional Analysis (EFA) theory was developed by Spakovsky and Evans (1993; 1993) and its basic decomposition is based on the method proposed by Frangopoulos (1983). In the EFA methodology, the thermoeconomic models exist on both system level and subgroup level (Von Spakovsky & Evans, 1993; R. Evans & Von Spakovsky, 1993). The model at both levels have information on internal geometry and material composition of each component/subgroup. The consistency of the subgroup optimums with the global optimum depends on the isolation of the subgroups established by optimization of system level thermoeconomic model. Optimization of both the interrelated models is possible by iterating the links between the models and the internal economy of the system. The decomposition methodology followed in both the calculus methods of thermoeconomics is based on the *Principle of Thermoeconomic Isolation* given by Evans (1980).

The structural theory of thermoeconomics

The structural theory was proposed as a standard mathematical formulation for all approaches in which the thermoeconomic models can be expressed by linear equations (Erlach et al., 1999). The Thermoeconomic Functional Analysis (TFA), the Theory of Exergetic Cost (TEC), SPECO/AVCO approach and the LIFO can be formulated based on the structural theory of thermoeconomics.

2.3. Exergoeconomic Analysis & Optimization

Why Exergoeconomics?

Exergoeconomic analysis aims at providing information on an energy conversion system that is not available from conventional thermodynamic and economic analysis and that is crucial to the cost effective design and operation of the system (Tsatsaronis & Cziesla, 2001). A major advantage is that it can be performed even if input data and functions for thermodynamic and economic model development are not available or not in required form. The optimization procedure in exergoeconomics is based on an iterative design improvement procedure that doesn't calculate a global optimum for a predefined objective function (Tsatsaronis, 1996). The procedure rather tries to optimize the parameters of the overall system design. Analytical and numerical optimization techniques can often be applied to one specific design only but costs maybe reduced through different design configurations. Such cost effective design changes can be suggested by exergoeconomic analysis and evaluation.

Exergoeconomics is based on the notion that exergy can be the only rational basis upon which a economic evaluation on an energy conversion system should be built (Tsatsaronis & Cziesla, 2001). The main objectives of exergoeconomic analysis are finding the cost of the products generated and to understand the cost formation process, optimizing specific variables in a single component or an entire system (Bejan et al., 1996). An exergoeconomic analysis will comprise of the following:

1. Exergy Analysis
2. Economic Analysis
3. Exergy Costing
4. Exergoeconomic evaluation

2.3.1. Exergy Analysis

An exergy analysis helps us determine the location and magnitude of thermodynamic inefficiencies in a thermal system. The flow sheet models developed in cycle tempo software has the ability to perform exergy calculations which can be further used for the exergy analysis of the systems. As exergy is a relative quantity it is important to specify the environment conditions based on which Cycle tempo performs exergy calculations. For all the exergy analysis performed in this research work and reported here, Baehr environment conditions at 15°C was used. In order to optimize the design of thermal systems based on thermoeconomic evaluation it is required to properly define exergetic efficiency of each component and their costing approach (Lazzaretto & Tsatsaronis, 1999).

Exergetic efficiency is the only variable that characterizes the performance of a thermal system without any ambiguity from a thermodynamic viewpoint as it only depends on the component considered (Tsatsaronis, 1999). Exergetic efficiency of a component is defined as the ratio between the product and fuel exergy flow in the component (Bejan et al., 1996).

For the k^{th} component of a system, the exergetic efficiency can be expressed as,

$$\varepsilon_k = \frac{\dot{E}_{P,k}}{\dot{E}_{F,k}} = 1 - \frac{\dot{E}_{D,k} + \dot{E}_{L,k}}{\dot{E}_{F,k}} \quad (2.2)$$

The product exergy, $\dot{E}_{P,k}$, denotes any desired result produced by the component like electricity, heating or cooling. The fuel exergy, $\dot{E}_{F,k}$ denotes any resources expended to generate the desired product like heat, electricity or mechanical work. $\dot{E}_{D,k}$ represents the rate of exergy destruction in a component and $\dot{E}_{L,k}$ represents the rate of exergy loss in the component (Bejan et al., 1996; Tsatsaronis & Czesla, 2001). The exergy rate balance at steady state can be expressed as,

$$\dot{E}_{P,k} = \dot{E}_{F,k} - \dot{E}_{D,k} - \dot{E}_{L,k} \quad (2.3)$$

The values of $\dot{E}_{D,k}$ and $\dot{E}_{L,k}$ depend on the definition of the component boundary regardless of which the sum of $\dot{E}_{D,k}$ and $\dot{E}_{L,k}$ values are the same at the inlet and outlet states (Bejan et al., 1996). The Exergy loss $\dot{E}_{L,k}$ in the k^{th} component is zero when the boundary of the component is at T_0 whereas the exergy loss in the overall system (\dot{E}_L) is equal to the exergy transfer from the system to the surroundings as heat or mass. This exergy loss is not considered further in this work as they represent only a small part of the total thermodynamic inefficiencies whereas the exergy destruction happening at each component together forms the major part. As recommended by Tsatsaronis et al. (2004), for this work the boundaries of the component analysis is taken at the reference environment temperature T_0 which means that all inefficiencies owing to frictional losses and thermodynamic irreversible losses at the component level is accounted exclusively by exergy destruction term $\dot{E}_{D,k}$ (Tsatsaronis & Czesla, 2004).

Apart from exergetic efficiency (ε_k) and exergy destruction ($\dot{E}_{D,k}$), the exergy destruction ratios $Y_{D,k}$ and $Y_{D,k}^*$ are also useful in the thermodynamic evaluation of a component.

$$Y_{D,k} = \frac{\dot{E}_{D,k}}{\dot{E}_{F,total}} \quad (2.4)$$

The exergy destruction ratio $Y_{D,k}$ compares the exergy destruction in the k^{th} component to the fuel exergy supplied to the entire system.

$$Y_{D,k}^* = \frac{\dot{E}_{D,k}}{\dot{E}_{D,total}} \quad (2.5)$$

The exergy destruction ratio $Y_{D,k}^*$ compares the exergy destruction in the k^{th} component to the total exergy destruction in the system.

The exergy rates associated with fuel and product of selected components of energy systems at steady state operation are defined as given in Figure 2.7:

Component	Schematic	Exergy rate of product \dot{E}_P	Exergy rate of fuel \dot{E}_F
Compressor, pump, quad or fan		$\dot{E}_2 - \dot{E}_1$	\dot{E}_3
Turbine or expander		\dot{E}_4	$\dot{E}_1 - \dot{E}_2 - \dot{E}_3$
Heat exchanger		$\dot{E}_2 - \dot{E}_1$	$\dot{E}_3 - \dot{E}_4$

Figure 2.7.: Exergy rates of fuel and product for selected components at steady state operation (Tsatsaronis & Cziesla, 2001)

The exergy definitions for heat exchanger in Figure 2.7 are given assuming that the purpose of a heat exchanger is to heat the cold stream ($T_1 > T_0$) but if its purpose is to provide cooling ($T_3 < T_0$) then the definition of fuel and product changes into $\dot{E}_P = \dot{E}_4 - \dot{E}_3$ and $\dot{E}_F = \dot{E}_1 - \dot{E}_2$ (Tsatsaronis & Cziesla, 2001). Also, as discussed in the work of Tsatsaronis (1996), certain system components have no meaningful purpose from an exergy point of view when considered alone. For example, throttling valve used in the refrigeration cycle serves another component and should always be evaluated in conjunction with the system component that it serves.

2.3.2. Economic Analysis

Cost evaluation and optimization of energy conversion systems requires comparison between annual values of carrying charges, fuel costs and operation and maintenance expenses. As these values vary over the timespan of the system's economic life, all charges has to be levelized based on certain economic parameters which are assumed or based on past data (Tsatsaronis & Cziesla, 2001). This section introduces the Total Revenue Requirement (TRR) method (Bejan et al., 1996) that will be used for the cost analysis performed as part of this work. The assumptions made for economic analysis are listed below:

Table 2.2.: Assumptions of various economic parameters

Economic Parameter	Values
Inflation rate	1.7%
Real Interest rate	2.75%
Economic life of the system	20 years
O&M cost/year	2% of TCI
Real Escalation rate	2%

The inflation rate taken is based on the inflation rate of USA as of July 2017 (USBLS, 2017). The real interest rate taken is based on the interest rate offered by US banks for long term savings as of July 2017. This is because the investment needed for the system is small and assuming an investor sees this as an alternative investment to saving. The system is small and developed for existing projects rather than as a standalone power system; meaning a loan would not be required and the profits from existing projects can be reinvested. The economic analysis in this work is based on this assumption.

When there is debt involved in an investment by an investor then there would be cost of debt. The cost of equity is the return expected by the investor for his own investment. The weighted average of cost of equity and debt gives the cost of capital for an investment. Cost of capital which is often used as the discount rate for a financed project varies widely depending on the sector of investment. A sensitivity analysis for the economics of the system based on cost of capital as interest rate would be done to see the effect of a different interest rate. The average value of cost of capital in USA considering a few application sectors for HSE systems. The average cost of capital found was 6.04% (Damodaran, 2017). Also, from the perspective of a developing country like India, sensitivity analysis will be performed with an interest rate of 7.72% and inflation rate of 3.36% .

Total Capital Investment

The cost estimates for equipments purchased for the system can be obtained from various sources like vendor's quotations, cost from past purchase orders, quotations from professional estimators, cost databases from companies and software packages. The estimates used in this work for components except the main cycle components are based on past purchase orders provided by Heat Source Energy Corporation. Also, due to unavailability of cost function for the scroll expander, the cost value given by the company for developing the scroll expander prototype has been used for analysis.

The cost functions given by the literature for heat exchangers that were used to estimate their cost depend on the area of the heat exchanger required. Since the heat exchangers in HSE systems were not optimized the required heat exchanger area was found from the UA values given as output by cycle-tempo for all heat exchangers in the flow sheet model. U refers to the heat transfer coefficient and A is the area of heat exchanger required. The UA values given by cycle tempo are based on LMTD calculation using inlet and outlet temperatures of the heat exchanger streams. The value of heat transfer coefficient (U) is taken as $3.4 \text{ kW/m}^2\text{K}$ based on the data sheet of heat exchangers provided by HSE. The cost function for plate type heat exchangers found from literature is given below (Guo-Yan, En, & Shan-Tung, 2008):

$$\text{Cost of plate type heat exchangers} = 635.14 * A^{0.778} \$ \quad (2.6)$$

Apart from the purchased equipment costs, the cost for instrumentation, piping, assembly, system structure and labour were included in the total capital investment calculation. The cost for insurance, taxes and retail markup was not considered as the economic analysis is done from the perspective of the manufacturer due to the non-commercial status of the technology which is in the prototype and testing stage. Also, they are not design dependent and the economic life which is taken as 20 years is a long period to consider taxes and insurance costs with certainty. The retail markup also depends on various factors depending on the application of the system and brings more ambiguity to the economic analysis when assumed.

Revenue Requirements and Levelized costs

Total Revenue Requirement calculations can be divided into two categories: carrying charges and expenses. Based on the economic parameters assumed for the economic analysis as given in Table 2.2, the following factors and rates are calculated which will be further used in this study while applying the total revenue requirement method to the different systems analyzed. The economic life is considered as 20 years and is assumed that all transactions take place at the end of respective years.

Nominal Interest Rate: The nominal interest rate for an investment is dependent on the real interest rate and inflation rate and can be calculated using the following equation:

$$(1 + i_n) = (1 + i_r) * (1 + e) \quad (2.7)$$

where,

i_n = nominal interest rate

i_r = real interest rate

e = inflation rate

The real interest rate is assumed as 2.75% and the inflation rate is assumed as 1.70%. Thus, the nominal interest rate found using the above equation is 4.5%.

Capital Recovery Factor(CRF): Capital Recovery Factor (CRF) is used for calculating the carrying charges and can be expressed as (Bejan et al., 1996):

$$CRF = \frac{i(1 + i)^n}{(1 + i)^n - 1} \quad (2.8)$$

Nominal Escalation Rate: The real escalation rate (r_r) of an expenditure, operation and maintenance costs in this case, is the annual rate at which an expenditure changes due to factors like resource depletion, technological changes and increase in demand. Although technological changes can lead to a negative escalation rate, the other factors lead to positive escalation rate. The real rate of escalation is assumed to be 2%. The nominal escalation rate (r_n) that incorporates the effect of inflation is found using the following equation:

$$(1 + r_n) = (1 + r_r) * (1 + e) \quad (2.9)$$

The nominal escalation rate was calculated as 3.73%.

Constant Escalation Levelization Factor (CELF): Applying escalation factor to an expenditure results in a non-uniform cost schedule. Therefore, the *Constant Escalation Levelization Factor (CELF)* that represents the relationship between an expenditure at the beginning and its annuity is used to find the levelized cost of operation and maintenance. The CELF factor can be found using the nominal escalation rate and nominal interest rate using the following equation:

$$CELF = \left(\frac{k(1 - K^n)}{1 - k} \right) CRF \quad (2.10)$$

where,

$$k = \frac{1 + r_n}{1 + i_n}$$

$$CRF = \text{Capital recovery factor (Eq 2.8)}$$

The O&M cost per year can be calculated from the assumption given in Table 2.2. The levelized costs of carrying charges (CCL) and operating and maintenance expenses (OML) per year for the entire system is then calculated using the assumptions and factors calculated based on them. Total revenue required per year is the sum of levelized cost of carrying charges and operation and maintenance cost per year. Also, the levelized costs are used for the calculation of \dot{Z}_k value needed for the cost balance equations as explained in section 2.3.3. The equation for \dot{Z}_k calculation is (Bejan et al., 1996),

$$\dot{Z}_k = \frac{(CC_L + OMC_L)PEC_k}{\text{Operation hours} * \text{Total PEC}} \quad (2.11)$$

The operation hours assumed for the economic analysis is 8000 hours considering only the downtime for maintenance. This signifies that the values obtained would be representative of the full potential of the system rather than a realistic application. Since the operation hours vary widely based on application, a sensitivity analysis for the values of \dot{Z}_k will be done for different operation hours.

2.3.3. Exergy Costing and Cost balance

Exergy analysis of a system gives information required to evaluate the design and performance of components from a thermodynamic viewpoint. However, it doesn't reveal how much does exergy destruction in a component costs the system operator. The information on this cost would be useful in improving the cost effectiveness of the system (Tsatsaronis & Czesla, 2001). For exergoeconomic evaluation and optimization, component related exergoeconomic variables that give the relation between investment, operation and maintenance cost and the thermodynamic inefficiencies of a component have to be calculated. These thermoeconomic variables will be calculated based on the cost rates associated with material and energy streams of the system. Based on a decision criteria and exergoeconomic variables, required changes in parameters and system structure can be identified. Also, the trade-offs between cost rates associated with capital investment and exergy destruction can be identified resulting in cost minimization for the overall system. Thus, the most basic step in the exergoeconomic analysis is exergy costing (Tsatsaronis & Czesla, 2001).

Exergy costing is the basic principle of exergoeconomics which states that exergy and not energy or mass should be the basis for costing of energy carriers. During this step, a cost rate is assigned to all the exergy streams in the system which can be expressed as, for j^{th} stream, the product of average cost per exergy unit c_j and the exergy rate of the stream \dot{E}_j :

$$\dot{C}_j = c_j \dot{E}_j$$

Also, a cost rate is assigned to exergy transfer rates involved in heat or work transfer in the system at steady state:

$$\dot{C}_q = c_q \dot{Q}$$

$$\dot{C}_w = c_w \dot{W}$$

Analogous to the fuel and product exergy rate definition in exergy analysis, the cost rates associated with fuel and product are defined for each component in the system. Figure 2.8 shows the cost rate definitions for selected components in the system at steady state operation.

Component	Schematic	Cost rate of product \dot{C}_P	Cost rate of fuel \dot{C}_F
Compressor pump, or fan		$\dot{C}_2 - \dot{C}_1$	\dot{C}_3
Turbine or expander		\dot{C}_4	$\dot{C}_1 - \dot{C}_2 - \dot{C}_3$
Heat exchanger		$\dot{C}_2 - \dot{C}_1$	$\dot{C}_3 - \dot{C}_4$

Figure 2.8.: Cost rates of fuel and product for selected components at steady state operation (Tsatsaronis & Czesla, 2001)

The cost rate definitions for heat exchanger in Figure 2.8 are given assuming that the purpose of a heat exchanger is to heat the cold stream ($T_1 > T_0$) but if its purpose is to provide cooling ($T_3 < T_0$) then the definition of fuel and product changes into $\dot{C}_P = \dot{C}_4 - \dot{C}_3$ and $\dot{C}_F = \dot{C}_1 - \dot{C}_2$ (Tsatsaronis & Czesla, 2001).

Cost balance equations are usually formulated for each component after exergy costing. A cost balance equation derived for the k^{th} component of a system defines that the total cost of exergy streams leaving a component is equal to the sum of total cost of exergy stream entering the component and the cost associated with investment, maintenance and operation expenses \dot{Z} . The value of \dot{Z}_k is the sum of \dot{Z}_k^{CI} and \dot{Z}_k^{OM} which represent the cost rate associated with capital investment and operation and maintenance respectively.

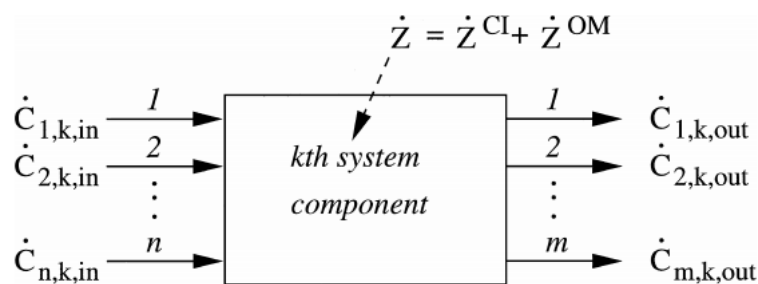


Figure 2.9.: Schematic to illustrate cost balance (Tsatsaronis & Czesla, 2001)

In exergoeconomic analysis it is assumed that the cost of exergy streams entering the k^{th} component is known and that is from the components they leave from or if the stream is entering the system then from the purchase cost. The \dot{Z}_k value is found from the economic analysis performed in the previous step of this methodology. Thus, the only unknown variables that have to be calculated from the cost balance equations are the costs per unit of exergy of the streams leaving the component.

2.3.4. Exergoeconomic evaluation

For exergoeconomic evaluation of thermal systems, the variables calculated from exergy analysis is not enough. The cost per unit of exergy in the streams calculated from the previous step is used to calculate the exergoeconomic variables which in addition with the exergetic variables enable design evaluation of the system and components. Thus, the exergetic and exergoeconomic variables calculated for the k^{th} component in a system are listed below (Tsatsaronis, 1996):

- Cost rate of Exergy Destruction, $\dot{C}_{D,k} = c_{F,k} \dot{E}_{D,k}$
- Cost rate of capital investment, \dot{Z}_k^{CI}
- Cost rate of operation and maintenance expenses, \dot{Z}_k^{OM}
- Sum of cost rates of both investment and operation and maintenance, $\dot{Z}_k = \dot{Z}_k^{CI} + \dot{Z}_k^{OM}$
- Relative cost difference, $r_k = \frac{c_{P,k} - c_{F,k}}{c_{F,k}} = \frac{1 - \varepsilon_k}{\varepsilon_k} + \frac{\dot{Z}_k}{\dot{C}_{D,k}}$
- exergoeconomic factor, $f_k = \frac{\dot{Z}_k}{\dot{Z}_k + c_{F,k} \dot{E}_{D,k}}$

The relative cost difference factor, r_k , expresses the relative increase in the average cost per unit of product exergy in comparison with the fuel exergy of the component. It is useful in evaluating and optimizing a system component especially when the cost of fuel to the component changes with each iteration. Thus, this factor holds more significance when the fuel exergy input to the system has a specific cost.

The exergoeconomic factor f_k expresses the contribution of non exergy related cost to the total cost increase as a ratio. A low value of f_k in a major component suggests that cost savings in the component can be achieved by improving the exergetic efficiency of the component even if the investment cost of the component increases due to the improvement. A high value of f_k suggests that the investment cost of the components should be reduced at the expense of exergetic efficiency. The typical values of f_k depend on the component type and can be used as a base to determine the direction in which the optimization has to proceed. The typical value of f_k for heat exchangers is 55%, between 35 and 75% for expanders and more than 70% for pumps (Bejan et al., 1996). These values give an understanding of which value of f_k for a particular component means that it is not in normal range and that the component should be considered for optimization depending on whether the value is lower or higher.

The guidelines given by Tsatsaronis (1996) that are to be followed while evaluating the k^{th} component of a system are explained below (Tsatsaronis & Czesla, 2001; Bejan et al., 1996):

1. The components should be ranked in the descending order based on the values of sum of \dot{Z}_k and $\dot{C}_{D,k}$. This value gives the total cost increase associated with the particular component and helps in prioritizing the components for optimization.
2. Consider design changes for components with high values of $\dot{Z}_k + \dot{C}_{D,k}$, especially when its relative cost difference (r_k) value is also high.
3. The value of exergoeconomic factor f_k reveals the major cost source:
 - If f_k is high, then it should be studied whether it is cost effective to reduce the investment on a component at the expense of its efficiency.
 - If f_k is low, then the component efficiency should be improved by increasing the investment.

4. Sub processes that increase exergy destruction without contributing to the reduction of investment for the component should be eliminated.
5. A component should be considered for improving exergetic efficiency if its exergetic efficiency is low or if it has relatively high value of exergy destruction.

2.3.5. Iterative Exergoeconomic Optimization Procedure

Conventional mathematical optimization methods based on analytical and numerical optimization techniques are generally applied to a thermal system with specific structure and generally require mathematical modelling of the entire system and input data in a certain form, for example, economic data as a function of thermodynamic variables. However, structural changes in a thermal system can result in significant reduction of product costs and it is not practical to develop mathematical models for all possible design configurations of the system to optimize. Also, the mathematical optimization techniques cannot suggest any structural changes to the system that can potentially improve cost effectiveness (Bejan et al., 1996)

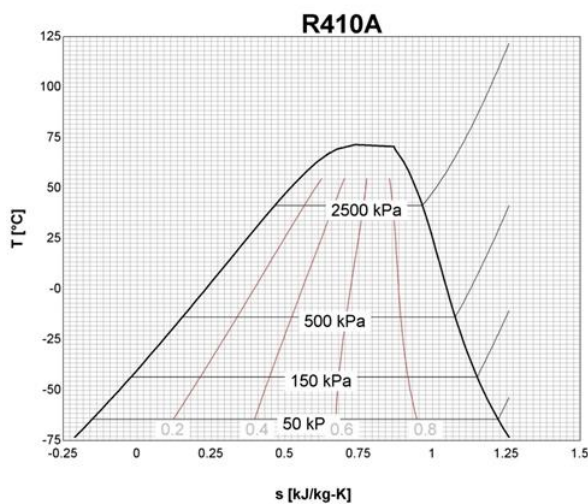
An alternative approach that can be used for such optimization is the iterative exergoeconomic procedure that consists of the following steps (Bejan et al., 1996):

1. Based on the results of exergoeconomic evaluation of the system, design changes are determined with an objective to improve the system design. In this step, only decision variables that affect *both* exergetic efficiency and investment costs are considered.
2. If the system has one or two components which have significantly higher $\dot{Z}_k + \dot{C}_{D,k}$ value than other components then one or two decision variables of the component should be changed with the objective of minimizing the relative cost difference value, r_k value. This step can be omitted if either \dot{Z}_k or $\dot{C}_{D,k}$ value do not significantly contribute to the $\dot{Z}_k + \dot{C}_{D,k}$ value.
3. Due to unavailability of equation that determines the relationship between the investment cost and the exergetic efficiency of the components, design changes can be suggested in this step based on the methodology explained in Section 2.3.4.
4. Based on steps 2 and 3, a new design is developed and the objective function is calculated. If the objective function improves, then we can go for another iteration with similar design changes and if it didn't then the steps will be repeated for another iteration.
5. Finally a parametric study can be performed to see the effect of some variables/assumptions on the optimization results.

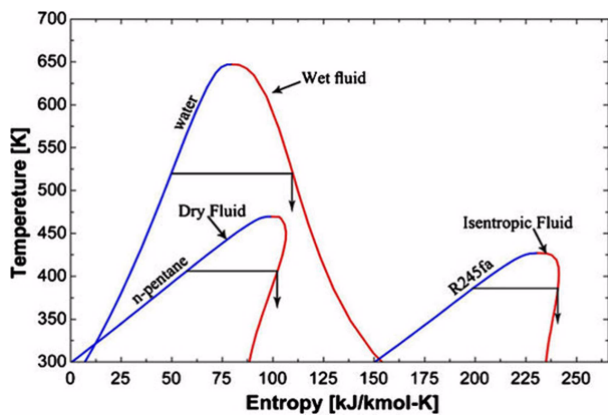
3. Modelling and Exergy Analysis

Flow sheet modelling software 'Cycle Tempo' was used to create the baseline model for the system. The output of the model gives both energy and exergy analysis which can be used for further analysis and optimization of the system. All systems were modelled in Cycle-Tempo with all the major components of a thermodynamic cycle. Other auxiliary components of the systems that could not be modelled in Cycle Tempo were excluded from the modelling. Also the use of internal heat exchanger or recuperator in the model developed for the basic ORC system was ruled out as the exhaust of the scroll expander was found to be in two phase and at temperatures not useful for preheating the working fluid in the economizer.

The reason behind the condensation of working fluid during expansion is that the working fluid R410A is a wet fluid and the system has been modelled assuming the working fluid is in saturated conditions before the inlet of the expander and the pump. Due to lack of super heat, the working fluid condenses during the expansion process and exits the turbine in two phase. From literature study it is known that too much super heat reduces the performance of the scroll expander which nullifies the advantages of recovering heat using a recuperator at the exit of the expander. The flow sheet model developed to check the usefulness of a recuperator in the basic ORC system can be found in Appendix A for reference. Figure 3.1a shows the T-S diagram of R410A fluid and from figure 3.1b it can be seen that the slope of the T-S diagram of the fluid depends on whether the type of fluid is wet, dry or isentropic.



(a) T-S diagram of R410a (Sakhrieh et al., 2016)



(b) T-S diagram of different fluids (Ataei et al., 2015)

Figure 3.1.: Comparing T-S diagram of R410A with other type of fluids

Dry fluids with a positive slope and lower critical point vaporize at low temperatures. Due to their overhanging two phase coexistence curve in the T-S diagram, they do not condense while passing through the turbine whereas Wet fluids on the other hand have a negative slope and tends to condense during the expansion process.

The thermal efficiency of a system is calculated as the ratio of electric power generated to the heat absorbed by the heat exchanger from the hot stream.

$$\eta_{th} = \frac{P_{el}}{Q_{input}} \quad (3.1)$$

The efficiency found from the above equation is called the gross thermal efficiency as it does not include the auxiliary power consumed. The following equation denotes the net thermal efficiency

$$\eta_{th,net} = \frac{P_{el} - P_{pump}}{Q_{input}} \quad (3.2)$$

As a special consideration in this work, the net thermal efficiency of the system is calculated by considering only the refrigerant pump work as the auxiliary power and in case of the cogeneration system including the compressor work required. The work done by hot and cold stream pumps are neglected as they are application specific and is not dependent on the thermodynamics of the organic rankine cycle itself. However, Cycle-Tempo's output for system efficiency includes the work of hot and cold stream pumps. Therefore, the values have been corrected according to the considerations of this work. The back work ratio is the ratio of auxiliary power to the total power produced by the system i.e the percentage of power self consumed by the system itself.

3.1. Modelling of HSE systems

Basic Organic Rankine Cycle with R410A

The model developed initially for this study was simulated with assumptions and process parameters close to what has been observed in various studies from the literature pool. As mentioned in section 2.1.1, HSE's claim of higher isentropic efficiency close to 90% has not been validated through standard experimental testing. Therefore, a base case value of 75% was assumed as the isentropic efficiency of the scroll expander. The input summary of the entire flow sheet model in cycle tempo can be found in Appendix A. However, the key assumptions are given below:

1. The system is in steady state: heat transfer to the environment is neglected.
2. The isentropic efficiency of the diaphragm pump is assumed to be 90%.
3. Scroll expander isentropic efficiency was assumed as 75%.
4. The temperature of the heat source was assumed to be constant at 80°C.
5. The inlet pressure of the expander was set at 42 bar.
6. The pressure drop for R410A in the plate type heat exchangers were assumed to be 0.1 bar.
7. The minimum temperature difference between the fluids in a heat exchanger is assumed to be 5K in all heat exchangers.
8. The cooling water entering the condenser is at environmental temperature and pressure.
9. Generator efficiency was assumed to be 95%.

Figure 3.2 shows the schematic of the basic ORC model. Further in this work all reference to a stream or component in the system would be based on the identifications specified in the schematic in figure 3.2.

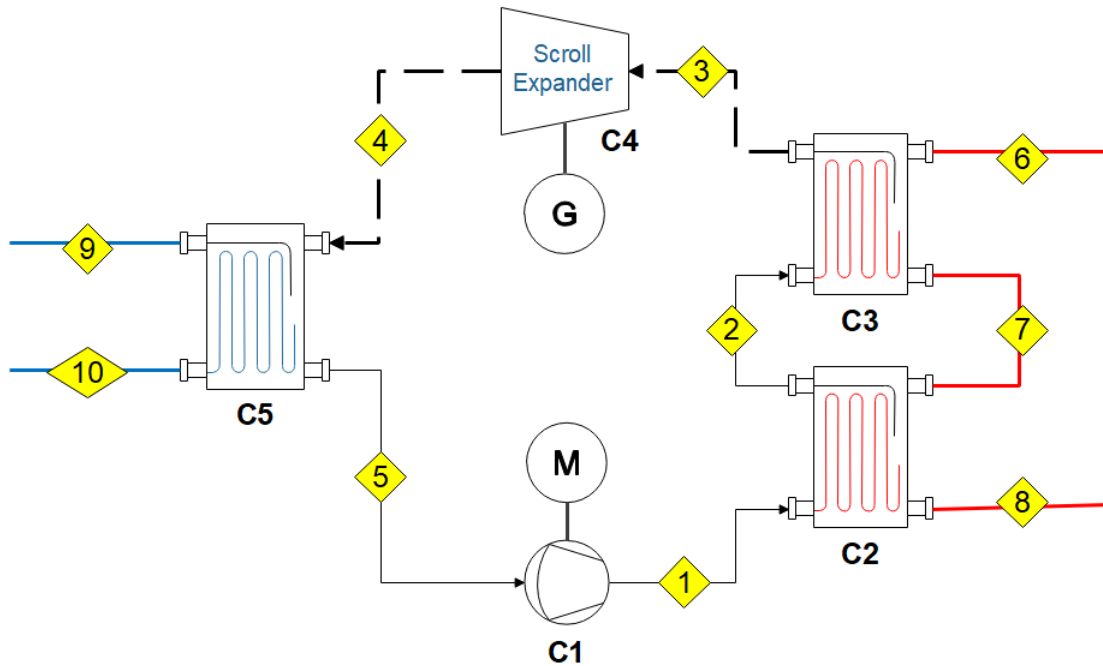


Figure 3.2.: ORC system with R410A as working fluid

The cycle tempo schematic of the system and output data can be found in Appendix A. The model was simulated for an electric power output of 40 kW based as the heat engine prototype developed by HSE has a rated power of 40 kW. The gross thermal efficiency achieved was 8.19% and the net thermal efficiency achieved was 6.38%. The back work ratio calculated for the pump is 22.1%. As discussed in Section 2.1.2, it is evident that the back work ratio of an ORC is relatively high. In this basic ORC system the pump consumes almost one fourth of the power produced by the system. Table 3.1 gives the thermophysical data and mass flow of each stream in the system.

Table 3.1.: Mass flow and thermophysical properties of streams

Stream ID	Mass flow [kg/s]	Pressure [bar]	Temperature [°C]	Exergy flow [kW]
1	2.65	42.20	27.01	211.98
2	2.65	42.10	65.04	233.08
3	2.65	42.00	65.06	278.35
4	2.65	16.46	25.00	222.74
5	2.65	16.36	24.66	205.54
6	7.19	1.41	80.00	192.39
7	7.19	1.21	70.04	140.53
8	7.19	1.01	63.78	111.63
9	21.70	1.21	15.00	0.43
10	21.70	1.01	20.00	3.90

The exergy flow rate of each stream given in Table 3.1 is calculated by Cycle-Tempo based on the environmental conditions specified. These values are then used in Section 3.2 to calculate the fuel and product exergy of each component based on its inlet and outlet streams.

ORC-Vapour compression based Cogeneration system

Sustainable development when defined from an energy policy perspective necessitates the reduction of environmental costs involved in energy production and use without compromising on the

accessibility and reliability of basic energy services like heating, cooling and lighting (Karbassi et al., 2007). Combining thermodynamic cycles to produce various forms of useful energy have become possible with cogeneration systems. Cogeneration systems for heat recovery have been extensively studied by various researchers as they have the potential to improve energy efficiency. This work investigates the performance of the cogeneration system proposed for low temperature thermal sources using exergoeconomic analysis based on average cost approach and iterative exergoeconomic optimization procedure (Tsatsaronis, 1996; Lazzaretto & Tsatsaronis, 1999).

The system is based on an organic rankine cycle for power generation and vapour compression cycle for refrigeration. The power cycle of this cogeneration system has the same features of the ORC heat engine described in Section 2.1 and therefore the assumptions considered are similar to the basic ORC model described in Section 3.1. For the refrigeration cycle it is to be noted that the refrigeration chamber was assumed to have only dry air as the presence of moisture has negligible effect on the exergy values calculated and also the Cycle Tempo exergy calculations were not reliable when refrigeration with moist air was simulated at or below 0°C. Thus, the presence of moisture in the stream of air being cooled is neglected.

The input summary of the process parameters for the Cycel-Tempo can be found in Appendix A. However, the key assumptions made while developing the flow sheet model for the cogeneration system are listed below:

1. The system is in steady state: heat transfer to the environment is neglected.
2. Diaphragm pump isentropic efficiency was assumed to be 90%.
3. The isentropic efficiency of the scroll expander was assumed to be 75% and the generator efficiency was assumed to be 95%.
4. The isentropic efficiency of the scroll compressor used in the refrigeration cycle was assumed to be 75%.
5. The refrigeration capacity is 3 refrigeration tonnes (RT) which roughly equals to 10.55 kW of heat load.
6. The refrigeration set temperature is assumed to be 0°C and an evaporation temperature of -2°C.
7. The temperature of the heat source was assumed to be constant at 80°C.
8. The inlet pressure of the expander was set at 42 bar.
9. The pressure drop for R410A in the plate type heat exchangers were assumed to be 0.1 bar.
10. The minimum temperature difference between the fluids in a heat exchanger is assumed to be 5K in all heat exchangers except the evaporating coils in the refrigeration cycle.
11. The cooling water entering the condenser is at environmental temperature and pressure.

Figure 3.3 shows the schematic of the cogeneration system modelled to represent HSE18R prototype.

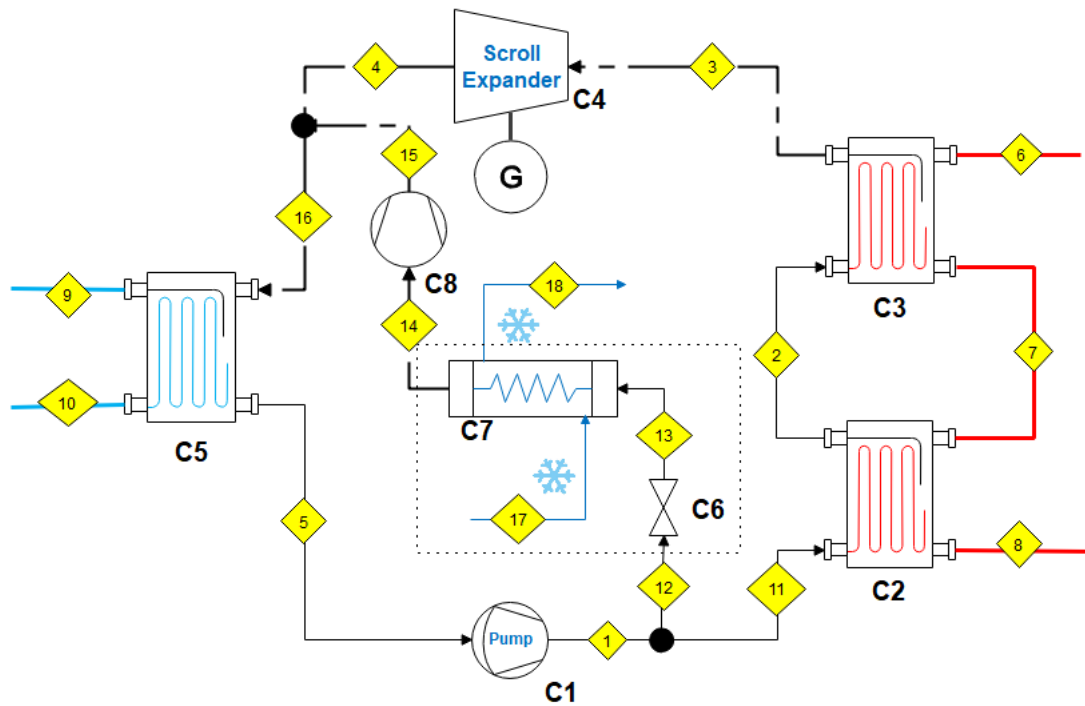


Figure 3.3.: Cogeneration system with R410A as working fluid

The schematic of the flow sheet model developed in cycle tempo and the corresponding The model was simulated for 25 kW of electric power and 3 tons of refrigeration (RT) which is approximately equal to 10.55 kW. The results of the simulation show that the gross thermal efficiency was 8.19% and the net efficiency was calculated as 5.43%. The back work ratio of the pump is 23.88 % where as for the compressor it is 9.8%. It is to be noted that the back work ratio is little higher for the cogeneration system. Table 3.2 gives the thermophysical properties of the working fluid in each stream of the system.

Table 3.2.: Mass flow and Thermophysical properties of fluid in each stream

Stream ID	Mass flow [kg/s]	Pressure [bar]	Temperature [°C]	Exergy flow [kW]
1	1.71	42.20	27.01	137.08
2	1.66	42.10	65.06	150.08
3	1.66	42.00	65.06	173.96
4	1.66	16.46	25.00	139.20
5	1.71	16.26	24.42	132.90
6	3.80	1.41	80.00	101.69
7	3.80	1.21	70.06	74.33
8	3.80	1.01	60.82	52.36
9	14.15	1.11	15.00	0.14
10	14.15	1.01	20.00	2.54
11	1.66	42.20	27.01	132.48
12	0.06	42.20	27.01	4.60
13	0.06	7.46	-2.08	4.25
14	0.06	7.46	-2.00	3.65
15	0.06	16.56	46.25	4.98
16	1.71	16.46	25.00	144.13
17	5.26	1.01	2.00	8.96
18	5.26	1.01	0.00	9.50

The exergy flow rate of each stream given in Table 3.2 is calculated by Cycle-Tempo based on the environmental conditions specified. These values are then used in Section 3.2 to calculate the fuel and product exergy of each component of the cogeneration system based on the inlet and outlet streams as defined in the schematic shown in Figure 3.3.

3.2. Exergy Analysis

First law based thermodynamic analysis and energy accounting usually leads to right conclusions. But the reason for a particular behaviour of a system or its component cannot be accurately predicted just with first law analysis. The reason is that the first law of thermodynamics does not embody any distinction between work and heat and has no provision to understand the quality of energy. These limitations, though not very serious when dealing with familiar systems, could make it difficult to understand the behaviour of novel thermal systems. However, a rigorous quantitative analysis based on second law of thermodynamics provides a better understanding while dealing with novel and complex thermal systems. The purpose of such an analysis employing both first and second law of thermodynamics is to analyze the performance of the thermodynamic processes in the reversible limit and to estimate the departure from this limit (irreversibility) (Mago et al., 2008).

Thermodynamics explains that different forms of energy are not equal and that less valuable forms of energy like heat cannot be converted into useful shaft work completely at all times. Exergy which can be described as a part of thermal energy that can be converted to shaft work completely represents the quality of energy or the energy that is actually available. Exergy analysis of a system thus helps in a deeper understanding of the thermodynamic irreversibilities in the system. Open literature indicates that several researches have laid the framework for exergy analysis. In this work, the exergy analysis is based on the work of Bejan et al. (1996). Refer to Section 2.3.1 for more details on the assumptions and definitions relating to exergy analysis done for this research.

According to the guidelines presented in Section 2.3.1, the rate of fuel and product exergy for each component in the basic ORC system and cogeneration system is defined and presented in Tables 3.3 and 3.4. Based on these definitions the exergetic variables are calculated which can be used to compare different systems or components of the same system.

Table 3.3.: Fuel and Product exergy definitions for each component of basic ORC system

Component	Fuel Exergy, \dot{E}_F [kW]	Product Exergy, \dot{E}_P [kW]
Pump C1	W_P	$\dot{E}_1 - \dot{E}_5$
Preheater C2	$\dot{E}_7 - \dot{E}_8$	$\dot{E}_2 - \dot{E}_1$
Evaporator C3	$\dot{E}_6 - \dot{E}_7$	$\dot{E}_3 - \dot{E}_2$
Expander C4	$\dot{E}_3 - \dot{E}_4$	W_T
Compressor C5	$\dot{E}_4 - \dot{E}_5$	$\dot{E}_{10} - \dot{E}_9$

In order to define the exergetic efficiency of each component in the cogeneration system, a special consideration has to be taken into account. As discussed in section 2.3.1, the throttling valve used in the refrigeration cycle should be evaluated in conjunction with the component that it serves. Therefore, the throttling valve (C6) in the refrigeration cycle is evaluated along with the evaporator (C7), meaning the exergetic efficiency of the evaporator is defined by considering the exergy reduction between streams 12 and 14 as the rate of fuel exergy (see Figure 3.3). The exergetic definitions for each component are presented below in Table 3.4:

Table 3.4.: Exergy definition for components of cogeneration system

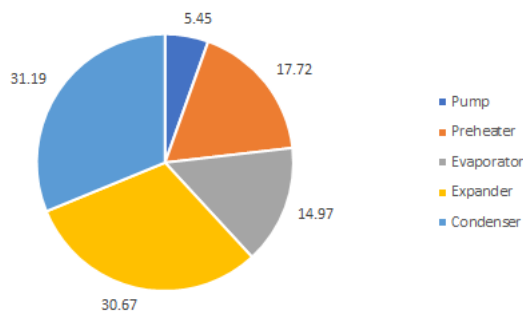
Component	Fuel Exergy, $E_{\{F\}}$ [kW]	Product Exergy, $E_{\{P\}}$ [kW]
Pump C1	W_P	$E_1 - E_5$
Preheater C2	$\dot{E}_7 - \dot{E}_8$	$\dot{E}_2 - \dot{E}_{11}$
Evaporator C3	$\dot{E}_6 - \dot{E}_7$	$\dot{E}_3 - \dot{E}_2$
Expander C4	$\dot{E}_3 - \dot{E}_4$	W_T
Compressor C5	$\dot{E}_{16} - \dot{E}_5$	$\dot{E}_{10} - \dot{E}_9$
Evaporator C7	$\dot{E}_{12} - \dot{E}_{14}$	$\dot{E}_{18} - \dot{E}_{17}$
Compressor C8	W_C	$\dot{E}_{15} - \dot{E}_{14}$

Based on the exergy definitions of each component and exergy calculations for each stream (given by cycle-tempo), the values of fuel, product exergy and exergy destruction are found for each component. Subsequently, the values were used to find the exergetic efficiency (ε) and exergy destruction ratios (Y_D and Y_D^*) for each component using Equations 2.2, 2.4 and 2.5. The exergetic efficiency of a component as given in Equation 2.2 is the ratio of product exergy to the fuel exergy of the component and the exergy destruction ratio, Y_D , is the ratio of exergy destruction in the component to the total fuel exergy supplied to the system. These two values help in comparing two similar components of different systems with same or similar fuels. In order to compare two dissimilar components of a system based on exergy destruction, the exergy destruction ratio Y_D^* is used as it is the ratio of exergy destroyed in a component to the total exergy destroyed in the system (Bejan et al., 1996).

Table 3.5.: Exergy calculations for each component of basic ORC system

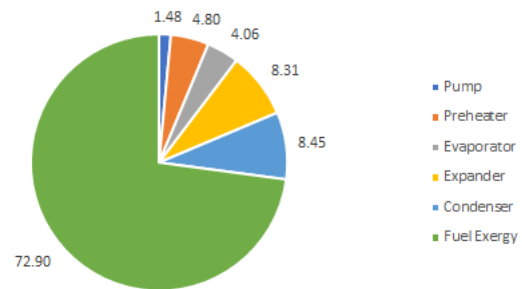
Component	\dot{E}_F [kW]	\dot{E}_P [kW]	\dot{E}_D [kW]	ε [%]	Y_D [%]	Y_D^* [%]
Pump (C1)	8.84	6.44	2.4	72.85	1.48	5.45
Preheater (C2)	28.9	21.1	7.8	73.01	4.80	17.72
Evaporator (C3)	51.86	45.27	6.59	87.29	4.06	14.97
Expander (C4)	55.61	42.11	13.5	75.72	8.31	30.67
Condenser (C5)	17.2	3.47	13.73	20.17	8.45	31.19

Contribution to Total Exergy Destruction (%)



(a) Exergy Destruction Ratio, Y_D^*

Fuel Exergy Destroyed (%)



(b) Exergy Destruction Ratio, Y_D

Figure 3.4.: Exergy Destruction in components of basic ORC system

From Table 3.3 and Figure 3.4 it is evident that the evaporator is the most efficient component with 87.29% efficiency from an exergy point of view and contributes to almost 15% of the total exergy destruction in the system. The preheater with a lower efficiency and higher

exergy destruction contributes to approximately 18% of the total exergy destruction. The other heat exchanger in the system, the condenser, is the least efficient component with a efficiency of 20.17% and contributes to 31.19% of the total exergy destruction. Considering the moving components of the system, the pump and the expander, the pump is less efficient but contributes to only a small fraction of the total exergy destroyed in the system whereas the expander at 75% exergy efficiency contributes to 31% of the total exergy destroyed.

Table 3.6.: Exergy calculations for each component in the cogeneration system

Component	\dot{E}_F [kW]	\dot{E}_P [kW]	\dot{E}_D [kW]	ε [%]	Y_D [%]	Y_{D}^* [%]
Pump	5.97	4.18	1.79	70.02	1.77	6.65
Preheater	21.97	17.6	4.37	80.11	4.31	16.25
Evaporator	27.36	23.88	3.48	87.28	3.44	12.94
Expander	34.75	26.32	8.43	75.74	8.32	31.34
Condenser	11.23	2.4	8.83	21.37	8.72	32.83
Evaporating coils	0.95	0.53	0.42	55.79	0.41	1.56
Compressor	2.46	1.33	1.13	54.07	1.12	4.20

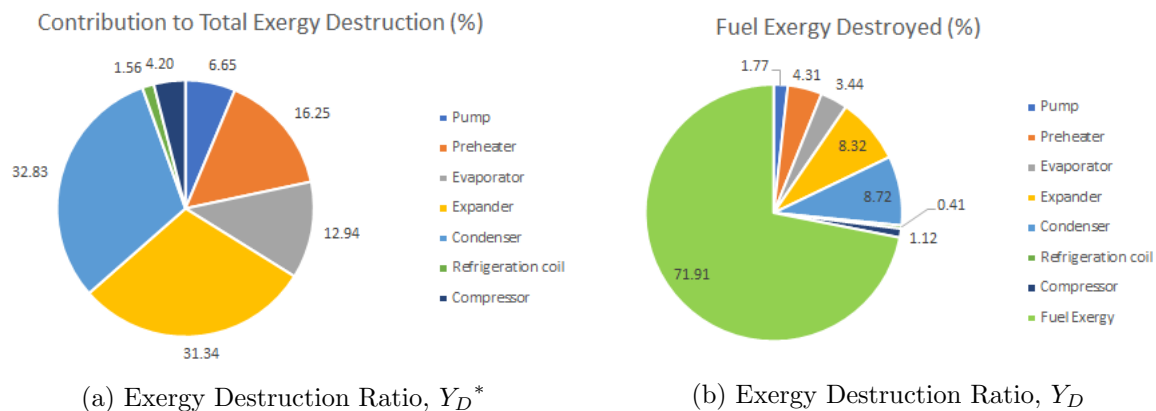


Figure 3.5.: Exergy Destruction in components of cogeneration system

From table 3.6 and Figure 3.5 it can be noted that the expander and condenser, similar to the basic ORC cycle, are the major contributors to total exergy destruction in the cogeneration system. The contribute to 31% and 33% of the total exergy destruction in the system. The expander and the evaporator have almost the same efficiency of 75% and 87% respectively as found in the basic ORC system. This is because the input parameters for the cycle tempo models of both systems is assumed to be same with respect to the power cycle. The exergy efficiency of the preheater is significantly higher in the cogeneration system at 80% compared to its efficiency of 73% in the basic ORC system. This is also reflected in the reduction of preheater's exergy destruction ratio based on the quantity of fuel exergy destroyed in the cogeneration system. It is also interesting to note that the exergetic efficiency of the pump is lower in the cogeneration system than the basic ORC system and also the fuel exergy destroyed by the pump is higher in case of the cogeneration system.

The exergetic efficiency of the refrigeration compressor and evaporating coils is low at 54% and 55.8% respectively, their contribution to total exergy destruction is low because of their relatively smaller capacity compared to the main power cycle. The refrigeration coils contribute to only 1.56% of total destruction whereas the compressor contributes a significant fraction of 4.2% to the total exergy destroyed in the system. Their contribution to exergy destruction can

increase to a more significant value if the refrigeration cycle in the system is scaled up to provide more cooling capacity.

It can be noted that in both the systems, the condenser exergetic efficiency was very low and the exergy destroyed by them contributed most to the total exergy destroyed in the systems. Due to the dissipative nature of the component and its purpose of sinking the heat in the cycle to the environment, the exergy destruction does not hold much significance compared to the exergy loss from the overall system. In the scope of this work the exergy lost from the system is not considered (Refer to Section 2.3.1) and the product exergy of the condenser is not used for any further purpose. The quantity of the product exergy, dependent on the exergetic efficiency of the condenser, is important only when the cooling water is utilized further down the system for other purposes. In the basic ORC system analyzed here, the exergy destruction in the condenser can be partially reduced, but the exergy being lost in the heat transfer process in the condenser is an unavoidable loss of exergy from the cycle.

Thus, from the exergy analysis of both the systems, it can be concluded that the exergy destruction at the expander alone is the major contribution to the thermodynamic irreversibility in the systems. Therefore, it is important to focus on improving the isentropic efficiency of the expander and operating it at optimal pressure ratios to reduce irreversible losses during expansion.

4. Economic Analysis

In order for a thermal design project to be successful, it is important to estimate the cost involved in the project. The most important factor that can affect a design option is the cost of the final products of the system. The market price of a product can depend on the production cost, desired profit and factors like demand and supply, competition, subsidies and regulations by governments. But from thermal system design point of view importance is given only to the production cost of the products of the system. Therefore, only the purchase cost of the system equipment and other investment needed to build the system are considered. Other cost components like retail markup, insurance and taxes are ignored as they are highly dependent on the market situation and does not have any influence on the product cost. In this chapter the total revenue requirement method (Bejan et al., 1996) is used to calculate the cost of the final product by finding the total revenue required by the system per year for feasible operation. The Total Revenue Requirement (TRR) method suggested by Bejan et al. (1996) is explained in more detail in Section 2.3.2.

4.1. Conventional economic analysis

The purchase costs of the main cycle components and other cost details of the cogeneration system can be found in Appendix B.1 and B.3. The total revenue required from the system for them to be economically feasible is calculated based on the equations 2.8, 2.7, 2.9 and 2.10. The total revenue required is the sum of the levelized carrying charges and levelized operation and maintenance costs per year. Table 4.1 gives the total costs involved in the system and the revenue required per year for both the basic ORC based system and the cogeneration system.

Table 4.1.: Cost of basic ORC and cogeneration system

Costs and Revenue Required	Basic ORC System [\$ /year]	Cogeneration system [\$ /year]
Total Investment Cost	67623	49879
Operation and Maintenance Cost	1352	998
Levelized carrying charges (CC_L)	5197	3833
Levelized OMC charges(OMC_L)	1857	1370
Total Revenue Requirement	7054	5203

Applying the TRR method to both the systems resulted in an annual revenue requirement of 7054 \$ for the basic ORC system and 5203 \$ for the cogeneration system. Energy costing of the products based on this annual revenue required is not done to prevent confusion in this work as we are more concerned about exergy costing than energy costing. In anyway, the energy costing results would not represent the actual costs of the system due to the limited boundaries of the economic analysis performed in this work which focuses only on the cost effectiveness of the system exclusively based on system manufacturing cost. This is explained in more detail in Section 2.3.2.

In exergoeconomic analysis the cost rates associated with the capital investment, operation and maintenance expenditure per year calculated in the following section is apportioned to the

various products of a system using exergy flows in the system as the criteria and individual components as the aggregation level for applying exergy costing approach.

4.2. Use of TRR method in Exergoeconomics

In exergoeconomics, the conventional economic analysis is necessary to understand the cost decomposition of the system and to find the yearly expenditure involved. Exergoeconomics is different only in the way that it builds up on a conventional economic analysis to apportion the levelized carrying charges and operation and maintenance cost per year among the different system components according to their contribution to the total purchased equipment cost. The cost rates associated with capital investment and operation and maintenance, \dot{Z}_k^{CI} and \dot{Z}_k^{OM} respectively, for each component is found using equation 2.11. The values calculated for \dot{Z}_k^{CI} , \dot{Z}_k^{OM} and $\dot{Z}_k(\dot{Z}_k^{CI} + \dot{Z}_k^{OM})$ for both the systems are given in Tables 4.2 and 4.3.

Table 4.2.: Cost rates associated with each component of basic ORC system

Component	\dot{Z}_k^{CI} [\$/hr]	\dot{Z}_k^{OM} [\$/hr]	\dot{Z}_k [\$/hr]
Pump C1	0.1056	0.0377	0.1433
Preheater C2	0.0298	0.0106	0.0404
Evaporator C3	0.0662	0.0237	0.0899
Scroll Expander C4	0.2132	0.0762	0.2893
Condenser C5	0.1109	0.0396	0.1505

From Table 4.2 it can be seen that the scroll expander has the highest total cost rate associated with it followed by the condenser and pump. In these components the main contribution to the total cost rate is the cost rate associated with capital investment, whereas the other two heat exchangers, preheater and evaporator, have more evenly distributed cost rates associated with capital investment and operation and maintenance expenditure.

From Table 4.3 that gives the cost rates associated with each component of the cogeneration system it is evident that the scroll expander ranks top in total cost rate followed by the condenser. The cost rate of pump is relatively less in the cogeneration system as a lower rated pump that suffices the requirement of the system is used. The main contribution to the total cost rate of these components is the capital investment unlike the other components that have a significant contribution from the O&M expenditure.

Table 4.3.: Cost rates associated with each system component

Component	\dot{Z}_k^{CI} [\$/hr]	\dot{Z}_k^{OM} [\$/hr]	\dot{Z}_k [\$/hr]
Pump C1	0.0514	0.0184	0.0698
Preheater C2	0.0252	0.0090	0.0342
Evaporator C3	0.0396	0.0141	0.0537
Scroll Expander C4	0.1398	0.0499	0.1897
Condenser C5	0.0790	0.0282	0.1073
Evaporator C7	0.0524	0.0187	0.0711
Compressor C8	0.0185	0.0066	0.0251

The \dot{Z} values for each component of both the system presented in Tables 4.2 and 4.3 is used in chapter 5 to calculate the exergoeconomic variables r_k and f_k and the term $\dot{Z}_k + \dot{C}_D$ based on which the components are prioritized for optimization using the iterative exergoeconomic optimization procedure proposed by Tsatsaronis (1996).

4.3. Sensitivity Analysis

Sensitivity analysis is one way to glean a sense of the possible outcomes of a particular investment by varying certain key variables to check the sensitivity of the investment to changes made to various assumptions. It is a way to check the risk involved with an investment.

Effect of key parameter changes on total revenue required per year

The effect of some key parameters on the annual total revenue required (TRR) for the systems is studied. For this sensitivity study 8 different scenarios were considered with each having at least one parameter change to see its effect on the total revenue requirement calculated. Table 4.4 gives the 8 different scenarios based on which the sensitivity for TRR is studied.

Table 4.4.: Different Scenarios considered for sensitivity analysis

Scenario	Change in Economic Parameter
1	20% increase in investment cost
2	20% decrease in investment cost
3	Real interest rate at 6.04%
4	Real interest rate at 7.72%
5	Inflation rate at 2.7%
6	Inflation rate at 3.36%
7	10 year economic life
8	15 year economic life

Scenario 1 and 2

In scenario 1 and 2, the investment cost of the systems were changed and it was observed that increasing or decreasing the investment cost proportionally increased or decreased the total revenue required per year for both the basic ORC and Cogeneration system. This is because the sensitivity analysis was performed by changing only one parameter at a time to see its effect on the TRR value obtained for the systems.

Scenario 3 and 4

In these scenarios, the effect of higher interest rate is investigated. Since the economic analysis in this work is performed based on the assumption that the investor is reinvesting his profits or savings, the interest rate used was very low. But in case of a financed project, that uses a weighted average cost of capital as the discount rate, the values are generally higher and varying according to the application sector. Scenario 3 and 4 looks at the effect of two interest rates 6.04% and 7.72%, calculated from the perspective of US and India, on the TRR of both systems. In Scenario 3 the inflation rate of US, 1.7% is used but in case of scenario 4 the inflation rate of India, 3.36% is used.

In Scenario 3 the total revenue requirement calculated was increased by almost 22% from the base case in both systems. The TRR is \$8596 in the basic ORC system and \$6341 in the cogeneration system. The total revenue requirement calculated as in for a developing country like India in

scenario 4 was 50% more than the base case value, indicating a significant difference in the economics of the system for different markets. The TRR of basic ORC system was increased to \$10631 and of cogeneration system was increased to \$7841.

Scenario 5 and 6

In scenario 5 and 6, the inflation rate was changed to see the effect on the total revenue required. When the inflation rate was to 2.7% in scenario 5, the total revenue required for the basic ORC system by approximately \$620 and for the cogeneration system by around \$460. The effect observed in both systems were less than 10% of the base case value when inflation rate was increased by only 1%. Thus, the effect of inflation rate is not very significant.

The effect of inflation rate on TRR would be more significant when the inflation rate is comparable with those of developing countries. For example, taking the present inflation rate of India which is at 3.36% as the inflation rate in Scenario 6 the total revenue required increased by almost 15% in both systems to \$8100 in the basic ORC system and \$5974 in the cogeneration system.

Scenario 7 and 8

The effect of changed economic parameters on TRR is significant when the economic life considered for analysis is reduced. Reducing the economic life to 10 and 15 years in scenario 7 and 8 respectively, the TRR increased by a significant fraction of the base case value. In Scenario 7 the TRR increased by around 65% to \$11598 for the basic ORC system and to \$8555 for the cogeneration system. In Scenario 8 the TRR increased by more than 20% to \$8544 for the basic ORC system and to \$6302 for the cogeneration system.

Table 4.5 gives the effect of all scenarios on TRR for both the basic ORC and cogeneration system. For more specific details of each scenario and the results refer to Tables B.2 and B.4 in Appendix B.

Table 4.5.: Effect of different scenarios on TRR of basic ORC and cogeneration system

Scenario	Basic ORC System [\$ /year]	Cogeneration system [\$ /year]
Base case	7054	5203
1	8465	6244
2	5643	4163
3	8597	6341
4	10632	7842
5	7677	5662
6	8100	5975
7	11598	8555
8	8545	6303

From the results of each scenario it can be concluded that the effect of interest rate has a very significant effect on the total revenue required by the systems. Especially when interest rate and inflation rate were taken from the perspective of a developing country, the TRR calculated was 50% more than the base case value. Also, using cost of capital for financed projects as discounting factor for levelization instead of long term savings interest rate produced a significant increase in TRR calculated. The TRR in this case increased by about 22% from the base case

value.

The other key assumption that produced large deviations from base case value is the economic life considered over which the costs are levelized. When 10 years was considered as economic life for levelization of costs, the TRR calculated was almost 65% more than the base case value in both systems. Although change in inflation rate alone had a significant effect it was not as high as the previous two parameters.

Effect of operation hours on cost rate associated with investment and operation

The operation hours assumed for this work is 8000 hrs taking into consideration only the down-time for maintenance. But this will vary widely depending on the application. Therefore, sensitivity analysis is performed on the total cost rate of investment, \dot{Z}_k value which directly depends on the annual operation hours of the system. The cost rate values then directly influence the results of exergoeconomic analysis. Tables 4.6 and 4.7 gives the value of \dot{Z}_k of each component in both the basic ORC and cogeneration systems.

Table 4.6.: \dot{Z}_k values of each component in basic ORC system

Component	Value of \dot{Z}_k based on operation hours in \$/hr			
	8000	7000	6000	5000
Pump	0.14	0.16	0.19	0.23
Preheater	0.04	0.05	0.05	0.06
Evaporator	0.09	0.10	0.12	0.14
Scroll Expander	0.29	0.33	0.39	0.46
Condenser	0.15	0.17	0.20	0.24

Table 4.7.: \dot{Z}_k values of each component in cogeneration system

Component	Value of \dot{Z}_k based on operation hours in \$/hr			
	8000	7000	6000	5000
Pump	0.07	0.08	0.09	0.11
Preheater	0.03	0.04	0.05	0.05
Evaporator	0.05	0.06	0.07	0.09
Scroll Expander	0.19	0.22	0.25	0.30
Condenser	0.11	0.12	0.14	0.17
Refrigeration Coils	0.07	0.08	0.09	0.11
Compressor	0.03	0.03	0.03	0.04

From Tables 4.6 and 4.7 it can be seen that reducing the operation hours of the system has a significant effect on the cost rates associated with investment and operation of a component. Comparing the effect on different components of the same system it was evident that the most expensive components in the system showed larger differences in the cost rate. This is because in the basic ORC system, the expander and the pump witnessed comparatively larger effect due to different operation hours. But in the cogeneration system the largest effect was seen in the cost rate of expander followed by the condenser.

5. Exergoeconomic Evaluation

Exergoeconomic evaluation is based on the results of economic and exergy analysis performed on a component level. The main part of this analysis is to calculate the cost per exergy unit of the product stream by studying the cost formation process. This requires formation of cost balance equations and auxiliary equations for each component solving which would give the cost of product exergy streams. The exergy costing method applied and cost balancing follows the average costing approach (Tsatsaronis, 1996; Lazzaretto & Tsatsaronis, 1999) as discussed in section 2.3.3.

Model Assumptions:

- All calculations are based on levelized annual costs comprising of carrying charges, operation and maintenance costs for a levelization time period of 20 years
- Zero unit cost is assumed for the hot water stream, cold water stream and the air entering the evaporator from the refrigeration chamber.

The cost per unit of exergy flow in the hot water stream is assumed zero as the value can be determined based on an application. It tends to vary widely based on application. So in this work, the cost rates obtained are solely based on the cost of purchasing system components and building the system. Applying exergy costing allows you to develop cost balance and auxiliary equations based on the cost rates assigned to each stream and the exergy flow in the streams. Auxiliary equation developed for components is based on the assumption that the unit cost of fuel exergy remains the same at the inlet and outlet of a component with only the cost rate changing its values based on the quantity of exergy used by the component (Bejan et al., 1996). The unknown cost rates of exergy streams are then found by solving the set of algebraic equations are used to calculate exergoeconomic variables. The exergoeconomic evaluation of the systems are based on these variables. Refer to Section 2.3.4 for detailed explanation on how exergoeconomic evaluation is performed and the guidelines given by Bejan et al. (1996) in their book.

5.1. Basic Organic Rankine Cycle with R410A

The cost rates associated with the exergy streams flowing through a component are defined in the same way as the exergy streams to form the cost balance equations. The cost balance equations for each component and its auxiliary equations are given below:

Pump (C1)

Cost balance:

$$\dot{C}_1 - \dot{C}_5 = \dot{C}_{Wp} + \dot{Z}_{C1}$$

$$\dot{C}_1 = \dot{C}_{Wp} + \dot{C}_5 + \dot{Z}_{C1}$$

Ignoring the losses during power transmission, the cost per unit of exergy in the power given to pump is equal to the cost per unit of exergy exported from the system by turbine work. Thus,

$$\frac{\dot{C}_{WP}}{W_P} = \frac{\dot{C}_{WT}}{W_T}$$

Preheater (C2)

Cost balance:

$$\dot{C}_2 - \dot{C}_1 = \dot{C}_7 - \dot{C}_8 + \dot{Z}_{C2}$$

$$\dot{C}_2 = \dot{C}_7 - \dot{C}_8 + \dot{C}_1 + \dot{Z}_{C2}$$

Auxiliary Equation:

Since $c_7 = c_8$,

$$\frac{\dot{C}_7}{\dot{E}_7} = \frac{\dot{C}_8}{\dot{E}_8} \quad \text{or} \quad \dot{C}_7 = \dot{C}_8 \frac{\dot{E}_7}{\dot{E}_8}$$

Evaporator (C3)

Cost balance:

$$\dot{C}_3 - \dot{C}_2 = \dot{C}_6 - \dot{C}_7 + \dot{Z}_{C3}$$

$$\dot{C}_3 = \dot{C}_6 - \dot{C}_7 + \dot{C}_2 + \dot{Z}_{C3}$$

Auxiliary Equation:

Since $c_6 = c_7$,

$$\frac{\dot{C}_6}{\dot{E}_6} = \frac{\dot{C}_7}{\dot{E}_7} \quad \text{or} \quad \dot{C}_6 = \dot{C}_7 \frac{\dot{E}_6}{\dot{E}_7}$$

Expander (C4)

Cost Balance:

$$\dot{C}_{WT} = \dot{C}_3 - \dot{C}_4 + \dot{Z}_{C4}$$

Auxiliary Equation:

Since $c_3 = c_4$,

$$\frac{\dot{C}_3}{\dot{E}_3} = \frac{\dot{C}_4}{\dot{E}_4} \quad \text{or} \quad \dot{C}_3 = \dot{C}_4 \frac{\dot{E}_3}{\dot{E}_4}$$

Condenser (C5)

Cost balance:

In the cost balancing of condenser, a dissipative component, the cost of the product stream that is the cooling water is 0. Therefore, there is no product stream exiting the condenser that can be burdened with the investment cost of condenser. But the exergy destruction cost of the component can be approximated by multiplying the exergy destruction at the condenser and the average cost per unit of exergy (c_F) of the fuel to the condenser ($\dot{E}_4 - \dot{E}_5$):

$$\dot{C}_D = c_F * \dot{E}_D$$

Auxiliary Equation:

Since $c_4 = c_5$,

$$\frac{\dot{C}_4}{\dot{E}_4} = \frac{\dot{C}_5}{\dot{E}_5} \text{ or } \dot{C}_4 = \dot{C}_5 \frac{\dot{E}_4}{\dot{E}_5}$$

Based on the assumption that the cost per unit of exergy for the hot stream and the cold water stream entering the condenser is zero (*i.e.* $c_6 = c_7 = c_8 = c_9 = c_{10} = 0$) and the value of \dot{Z} for each component found by economic analysis, a set of cost balance equations are derived. By solving the equations for the unknowns, the cost rates of all exergy streams are found which is used for calculating the exergoeconomic variables required for exergoeconomic evaluation and optimization.

As discussed in section 2.3.4 the design evaluation methodology states that the components should be ranked in the descending order of cost importance based on the values of $\dot{Z}_k + \dot{C}_{D,k}$ which represents the total increase in costs at the component. Table 5.1 ranks the components based on their $\dot{Z}_k + \dot{C}_{D,k}$ value.

Table 5.1.: Components ranked according to $\dot{Z}_k + \dot{C}_{D,k}$ value

Rank	Component	c_f [\$/kWh]	c_p [\$/kWh]	$\dot{C}_{D,k}$ [\$/hr]	\dot{Z}_k [\$/hr]	$\dot{Z}_k + \dot{C}_{D,k}$ [\$/hr]	r_k	f_k
1	Expander C4	0.01	0.014	0.19	0.29	0.48	1.58	0.60
2	Pump C1	0.01	0.042	0.10	0.14	0.24	1.95	0.59
3	Condenser C5	0.01	0.000	0.08	0.15	0.23	3.96	0.67
4	Evaporator C3	0.00	0.002	0.01	0.09	0.10	0.15	0.87
5	Preheater C2	0.00	0.002	0.01	0.04	0.06	0.37	0.73

From Table 5.1 it is evident that the expander is the first component to be considered for optimization. The f_k value of the expander is 0.6 which is well within the typical f_k value range of 0.35 and 0.75 for compressors and turbines (Bejan et al., 1996). Therefore, the expander should be mainly considered for improving its exergetic efficiency even if investment cost increases as the exergy destruction in the component and the cost rate associated with it is significantly higher than other components. The refrigerant pump which ranks second has almost equal contribution from both investment cost and cost of exergy destruction. The lower f_k value of the pump (typically >70% for pumps) means that it should also be considered for efficiency improvement at the expense of higher investment.

Looking at the heat exchangers, the condenser has high $\dot{Z}_k + \dot{C}_{D,k}$ value with main contribution from its investment cost. Thus, the condenser should be considered for reduction in investment cost at the expense of its exergetic efficiency which means the condenser of the system can be undersized if that contributes to cost savings. The other heat exchangers, preheater and the evaporator, have really high f_k values implying that it is cost effective to reduce their cost of investment at the expense of their exergetic efficiency. Thus, all heat exchangers in the systems can be undersized if the other components *i.e.* expander and pump are performing well, from an exergy point of view, to improve the cost effectiveness of the entire system.

Among all the system components, the total cost increase associated with the expander, $\dot{Z}_k + \dot{C}_{D,k}$, is significantly higher than other components. Thus, design changes made to significantly reduce this would have the greatest effect on the cost effectiveness of the basic ORC system.

5.2. Cogeneration System with R410A

The cost rates associated with a component's inlet and outlet exergy streams can be defined in the same way as the exergy streams to form the cost balance equations. The cost balance equations for each component and its auxiliary equations are given below:

Pump (C1)

Cost balance:

$$\dot{C}_1 - \dot{C}_5 = \dot{C}_{WP} + \dot{Z}_{C1}$$

$$\dot{C}_1 = \dot{C}_{WP} + \dot{C}_5 + \dot{Z}_{C1}$$

The cost per unit of exergy in the power given to pump is equal to the cost per unit of exergy exported from the system by turbine work given the transmission losses are neglected. Thus,

$$\frac{\dot{C}_{WP}}{W_P} = \frac{\dot{C}_{WT}}{W_T}$$

Preheater (C2)

Cost balance:

$$\dot{C}_2 - \dot{C}_{11} = \dot{C}_7 - \dot{C}_8 + \dot{Z}_{C2}$$

$$\dot{C}_2 = \dot{C}_7 - \dot{C}_8 + \dot{C}_{11} + \dot{Z}_{C2}$$

Auxiliary Equation:

Since $c_7 = c_8$,

$$\frac{\dot{C}_7}{\dot{E}_7} = \frac{\dot{C}_8}{\dot{E}_8} \quad \text{or} \quad \dot{C}_7 = \dot{C}_8 \frac{\dot{E}_7}{\dot{E}_8}$$

Evaporator (C3)

Cost balance:

$$\dot{C}_3 - \dot{C}_2 = \dot{C}_6 - \dot{C}_7 + \dot{Z}_{C3}$$

$$\dot{C}_3 = \dot{C}_6 - \dot{C}_7 + \dot{C}_2 + \dot{Z}_{C3}$$

Auxiliary Equation:

Since $c_6 = c_7$,

$$\frac{\dot{C}_6}{\dot{E}_6} = \frac{\dot{C}_7}{\dot{E}_7} \quad \text{or} \quad \dot{C}_6 = \dot{C}_7 \frac{\dot{E}_6}{\dot{E}_7}$$

Expander (C4)

Cost Balance:

$$\dot{C}_{WT} = \dot{C}_3 - \dot{C}_4 + \dot{Z}_{C4}$$

Auxiliary Equation:

Since $c_3 = c_4$,

$$\frac{\dot{C}_3}{\dot{E}_3} = \frac{\dot{C}_4}{\dot{E}_4} \quad \text{or} \quad \dot{C}_3 = \dot{C}_4 \frac{\dot{E}_3}{\dot{E}_4}$$

Condenser (C5)

Cost balance:

In the cost balancing of condenser, a dissipative component, the cost of the product stream that is the cooling water is 0. Therefore, there is no product stream from the condenser to be burdened with the investment cost of condenser. But the component in itself has exergy destruction cost of which can be approximated by finding the average cost per unit of exergy (c_F) of the fuel to the condenser ($\dot{E}_{16} - \dot{E}_5$).

Auxiliary Equation:

Since $c_{16} = c_5$,

$$\frac{\dot{C}_{16}}{\dot{E}_{16}} = \frac{\dot{C}_5}{\dot{E}_5} \text{ or } \dot{C}_{16} = \dot{C}_5 \frac{\dot{E}_{16}}{\dot{E}_5}$$

Refrigeration coil (C7)

Cost balance:

$$\dot{C}_{18} - \dot{C}_{17} = \dot{C}_{12} - \dot{C}_{14} + \dot{Z}_{C7}$$

$$\dot{C}_{18} = \dot{C}_{12} - \dot{C}_{14} + \dot{C}_{17} + \dot{Z}_{C7}$$

Auxiliary Equation:

Since $c_{12} = c_{14}$,

$$\frac{\dot{C}_{12}}{\dot{E}_{12}} = \frac{\dot{C}_{14}}{\dot{E}_{14}} \text{ or } \dot{C}_{12} = \dot{C}_{14} \frac{\dot{E}_{12}}{\dot{E}_{14}}$$

Compressor (C8)

Cost balance:

$$\dot{C}_{15} - \dot{C}_{14} = \dot{C}_{W_C} + \dot{Z}_{C8}$$

$$\dot{C}_{15} = \dot{C}_{W_C} + \dot{C}_{14} + \dot{Z}_{C8}$$

The cost per unit of exergy in the power given to compressor is equal to the cost per unit of exergy exported from the system by turbine work when losses are neglected. Thus,

$$\frac{\dot{C}_{W_C}}{W_C} = \frac{\dot{C}_{W_T}}{W_T}$$

The cost per unit of exergy for the hot water streams, cold water streams and the air entering the evaporator from refrigeration chamber was assumed to be zero (*i.e.* $c_6 = c_7 = c_8 = c_9 = c_{10} = c_{17} = 0$) and the value of \dot{Z} for each component found by economic analysis was used to formulate the cost balance equations which can be found in Appendix C. Solving the equations in Maple for all the unknowns gives the cost rate of all exergy streams in the system. Based on this and the economic analysis all exergoeconomic variables required for exergoeconomic evaluation and optimization are calculated and presented in Table 5.2.

Based on the exergoeconomic design evaluation methodology discussed in section 2.3.4 the components of the cogeneration system are ranked in the descending order of cost importance based on the values of $\dot{Z}_k + \dot{C}_{D,k}$ which represents the total increase in cost rate associated with the component. Table 5.2 ranks the components based on their $\dot{Z}_k + \dot{C}_{D,k}$ value.

Table 5.2.: Components ranked based on $\dot{Z}_k + \dot{C}_{D,k}$ value

Rank	Component	c_f [\$/kWh]	c_p [\$/kWh]	$\dot{C}_{D,k}$ [\$/hr]	\dot{Z}_k [\$/hr]	$\dot{Z}_k + \dot{C}_{D,k}$ [\$/hr]	r_k	f_k
1	Expander C4	0.01	0.016	0.135	0.19	0.32	1.41	0.58
2	Condenser C5	0.01	0.000	0.062	0.11	0.17	3.68	0.63
3	Pump C1	0.02	0.040	0.071	0.07	0.14	1.47	0.50
4	Evaporator C7	0.01	0.149	0.062	0.07	0.13	17.47	0.53
5	Compressor C8	0.02	0.048	0.055	0.03	0.08	2.03	0.31
6	Evaporator C3	0.00	0.002	0.008	0.05	0.06	0.15	0.87
7	Preheater C2	0.00	0.002	0.008	0.03	0.04	0.25	0.80

From Table 5.2 it is evident that the expander tops the list for considering design changes during optimization. The expander with its relatively high $\dot{Z}_k + \dot{C}_{D,k}$ should get first priority among all other design considerations. The expander efficiency should be increased at the expense of its investment cost as the f_k value is relatively low and has room for a higher capital investment on the expander.

The condenser cost which ranks second in the list should be considered for reduction in investment cost at the expense of its efficiency. This is because the contribution of investment cost rate to the total cost rate increase associated with it is significantly higher. The pump which is ranked third has a low f_k value compared to its typical value of more than 70%. Thus, it should be considered for improving the exergy efficiency with higher investment on it.

The refrigeration evaporator has a high total cost rate increase associated with it. Since the exergoeconomic factor, f_k , value of it is typical of a heat exchanger, the evaporator will be considered for design optimization only if that improves the cost effectiveness of the refrigeration cycle or the overall system. The scroll compressor used in the refrigeration cycle has low f_k value, implying that a compressor with higher exergetic efficiency is needed to reduce the cost of exergy destruction. The exergetic efficiency can be improved by changing the design parameters of the refrigeration cycle or by investing to improve the efficiency of the compressor. Since the cost of exergy destruction is more than the cost rate associated with investment any improvement on the performance of the scroll compressor improves the cost effectiveness of the refrigeration cycle and thus the overall system.

The evaporator and preheater in the power cycle of the cogeneration system have very low cost of exergy destruction and a high cost rate associated with the investment cost. Therefore, both the components should be considered for cost reduction at the expense of their exergy efficiency due their high f_k value.

Similar to basic ORC system, the expander among all other components stands out to be the one with significantly high value of total cost rate increase, $\dot{Z}_k + \dot{C}_{D,k}$, associated with it. Thus, even a small improvement in the exergetic efficiency would have a significant impact of the cost effectiveness of the entire system.

Sensitivity check on the cost rate of products

From the sensitivity analysis done in Section 4.3 to see the effect of different operation hours, the \dot{Z}_k values calculated were significantly higher than the base case values. Therefore, exergoeconomic evaluation of the base case cogeneration system with operation hours of 5000 hrs is

done to see its effect on the total cost of products per unit of exergy.

Table 5.3.: Effect of operation hours on the total cost rate of products in the cogeneration system

Variable	8000 hrs	5000 hrs
$c_{p_{elec}}$	0.016	0.026
$c_{p_{cooling}}$	0.149	0.238
$c_{p_{tot}}$	0.165	0.263
$\dot{C}_{D_{tot}}$	0.401	0.642

From Table 5.3 it can be concluded that operation hours have a significant effect on the total cost of products. The cost calculated at 5000 hrs of operation was 10 ¢/kWh higher than what was calculated for 8000 hours of operation. The total cost rate of products calculated is 0.26 \$/kWh. The total cost rate associated with exergy destruction was calculated as 0.64 \$/hr of exergy whereas in the base case it was 24 cents lower at 0.4 \$/hr of exergy flow.

6. Exergoeconomic Optimization

Optimization of a thermal system is a mathematical process wherein certain process parameters are varied with the aim to minimize or maximize the objective function in the system. Iterative exergoeconomic optimization procedure aims at reducing the average cost per unit of exergy or the cost rate of exergy in the product streams of a system, be it electricity or other forms of energy. This is possible with the help of exergy and economic analysis, combining which, the cost rate of all exergy streams in the system can be found using cost and exergy balance. Chapter 5 describes how this is done and also evaluates each system based on the exergoeconomic variables calculated from the cost rates found.

The exergoeconomic optimization procedure applied here, unlike rigorous optimization procedures, is based upon on the judgment of the engineer who considers design changes before each iteration. The design changes considered are in effect implemented by changing the decision variables. These decision variables are process parameters that directly have an effect on the exergetic efficiency of one or more components and should be an input parameter in the flow sheet models developed. The decision variables have to be changed based on the parametric study as it gives the knowledge of the degree of effect of changing a certain decision variable. Refer to Section 2.3.5 for more details on the iterative exergoeconomic optimization procedure.

One important assumption considered during the optimization is that the expander can perform at a high isentropic efficiency of 90% as claimed by the company. From exergoeconomic evaluation it is understood that the expander efficiency would play an important role in reducing the cost and exergy destruction in the system. Although an isentropic efficiency of 75% for the expander has been validated through experimental analysis in Chapter 7, an isentropic efficiency of up to 90% was considered for the expanders during optimization. This would enable us to see how operating the expander at high efficiency as claimed would bring down the costs associated with the system. A sensitivity analysis is also performed to see how a lower isentropic efficiency affects the cost effectiveness of the system.

6.1. Basic ORC system with R410A

The decision variables chosen to vary the design options in the basic ORC system are the expander inlet pressure, expander isentropic efficiency, pinch temperature of condenser and evaporator. The system has to be optimized without compromising on the cost rate of products generated by the system. The total cost rate of products in the system can be the objective function for the optimization procedure if the product of the system is fixed (Bejan et al., 1996). Therefore, \dot{C}_{WT} is the objective function of the basic ORC system with a fixed output of 40 kW electricity. During each iteration the value of decision variables will be chosen based on the trade offs established with the help of exergoeconomic evaluation in section 5.1. Since the trade offs established is between the investment cost of the system components and their exergetic efficiency, it is important to know how the efficiency changes with respect to change in decision variables.

From the exergoeconomic evaluation of the base case model in Section 5.1, it can be deduced that the expander and the pump are the most important components to be optimized. As dis-

cussed, they have to be considered for improving the exergetic efficiency even if it means higher investment cost on the components. Decision variables are changed based on parametric study to implement the design changes considered based on evaluation. The results of the parametric study done for each decision variable is given in Appendix D.

From parametric study on the decision variables it is observed that the exergetic efficiency of the expander can be enhanced by increasing the isentropic efficiency of the expander but this also decreased the pump efficiency by a small margin. When there is conflict in design changes, the changes affecting component with higher $\dot{Z}_k + \dot{C}_D$ value prevails (Tsatsaronis, 1996). Therefore, the first priority in optimizing the system would be to increase the isentropic efficiency of the scroll expander.

Increasing the expander inlet pressure slightly increased the pump exergy efficiency and the evaporator efficiency but decreased the preheater efficiency. Since pump ranks higher in $\dot{Z}_k + \dot{C}_D$ value, the expander inlet pressure should be increased. Increasing the pinch temperature in the condenser, which ranks third, decreases its exergy efficiency but then the area of heat exchanger required is lower. Also, it had a mild positive effect on the exergetic efficiency of expander and pump. As the f_k value of condenser is high, pinch temperature is increased to reduce its area and thus its investment cost.

Increasing the evaporator pinch temperature reduces the area of heat exchanger required and thus the cost at the expense of the exergetic efficiency. From parametric study it was evident that the evaporator efficiency decreased slightly whereas the preheater had a significant decrease in its exergetic efficiency, almost double that of the evaporator.

Figure 6.1 gives the values of decision variables for each iteration. Based on the new values of the decision variables exergoeconomic analysis is performed to find the cost rate of product of the system. The iterations are continued until it is observed that the cost rate of product cannot be significantly reduced anymore.

<i>Iteration 1</i>				<i>Iteration 2</i>			
Variable	Suggestion	Initial Value	Final Value	Variable	Suggestion	Initial Value	Final Value
Expander efficiency [%]	Increase	75	80	Expander efficiency [%]	Increase	80	85
Expander inlet pressure [bar]	Increase	42	45	Expander inlet pressure [bar]	Increase	45	47
Pinch T of Condenser [K]	Increase	5	7	Pinch T of Condenser [K]	Increase	7	10
Pinch T of Evaporator [K]	Increase	5	7	Pinch T of Evaporator [K]	Constant	7	7
<i>Iteration 3</i>				<i>Iteration 4</i>			
Variable	Suggestion	Initial Value	Final Value	Variable	Suggestion	Initial Value	Final Value
Expander efficiency [%]	Increase	85	90	Expander efficiency [%]	Constant	90	90
Expander inlet pressure [bar]	Constant	47	47	Expander inlet pressure [bar]	Constant	47	47
Pinch T of Condenser [K]	Constant	10	10	Pinch T of Condenser [K]	Decrease	10	7
Pinch T of Evaporator [K]	Constant	7	7	Pinch T of Evaporator [K]	Constant	7	7

Figure 6.1.: Changes in decision variables at each iteration

First Iteration

The values of decision variables for 1st iteration can be found in Figure 6.1. Based these values the system is simulated once again to obtain all results required for the exergoeconomic evaluation. Table 6.1 gives the results of the 1st iteration with respect to cost rate of product, cost of the system, exergy destruction and cost rate of exergy destruction.

Table 6.1.: Results of 1st iteration

Output	Base Case	1st Iteration
\dot{C}_{W_T} [¢/hr]	59.34	58.79
TRR [\$ /year]	7054.42	6829.09
$\dot{E}_{D,tot}$ [KW]	44.02	42.5
$\dot{C}_{D,tot}$ [\$ /hr]	0.39	0.35

The small reduction in the objective function justifies the direction in which design changes are considered. But the reduction is not very significant. The iteration is continued with similar changes in decision variables to see if there is significant reduction in the cost of product in further iterations. However the pinch temperature of the evaporator is not changed to allow for a significant temperature difference available at the evaporator for heat transfer.

Second Iteration

In this iteration the isentropic efficiency of the expander, expander inlet pressure and the pinch temperature of the condenser was increased.

Table 6.2.: Results of 2nd iteration

Output	Base Case	2nd Iteration
\dot{C}_{W_T} [¢/hr]	59.34	58.18
TRR [\$ /year]	7054.42	6724.19
$\dot{E}_{D,tot}$ [KW]	44.02	41.8
$\dot{C}_{D,tot}$ [\$ /hr]	0.39	0.32

Table 6.2 shows that there is reduction in total cost due to smaller heat exchangers especially the condenser. Although the condenser exergy destruction significantly increases in this iteration, its lower cost rate of destruction, determined by its relative position in the system, justifies the change.

3rd Iteration

In this iteration only the expander efficiency was improved to check the effect of expander on the product cost and exergy destruction. From Table 6.3 it is evident that the effect of improving expander efficiency has a significant effect even without other trade offs in reducing cost and exergy destruction.

Table 6.3.: Results of 3rd iteration

Output	Base Case	3rd Iteration
\dot{C}_{W_T} [¢/hr]	59.34	57.62
TRR [\$ /year]	7054.42	6683.93
$\dot{E}_{D,tot}$ [KW]	44.02	37.21
$\dot{C}_{D,tot}$ [\$ /hr]	0.39	0.28

The contribution of condenser to total exergy destruction now is almost 46% and the cost rate of this destruction is also high. The cost rate of exergy destruction for pump which contributes to only 6.48% of total destruction is also high due to its higher specific cost of product. Since,

pump is already considered as a highly efficient component, the exergy destruction can only be reduced by decreasing the pinch temperature of condenser or evaporator.

4th Iteration

In this iteration the pinch temperature of condenser is reduced back to 7 K in order to check whether the exergy destruction can be reduced without increasing the objective function. The results shown in Table 6.4 that the exergy destruction rate can be reduced for a negligible increase in the objective function (\dot{C}_{W_T}) of 0.02¢/hr.

Table 6.4.: Results of 4th iteration

Output	Base Case	4th Iteration
\dot{C}_{W_T} [¢/hr]	59.34	57.64
TRR [\$/year]	7054.42	6737.96
$\dot{E}_{D,tot}$ [KW]	44.02	33.25
$\dot{C}_{D,tot}$ [\$/hr]	0.39	0.26

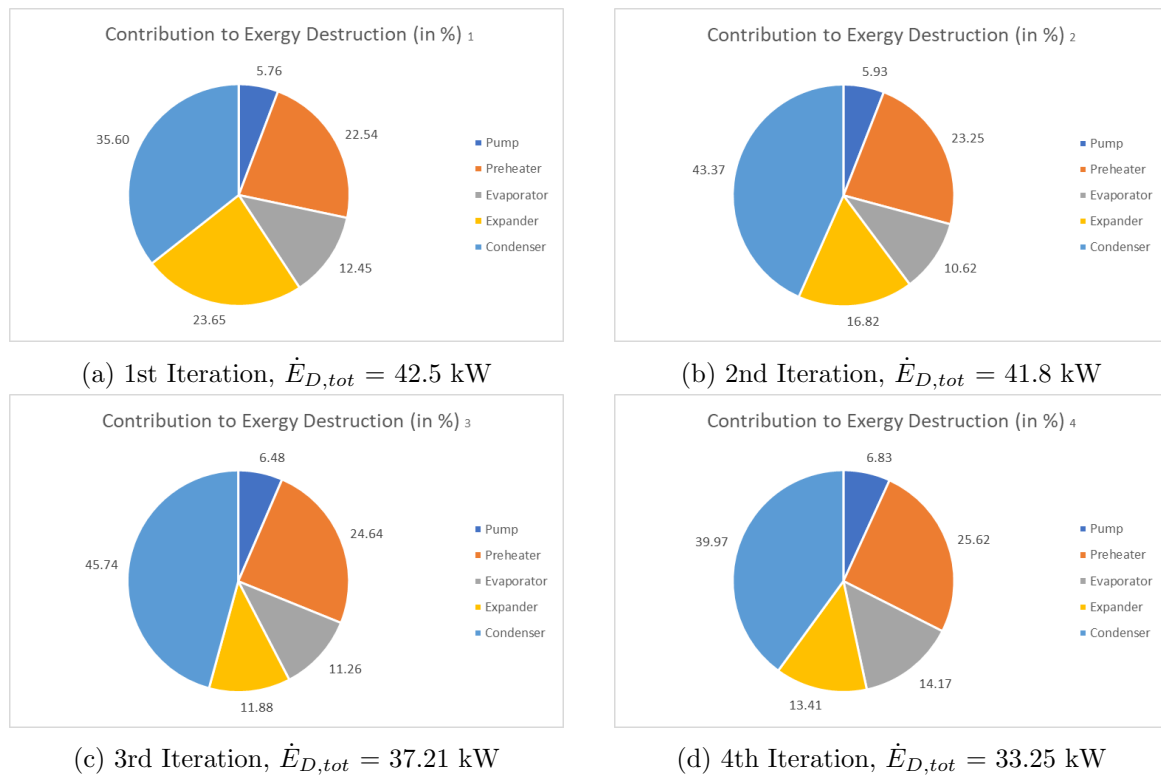


Figure 6.2.: Contribution to Exergy Destruction by system components

Results of Optimization

From the iterations it is understood that the efficiency and cost of expander and pump has a major influence in the cost rate at which the electricity is produced. This implies that for the basic ORC system it is cost effective to have undersized heat exchangers given the expander and pump is performing optimally. Since the 4th iteration has the best results, neglecting the mild increase in the objective function, the decision variables used for it is considered to produce the most cost effective system. The cost rate of electricity has reduced by 1.7 ¢/hr in the cost

effective system and this is not a very significant improvement in cost effectiveness but the exergy destruction in the system and the cost associated with it has been considerably reduced. In the final iteration it can be noted that the exergy destruction at the preheater contributes a major share in the system's total exergy destruction. Therefore, the system was simulated without the preheater and an exergy analysis was performed to see if there is a reduction of total exergy destruction in the system. Table 6.5 gives the results of the exergy analysis done on the basic ORC system without the preheater.

Table 6.5.: Exergy analysis of the basic ORC system without the preheater

Component	$\dot{E}_{D,k}$	ε_k	$Y_{D,k}$	$Y_{D,k}^*$
Pump	2.39	72.87	1.47	5.45
Evaporator	14.25	82.33	8.78	32.48
Expander	13.5	75.72	8.32	30.77
Condenser	13.73	20.17	8.46	31.30

From the exergy analysis it was found that the total exergy destruction in the system increased when the system was simulated without the preheater, thus justifying its presence. Also, the economic analysis revealed that the effect of removing the preheater on the TRR for the system was around \$300 and the cost rates apportioned to the system components didn't have a significant difference compared to the system with preheater.

6.2. Cogeneration system with R410A

The decision variables in the cogeneration chosen to change the design options are expander and compressor isentropic efficiency, expander inlet pressure, refrigeration temperature, pinch temperature of condenser and evaporator. The exergoeconomic evaluation of the base case cogeneration system in Section 5.2 helps in making the trade-off between cost and efficiency whereas the parametric study done for the decision variables gives the knowledge of the effect of the variables on the efficiency of the system components. The objective function for the cogeneration cost is total cost per unit of exergy of products, c_{ptot} which is the sum of average cost per unit of exergy for electricity produced and cooling capacity provided.

As discussed in Section 5.2 the expander stands out to be the most important component to be optimized especially for its exergy efficiency due to low f_k value. From parametric study results (refer Appendix D) it can be seen that increasing the isentropic efficiency of the expander proportionally increases its exergy efficiency and marginally reduces the pump efficiency. Also, increasing the condenser pinch temperature marginally increases the expander efficiency. The condenser which ranks second after the expander in the $\dot{Z}_k + \dot{C}_{D,k}$ value based prioritization, has a higher \dot{Z}_k contribution and thus a higher f_k value. Therefore, the pinch temperature of the condenser has to be increased to decrease the investment cost at the expense of its exergetic efficiency. Also, increase in expander efficiency also reduces the area required by the condenser.

Increasing the expander inlet pressure had a small positive effect on the pump efficiency and reduced the area required for the condenser thereby reducing its investment cost. The $\dot{Z}_k + \dot{C}_{D,k}$ value of the refrigeration coil has almost equal contribution from both investment cost and exergy destruction. Its efficiency can be improved or cost can be reduced only by reducing the evaporation temperature. Since reducing the evaporation temperature reduces the cooling capacity, given compressor is the same, cost considerations are important before changing the evaporation temperature of the refrigeration coil.

Similar to the basic ORC system, the main evaporator and the preheater have very less contribution towards the cost of the system. Their pinch can be increased to reduce their area, requiring lesser investment. The pinch temperature is not increased more than 7 as the system is simulated for a hot water temperature of 80 °C and at higher pressures the preheater output is close to 70 °C. Considering pinch value more than 7 would reduce the heat rate available for evaporator especially if the mass flow of water has to be kept in a normal range.

Iteration 1				Iteration 2			
Variable	Suggestion	Initial Value	Final Value	Variable	Suggestion	Initial Value	Final Value
Expander efficiency [%]	Increase	75	80	Expander efficiency [%]	Increase	80	85
Expander inlet pressure [bar]	Increase	42	45	Expander inlet pressure [bar]	No change	45	45
Pinch T of Condenser [°C]	Increase	5	7	Pinch T of Condenser [°C]	No change	7	7
Pinch T of Evaporator [°C]	Increase	5	7	Pinch T of Evaporator [°C]	No change	7	7
Compressor efficiency [%]	Increase	75	80	Compressor efficiency [%]	Increase	80	85
Refrigeration temperature [°C]	No change	0	0	Refrigeration temperature [°C]	Decrease	0	-5
Iteration 3				Iteration 4			
Variable	Suggestion	Initial Value	Final Value	Variable	Suggestion	Initial Value	Final Value
Expander efficiency [%]	Increase	85	90	Expander efficiency [%]	No change	90	90
Expander inlet pressure [bar]	No change	45	45	Expander inlet pressure [bar]	No change	45	45
Pinch T of Condenser [°C]	No change	7	7	Pinch T of Condenser [°C]	No change	7	7
Pinch T of Evaporator [°C]	No change	7	7	Pinch T of Evaporator [°C]	No change	7	7
Compressor efficiency [%]	Increase	85	90	Compressor efficiency [%]	No change	90	90
Refrigeration temperature [°C]	Decrease	-5	-10	Refrigeration temperature [°C]	Decrease	-10	-15

Figure 6.3.: Changes in decision variables at each iteration

First Iteration

Table 6.6 gives the total unit cost of products, total revenue required per year, exergy destruction and the monetary loss associated with it for the cogeneration system. From results it is clear that we are heading in the wrong direction as the objective function, $c_{p_{tot}}$, increased by a small margin instead of decreasing.

Table 6.6.: Results of 1st iteration

Output	Base Case	1st Iteration
$c_{p_{elec}}$ [\$/kWh]	0.016	0.0157
$c_{p_{cooling}}$ [\$/kWh]	0.1486	0.1533
$c_{p_{tot}}$ [\$/kWh]	0.1646	0.169
TRR [\$/year]	5203.38	5037.43
$\dot{E}_{D,tot}$ [KW]	28.45	28.29
$\dot{C}_{D,tot}$ [\$/hr]	0.40	0.37

In this iteration design changes were made to the power cycle similar to the basic ORC system in which it resulted in cost reduction. The expander efficiency was improved and other design changes were aimed at reducing the condenser cost and improving the pump efficiency. This decision resulted in electricity cost reduction, although marginally, but the refrigeration cycle was burdened more with the cost where only the compressor efficiency was increased and the remaining variables were kept unchanged. This resulted in the total product cost being more than the base case value. Thus, new design changes are considered in the next iteration where the evaporation temperature is varied to increase the efficiency of refrigeration process.

Second Iteration

In this iteration the pinch temperature variables and turbine inlet pressure were kept unchanged as they had a negative impact on the exergetic efficiency of the refrigeration coil. In order to improve the power cycle only the expander isentropic efficiency is considered as it dominates the effect of other variables as seen in optimization of basic ORC system. On the refrigeration side, compressor efficiency was increased and the evaporation temperature was decreased.

Table 6.7.: Results of 2nd iteration

Output	Base Case	2nd Iteration
$c_{p_{elec}}$ [\$/kWh]	0.016	0.0154
$c_{p_{cooling}}$ [\$/kWh]	0.1486	0.1312
$c_{p_{tot}}$ [\$/kWh]	0.1646	0.1467
TRR [\$/year]	5203.38	4986.88
$\dot{E}_{D,tot}$ [KW]	28.45	25.03
$\dot{C}_{D,tot}$ [\$/hr]	0.40	0.32

From Table 6.7 it is evident that there is a significant reduction in the total product cost. Thus, the decision variables were changed in the similar manner in the next iteration to see their effect on the total unit cost of products.

Third Iteration

In this iteration the isentropic efficiency was further increased for the expander and compressor while the refrigeration temperature was further decreased.

Table 6.8.: Results of 3rd iteration

Output	Base Case	3rd Iteration
$c_{p_{elec}}$ [\$/kWh]	0.016	0.0152
$c_{p_{cooling}}$ [\$/kWh]	0.1486	0.123
$c_{p_{tot}}$ [\$/kWh]	0.1646	0.138
TRR [\$/year]	5203.38	4941.35
$\dot{E}_{D,tot}$ [KW]	28.45	22.03
$\dot{C}_{D,tot}$ [\$/hr]	0.40	0.28

From Table 6.8 it can be seen that the unit cost of the products further reduced. Since 90% is considered as the maximum for increasing the isentropic efficiency, in the next iteration the evaporation temperature was reduced further to see its effect on the system cost.

Fourth Iteration

Table 6.9.: Results of 4th iteration

Output	Base Case	4th Iteration
$c_{p_{elec}}$ [\$/kWh]	0.016	0.0152
$c_{p_{cooling}}$ [\$/kWh]	0.1486	0.121
$c_{p_{tot}}$ [\$/kWh]	0.1646	0.137
TRR [\$/year]	5203.38	4927.14
$\dot{E}_{D,tot}$ [KW]	28.45	22.03
$\dot{C}_{D,tot}$ [\$/hr]	0.40	0.28

From Table 6.9 it is evident that there was no significant reduction in the cost when only the evaporation temperature was reduced. The optimization is stopped with this iteration.

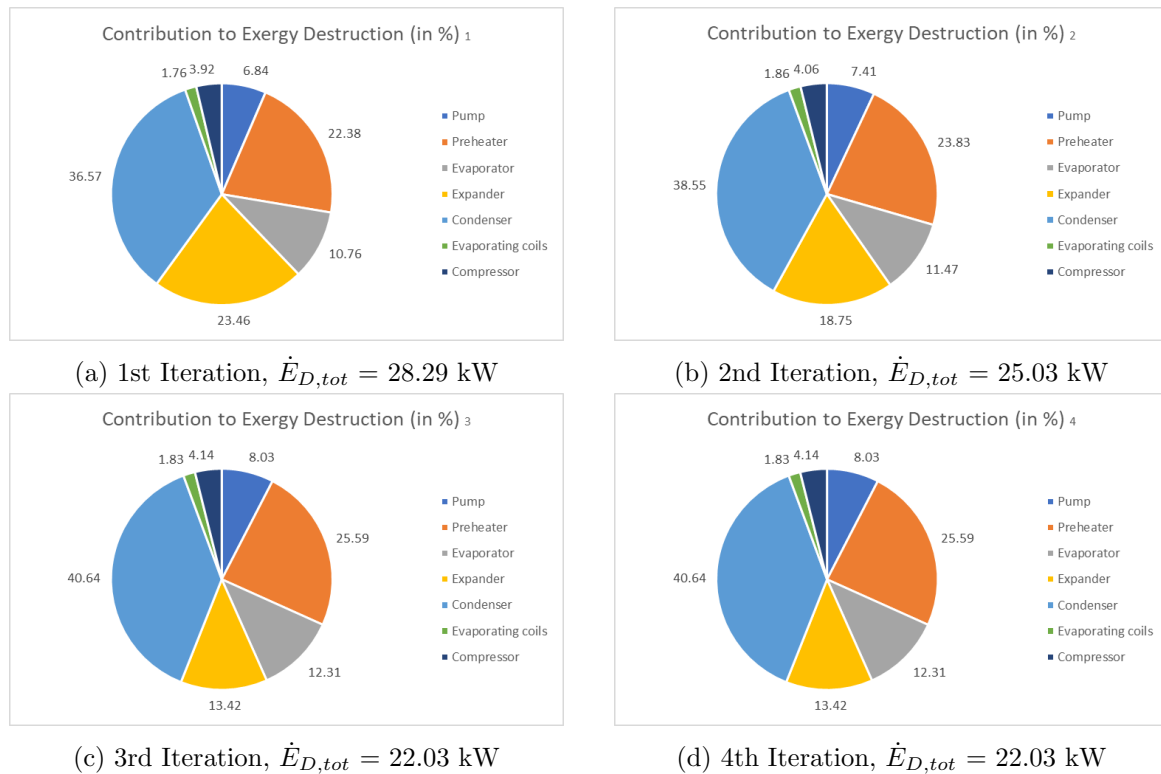


Figure 6.4.: Contribution to Exergy Destruction by system components

Results of Optimization

The decision variables used in Iteration 3 are considered as the optimum values for cost effectiveness as it has the lower product cost almost as same as Iteration 4 but has a higher cooling capacity due to higher evaporation temperatures. Similar to the basic ORC system the exergy destruction at the preheater in the final iteration considered contributes a major share to the total exergy destruction in the system.

In iteration 1 changing the parameters of the power cycle alone didn't improve the cost effectiveness of the system and similarly changing the refrigeration temperature in the 4th iteration alone didn't produce any significant reduction in the cost. Thus, from iterations 1 and 4 it is understood that the total unit cost of products from the system reduces only when the parameters of both the cycles are optimized even though the refrigeration cycle is relatively smaller compared to the power cycle.

The optimized system based on the parameters of iteration 3 has a total product cost that is 2.6  less than the base case system per kWh of exergy. The exergy destruction at the system and the cost associated with it has also been considerably reduced. From Figure 6.4 it is evident that the exergy destruction at the condenser and preheater dominates the exergy destruction at the expander after optimization, but due to their lower unit product/fuel cost, the total cost rate of exergy destruction is lower. The reduction in exergy destruction and its cost rate witnessed is mainly due to the increased exergetic efficiency of the expander which had the highest cost rate of exergy destruction. It is to be noted that the significant increase in exergetic efficiency was possible only when the efficiency of the expander was varied up to 90%, a technological claim which has not been validated yet.

7. Experimental Results and Discussion

The HSE18R prototype, which has a refrigeration cycle integrated to the basic ORC cycle, was first tested at a technology expo organized at Codale Inc, Salt Lake City; a preferred component supplier of HSE. To run the prototype standalone in any place a hot water supply unit fuelled by bottled gas and a cooling circuit with a small cooling tower to provide the cold-water stream were attached to the machine. The entire setup can be transported on a trailer behind a truck. Since, the conditions at the expo were not favourable for data collection, both testing and data collection was separately performed on 20th May 2017 at the registered location of HSE under the supervision of Dr Kas Hemmes.

The test run included a demonstration of the cooling cycle integrated into the system but no precise (efficiency) measurements could be made at this point due to lack of standard testing conditions. During the test run both electric and thermodynamic data were collected to analyze the overall performance of the system, including the inlet and outlet conditions of certain components, to assess the performance of the individual processes. In particular, the inlet and outlet conditions of working fluid for scroll expander, refrigeration compressor and the hot and cold streams were measured. The data was collected in the form of screenshots of the PLC program due to lack of data logging setup at the time of testing. The data from the screenshots were then translated into data entries in excel for further analysis.

It is to be noted that the net efficiency calculation includes only the auxiliary power consumed by the compressor and the refrigerant pump in the unit but not the pumping power needed in the hot and cold water supply system. It was assumed that in practical applications these hot and cold water streams are readily available. In any way, this will largely depend on the local circumstances of an application and are not a unique characterization of the prototype under consideration.

7.1. Performance of HSE18R prototype

System Efficiency Vs Power Output

By varying the electric load applied to the system, the output power can be controlled. The load applied consisted of a water cooled (water heating elements were present in the return hot water flow) resistor bank and electric lights connected to the output that can be switched on and off according to the load setting required. To analyze the performance at various loading rates, at each of five different load settings four readings were taken. The readings at each load setting were averaged to reduce the measurement error. The gross efficiency is calculated according to Equation 3.1 and the net efficiency is calculated based on Equation 3.2.

From Figure 7.1 it is evident that the system efficiency depends on load conditions and that for low load conditions i.e. low electric power output, the gross efficiency is more or less proportional with output power up to about 50% of the maximum power; 10 kW this case. At higher load and higher output power the gross efficiency levels off to a maximum of about 9.4% in this case. The system performs better at high and full load conditions, but part load conditions can be

maintained up to about 50% of the maximum power without sacrificing too much in efficiency (still 8% at 11 kW see Figure 7.1).

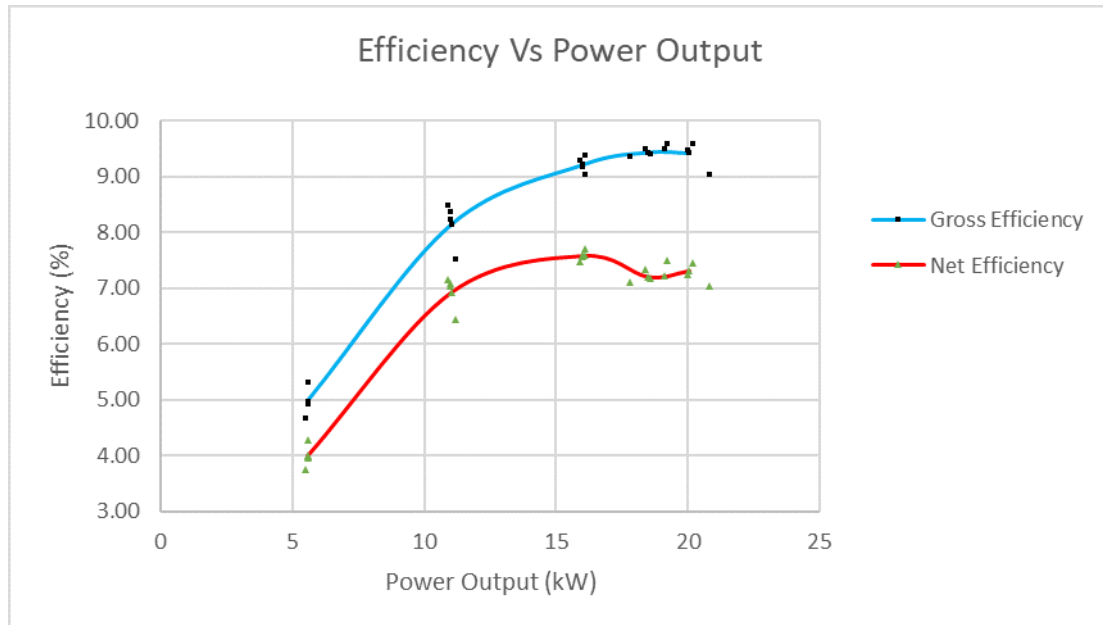


Figure 7.1.: Gross and Net thermal efficiency Vs Power Output

In the pilot set-up, the rotation speed of the hydraulic pump can be adjusted either manually or automatic using the software. The automatic control setup using constant voltage output as the control parameter. Therefore, in most of the experiments the speed was adjusted manually based on the experience of the operator in order to achieve optimum performance. The auxiliary power needed for the hydraulic pump increases with load, which is effectively reflected by the net efficiency curve for higher loads. (See red curve in Figure 7.1).

Maximum net efficiency of 7.7% is obtained at around 16 kW electric power output. Going to full power (20 kW) decreased the net efficiency by about point 0.5% to a little more than 7%. This drop in net efficiency can be attributed to the limitations of the generator connected to the expander. The generator used in the test set up had 4 poles which limited the generator speed to 1800 RPM at a frequency of 60HZ (refer Equation 7.1). Thus, a 2-pole generator with rotational speed up to 3600 rpm obtains more efficiency at higher loads because the optimum performance of the design scroll expander ranges between 2900 RPM at 50HZ and 3600RPM at 60HZ. From the work of Yanagisawa et al. (2001) it is understood that at lower RPM the leakage losses dominate and the performance of the expander decreases.

$$N = \frac{120 * f}{P} \quad (7.1)$$

where,

f = frequency,

P = no of poles,

N = rotational speed.

System efficiency as a function of temperature of the hot stream:

To look at the influence of varying source temperature and heat input rate on the system performance, the temperature of the hot water inlet was continuously allowed to drop and the corresponding measurements were taken. When the gas heaters were switched off, the

recirculated hot water stream is not reheated and the heat is continuously extracted from the flow by the setup, lowering its temperature. The load applied to the system was also adjusted according to the heat available from the hot source.

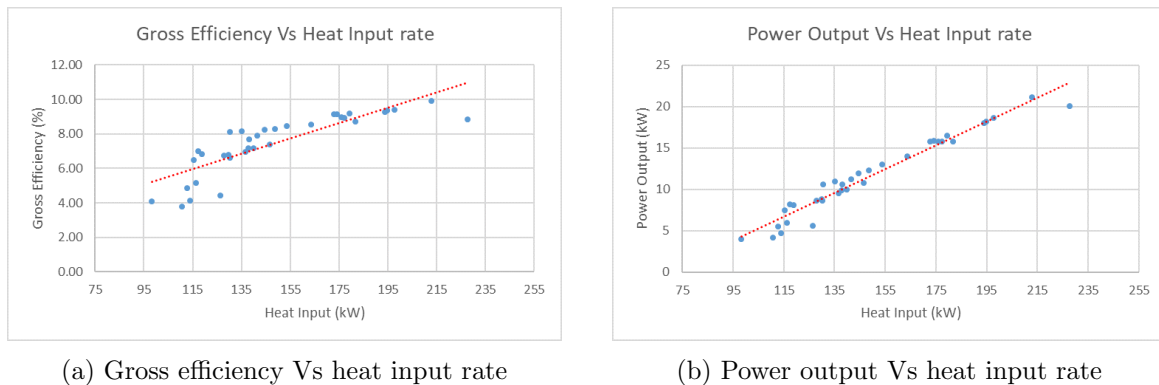


Figure 7.2.: Effect of heat input rate on the system performance

Figure 7.2 gives the power output and efficiency of the system with respect to increasing heat input rate. The drop in efficiency and output at lower heat rates could be due to losses caused by un-adapted pressures at the expander (Kane et al., 2003).

7.2. Performance of the Scroll Expander:

In order to understand the performance of the scroll expander pressure and temperature data at the inlet and outlet of the expander was collected. This data is enough to know the enthalpy and entropy of the fluid at the inlet and outlet state points of the expander. A simple MATLAB code was developed to use this data and the NIST Refprop database to calculate the isentropic efficiency of the expander at each data point. The MATLAB code can be found in Appendix E.

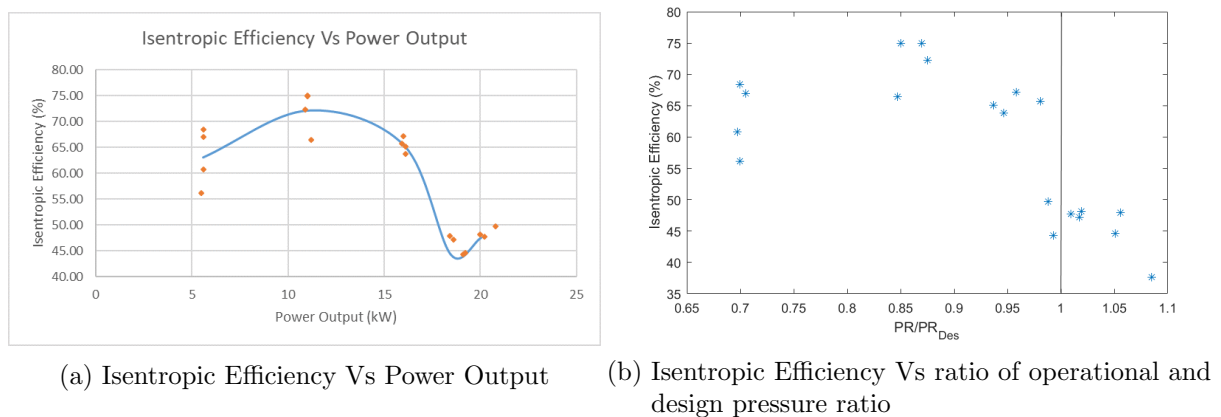


Figure 7.3.: Performance of scroll expander under varying load

From Figure 7.3a, it can be noted that the maximum isentropic efficiency achieved was 75.01% under part load conditions. When the system was continuously ramped up for higher power output, the isentropic efficiency started reducing instead of having an increasing trend towards the design pressure ratio, as one would expect given the pressure ratio increases with the power output. Although the exact reason for this reducing trend (see Figure 7.3b) could not be pinpointed, the company speculates that the issue could be with the oil separator, malfunctioning at the time of testing, which blocked the flow from exhaust of the expander and condensed the

refrigerant as seen through the sight glasses due to pressure drop across the separator. Due to lack of information to understand why this is happening and its effect on the isentropic efficiency, a reason could not be stated with certainty for the drop in isentropic efficiency observed in our experiment.

From Figure 7.3b it is also clear that the expander performs the worst when the ratio of the operational pressure ratio and the design value is more than unity. This can be attributed to the over expansion that affects the expander performance due to losses caused by back flow and re-compression. From literature it is also known that over expansion affects the expander more than under expansion (refer to Section 2.1.1) and hence the poor performance of the expander.

Based on the data collected while studying the influence of varying heat source temperature and input rate on system performance, the isentropic efficiency of the expander at varying scroll inlet temperatures was calculated. A third order polynomial fit was used (refer Figure 7.4) to obtain the trend of varying isentropic efficiency which is constantly fluctuating due to gliding pressures caused by continuously varying heat rate.

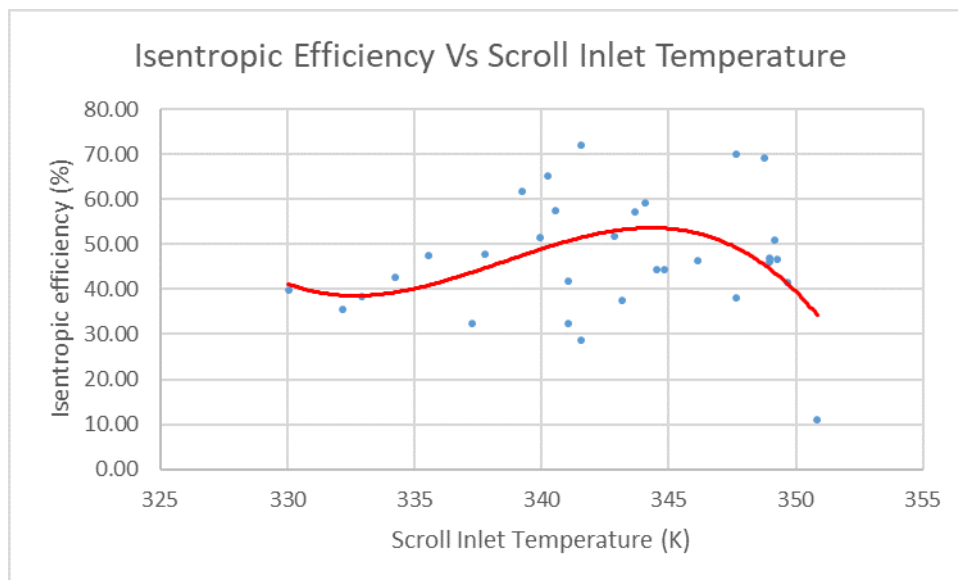


Figure 7.4.: Isentropic Efficiency of Expander Vs Scroll Inlet Temperature

From Figure 7.4, it is evident that the isentropic efficiency increases with inlet temperature of the expander until a temperature of 341.55 K and then it begins to drop. This trend in the isentropic efficiency is in accordance with the study of Garg et al. (2016) where they observed a drop in isentropic efficiency and increase in volume expansion ratio with increasing scroll inlet temperatures for all working fluids tested. The drop in isentropic efficiency could be attributed to the increase in specific volume of the super heated working fluid, at the inlet of the expander, when the temperature increases. This results in mismatch of the built in volume ratio of the expander and the volume expansion ratio of the fluid. Thus, under expansion losses increase leading to drop in isentropic efficiency.

7.3. Performance of the Refrigeration Cycle:

At the end of experiments with the power cycle, the cooling circuit that was added to the pilot setup was also tested. It is emphasized here again that the test was performed only to demonstrate the possibility of cooling. No dedicated preparations were made to measure its

performance or standardize the test conditions for determining an accurate COP of the refrigeration cycle. Therefore the measurements performed and reported here are very preliminary and lacks the level of accuracy expected from a standard test run. Based on the few data points collected an attempt was made to reconstruct the performance of the cooling circuits integrated with the HSE power producing unit.

The scroll compressor from Danfoss (HRH038U2LP6) used in the refrigeration circuit consumes on an average 1.7 to 2.0 kW of electricity produced by the system. This parasitic power would bring down the net efficiency of the system. The net efficiency would therefore drop when the refrigeration circuit starts producing cold. This shows a window of opportunity in which the system would perform optimally based on need for electricity and/or cold at high efficiency. The system could produce cold however at the expense of producing less power than the rated value. Thus, an optimized control system is needed to continuously run the cogeneration system at the best synergy possible between the two cycles for specified operating conditions adapted to specific, probably time varying, demand for cold and electricity.

The refrigeration cycle and the power cycle have two components in common namely the condenser and the pump. The condenser condenses the compressed gas coming from the refrigeration compressor along with the two-phase exhaust coming from the scroll expander of the power cycle. The refrigerant hydraulic pump in the power cycle provides high pressure liquid to both the power cycle and the refrigerant cycle. The refrigerant mass flow required for refrigeration does not significantly affect the system as it is very low in comparison to the overall mass flow requirements. Therefore, the extra work done by the main refrigerant pump is small enough to be ignored. But this might not be the case when the prototype is scaled up to provide higher refrigeration capacity relative to the power produced. It is to be noted here that as the pressure increases from the inlet to the outlet of the refrigerant pump there was no measurable difference in refrigerant temperature from the suction side of the pump to the high-pressure side, implying that the pumping process is very efficient.

The performance of the refrigeration circuit can be determined by its Coefficient of Performance (COP). The COP of a refrigeration cycle can be defined as the ratio of the refrigeration load to the work done by the compressor. Due to lack of sensors across all refrigeration components at the time of testing, a few assumptions were made, to be able to determine the performance of the refrigeration cycle, like that the refrigerant at the pump outlet is a saturated liquid and that the thermal expansion valve (metering valve) is perfectly isenthalpic.

These assumptions allow us to use the high-pressure value from the main cycle and saturation conditions to calculate the enthalpy of the refrigerant liquid after the pump. A small amount of this liquid is taken and then passed through the thermal expansion valve for the refrigeration circuit. Since the thermal expansion valve is assumed to be isenthalpic, the liquid enthalpy value can be used as the enthalpy of the inlet to the evaporator. Thus, the evaporator inlet enthalpy ($h_{evap,in}$) is found as 291.08 kJ/kg at one of the few data points collected for the refrigeration cycle.

The refrigerant load can be found using the following equation,

$$Q_{ref} = m_{ref} * (h_{evap,in} - h_{evap,out}) \quad (7.2)$$

The mass flow rate of the refrigerant cycle can be found from the scroll compressor parameters using the following equation,

$$m_{ref} = \frac{(V_s * N)}{suc} \quad (7.3)$$

where,

V_s = Swept volume of the compressor ($36.54cm^3$ from data sheet)

N = Rotational speed of the compressor (3500 rpm 60 Hz from data sheet)

v_{suc} = Specific volume of refrigerant at the inlet of the compressor (m^3/kg)

The Carnot COP of the cycle can be calculated using the following equation,

$$COP_{Carnot} = \frac{T_{cold}}{(T_{hot} - T_{cold})} \quad (7.4)$$

The actual COP of a refrigeration cycle is calculated as,

$$COP_{actual} = \frac{m_{ref} * (h_{evap,in} - h_{evap,out})}{Q_c} \quad (7.5)$$

COP of a refrigeration circuit is very sensitive to the refrigeration conditions achieved with the cycle. COP of refrigeration directly depends on the evaporation and condensation temperatures of the refrigeration cycle as shown by the expression for COP_{Carnot} . Thus, the COP decreases with decrease in evaporation temperature (T_{cold}). For $T_{cold} = 251.65K$ and $T_{hot} = 304.65K$, the theoretical coefficient of performance (COP_{Carnot}) is calculated as 4.75.

Using NIST Refprop database and compressor data sheet the mass flow rate was calculated as 0.0223 kg/s and the actual COP of the refrigeration cycle as 1.4. Although the COP found is nowhere accurate due to the assumptions considered and absence of proper test setup. The COP thus obtained is much lower than the COP given by the compressor data sheet for similar process parameters. The main reason for this is the difference in test conditions. While Danfoss followed AHRI standards for compressors for all its tests required to create the data sheet, the testing conditions for the refrigeration system in HSE18R didn't follow any standards and had a continuous influx of heat through imperfectly sealed or closed doors, unlike a typical refrigeration space that has no continuous influx of heat from external sources. The longer the compressor runs to cool the space due to high input heat load, it gets loaded if it cannot reduce the inside temperature and this results in lower COP.

7.4. Comparison with Modelling results

The maximum gross thermal efficiency achieved with the system during the test run in Salt Lake city was 9.60%. The cycle tempo model developed for the heat engine achieved a gross thermal efficiency of 9.44% in the base case. Thus, theoretical simulation validates the performance of the system during the test run. Although the values are relatively comparable, the smaller value of the theoretical simulation result could be because the experimental setup of the prototype was not entirely replicated in cycle tempo. The cycle tempo scheme of the heat engine simulated for comparison with experimental result is given in Appendix A.

During the previous tests performed on the system a maximum thermal efficiency of 10.67% was recorded by the company. But the parameters available from the test were not enough to simulate in cycle tempo for comparison.

8. Future of HSE systems

8.1. Transcritical CO₂ power cycle

Transcritical CO₂ cycle is seen as an attractive alternative for the ORC system with R410A as working fluid. Although both ORC and transcritical CO₂ (tCO₂) cycles are attractive technologies for conversion of low grade heat source into electricity, the ORC system is relatively simple due to lower operating pressure and lower cost. Appropriate organic working fluids can be used for ORC systems depending on the type of heat source and their temperature ranges. But the main drawback is the constant evaporation temperature that causes mismatch between the hot and cold stream fluids, called the pinch point problem, in heat exchangers which result in loss of exergy available from the heat source. In case of transcritical CO₂ cycles, the temperature glide CO₂ in the supercritical region generates a closer fit of the temperature curves thereby preventing the pinch limitation (X. Wang & Dai, 2016).

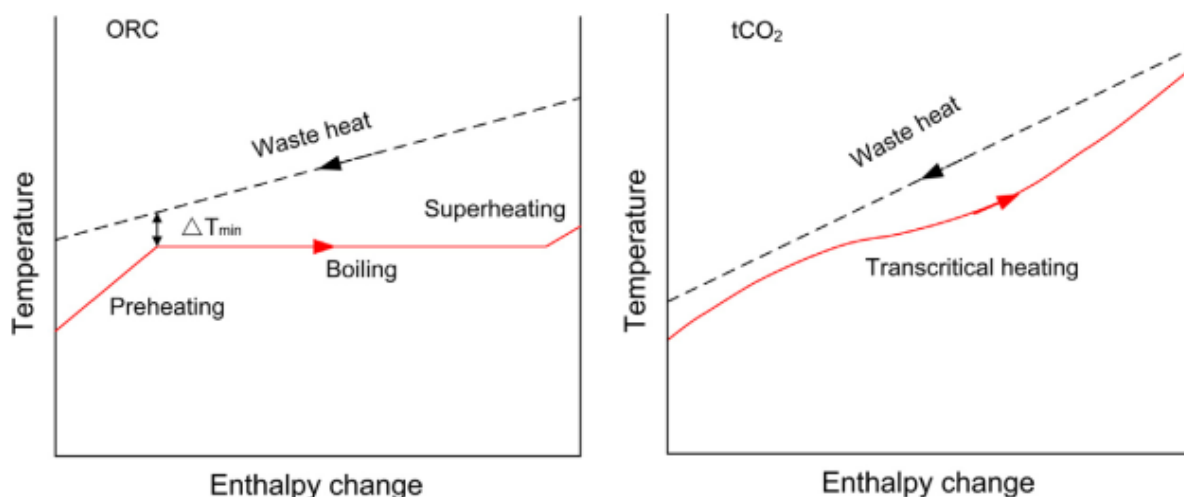


Figure 8.1.: Temperature variation in heat exchangers for ORC and tCO₂ systems (X. Wang & Dai, 2016)

Comparative study by Chen et al. (2006) between an ORC system with R123 as working fluid and transcritical CO₂ cycle shows that the tCO₂ cycle has a higher power output and is more compact than the ORC system. But the main disadvantage of the transcritical CO₂ cycle is the high absolute pressure of CO₂ under supercritical conditions which shifts the attention more towards the ORC cycles.

R744 as a working fluid has unique thermophysical properties. The supercritical region of CO₂ is readily accessible at lower temperatures due to the low critical temperature of 30.98°C. This makes it an ideal working fluid for use in transcritical power cycles at low temperature ranges. However, the anomalously high critical pressure of CO₂ can be problematic for practical applications. The safety aspects of CO₂ like non-flammability, non-toxic, low TLV (threshold limit value), inert nature and its “green” status owing to zero ozone depleting potential (ODP)

and a global warming potential (GWP) of 1 makes it an attractive alternative (Beckman, 2004). Table 8.1 gives the physical properties of R744 (Span & Wagner, 1996).

Table 8.1.: Physical Properties of R744

Properties of R744	Values
Boiling Point at 1 atm	-78.46°C
Molecular Weight	44.01 kg/kmol
Critical Temperature	30.98°C
Critical Pressure	73.77 bar
Critical Density	467.6 kg/m ³
ASHRAE Safety Category	A1
Ozone Depletion Potential (ODP)	0
Global Warming Potential (GWP)	1

In order to simulate the performance of the ORC cycle with CO₂ as working fluid for low temperature applications, the basic ORC heat engine model was modified and simulated for a power of 40kW and the corresponding results are discussed in this section. The significant difference in the CO₂ model is that it uses a regenerator to heat the working fluid before the main evaporator. Figure 8.2 shows the schematic of the model developed and the key assumptions are as follows:

1. The isentropic efficiency of the scroll expander is assumed as 75%.
2. Isentropic efficiency of the pump is taken as 90%.
3. The turbine inlet pressure is taken as 100 bar.

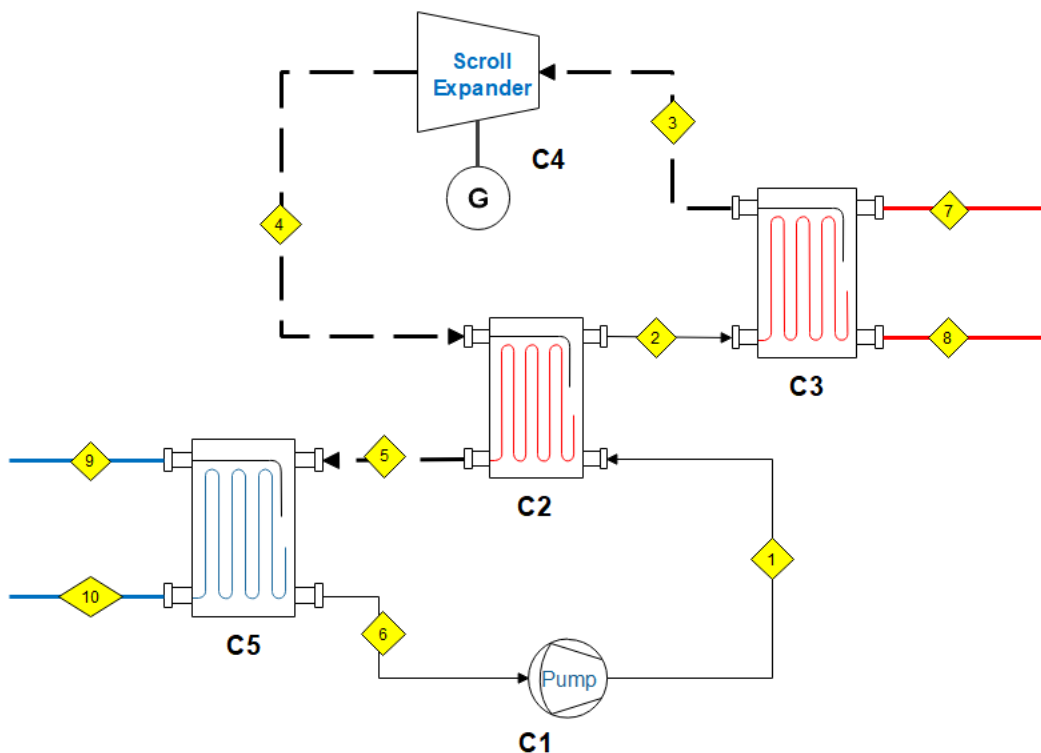


Figure 8.2.: Schematic of the Transcritical CO₂ cycle

The cycle tempo schematic and input summary is given in Appendix A. The gross thermal efficiency achieved by the simulation model was 7.98% and the net thermal efficiency was 4.04%. The back work ratio of the pump with R744 as fluid is 49.35% meaning a significant portion of the power produced is used for auxiliary consumption. Since the back work ratio is really high, it is important to operate the pump at optimal conditions for better dynamic performance of the system.

Exergy analysis was performed to analyze the exergetic efficiency of each component and the system. Table 8.2 gives the results of the exergy analysis on the transcritical CO₂ system.

Table 8.2.: Exergetic variables calculated for Transcritical CO₂ cycle

Component	\dot{E}_F [kW]	\dot{E}_P [kW]	\dot{E}_D [kW]	ε [%]	Y_D [%]	Y_{D}^* [%]
Pump	19.74	15.12	4.62	76.60	2.90	11.56
Regenerator	4.41	2.83	1.58	64.17	0.99	3.95
Evaporator	65.97	55.65	10.32	84.36	6.48	25.82
Expander	55.03	42.11	12.92	76.52	8.11	32.32
Condenser	14.16	3.63	10.53	25.64	6.61	26.34

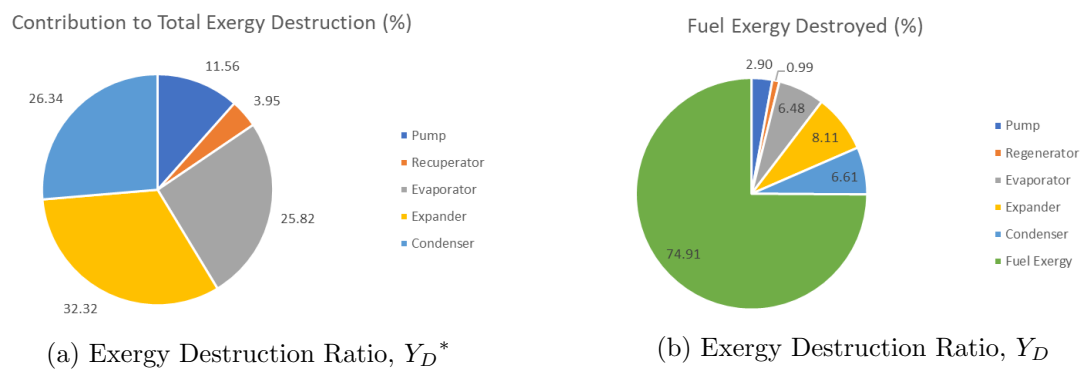


Figure 8.3.: Exergy Destruction in components of transcritical CO₂ system

From Table 8.2 and Figure 8.3 it is evident that the evaporator is the most efficient component in the system from exergy point of view but contributes to almost 26% of the total exergy destruction. The condenser also contributes almost the same fraction to the total exergy destruction. The expander with an efficiency of 76.5% contributes the largest share of 32% to the total exergy destruction. The pump in this system destroys a significant quantity of exergy during the pumping process. It contributes to 11.5% of total exergy destruction in the system. The total quantity of exergy destroyed by the transcritical CO₂ system is approximately 40 kW.

8.2. Potential Applications

HSE system for Ships

Maritime Transport is a major energy consuming sector on a global scale. The energy required on board a ship is typically produced by diesel engines that produce power for propulsion and electricity for on board consumption. Environmental and economic concerns have pushed the maritime sector to look for alternative options to improve energy efficiency of the ships. About 3.3% of the global CO₂ emissions is due to maritime transport (Salmi, Vanttola, Elg, Kuosa, & Lahdelma, 2017). The International Maritime Organization (IMO) has adopted the 'Energy

Efficiency Design Index' (EEDI) from July 2011 which sets the minimum energy efficiency requirements for ships built from 2013 to 2025. This index, though witnessed to be not very effective alone, can be used in conjunction with other international efforts to increase energy efficiency of newly built ships.

Figure 8.4 represents the typical heat balance in a MAN diesel engines operating at 100 SMCR rating. SMCR, Specified Maximum Continuous Rating, is the maximum power the diesel engine can produce while running continuously at safe conditions. It is specified on the engine nameplate and important engine parameters like specific fuel consumption, engine performance etc. are based on SMCR rating of the engine.

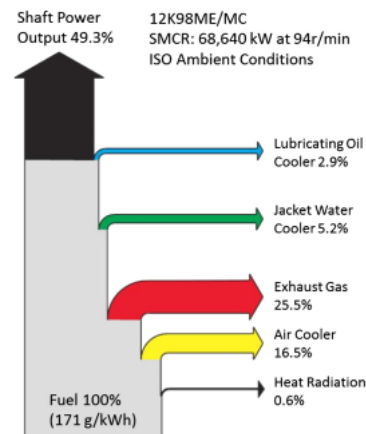


Figure 8.4.: Heat Balance for MAN Diesel engine operating at 100 SMCR rating (Singh & Pedersen, 2016)

The jacket cooling water temperatures of 80 to 90°C are fairly standard for all ships and can be utilized for power production. The thermal energy carried away by the jacket cooling water of diesel engines in a ship is either used for fresh water production from seawater for on board consumption or lost to the atmospheric environment via heat-exchangers. This thermal energy despite being a low grade heat source is large in quantity and is continuously available when the engine is running. ORC systems suitable for the temperature range makes a good candidate for WHR application in this waste heat stream of ships (Singh & Pedersen, 2016).

The properties of the working fluid is crucial for marine WHR applications as it is difficult to heat water to its critical point (Singh & Pedersen, 2016). For using HSE systems for marine applications, R407C is suggested as it has a better thermal matching than R410A for the temperature range of 70 to 90 °C. This is because R407C has a higher critical temperature and lower pressures reducing pump work and a better temperature curve fit for 90°C. Since R407C is a zeotropic mixture there will be a small temperature glide during the heat transfer processes.

The basic ORC system model developed was simulated for hot water stream at 90°C and cold water stream at 20°C. The expander inlet pressure was set at 39 bar. The expander and pump isentropic efficiency was assumed as 75% and 90% respectively. Simulating the model for 40 kW power output resulted in a gross efficiency of 9.38% and a net efficiency of 7.45%.

HSE systems having the ability to be retrofitted in the engine room of ships owing to its compact size can be installed in existing fleet as well. Considering the fact that there are more than 50,000 merchant ships in the merchant fleet trading globally, the theoretical potential of the application would be rather high. But market specific and realizable potential will depend on

various factors like market barriers, national and international regulations etc.

Although marine application for HSE systems seems attractive, a detailed market study would be needed to understand the maritime transport markets around the globe and their openness towards CO₂ emission reduction efforts according to the international norms and the current trend. The global maritime industry, though had started moving towards energy efficient marine fleet, has a long way to go to achieve the global CO₂ emission targets.

HSE system for OTEC platforms

One of the vast renewable sources of energy but the least tapped are the oceans, containing energy in the form of heat and movement that is enough to power the entire world. But the economic and technical feasibility is what is hindering the progress of developing these alternative sources of energy. Thus, there are many challenges associated with the realization of ocean technologies including the reduction of the costs per kWh and in some cases specialized engineers. Ocean energy technologies are also still at an early stage of development. Ocean Thermal Energy Conversion (OTEC) can offer a baseline power generation for remote and isolated regions around the Equator and others such as Tidal and Ocean currents are already demonstrating successful results.

In order to check the technical feasibility of using HSE system for OTEC, a cycle tempo was developed based on certain assumptions. The head loss in cold sea water pumping was taken as 5.6m and in warm sea water pumping as 2.5m (Aydin, 2013). The cold sea water was assumed to be at 5°C and the warm sea water was assumed to be at 28°C. The isentropic efficiency of the expander and pump was taken as 90%. Using R410A as working fluid the net efficiency calculated by the model was 1.40%. Thus, the HSE system can be theoretically used for OTEC application. But it is to be noted that the scroll expanders cannot be scaled up due to its complex geometry and casting challenges encountered. The largest scroll expander manufactured is 55 kW in size. This means that the scroll expanders have to be stacked in parallel to achieve practical usage in OTEC platforms which is not an economically and practically feasible solution. The HSE systems on the other hand can be readily used for testing purposes as they are compact and can be retrofitted with existing infrastructure.

9. Conclusions and Recommendations

9.1. Conclusions

The cycle tempo models developed for the basic ORC system and cogeneration system calculated a net efficiency of 6.38% and 5.43% respectively. From the exergy analysis of both the systems, it can be concluded that the exergy destruction at the expander alone is the major contribution to the thermodynamic irreversibility in the systems. Although the exergy destruction at the condenser has a major share in the total exergy destruction, it doesn't hold any significance due to the dissipative nature of the component. The exergy loss from the condenser is unavoidable and exergy loss to the environment is not within the scope of this work considering the exergy lost from the system is not used anywhere. Therefore, it is important to focus on improving the isentropic efficiency of the scroll expander and operating it at optimal pressure ratios to reduce leakage losses during expansion, a major reason for losses in the expander.

Exergoeconomic analysis of both the basic ORC system and the cogeneration system was done to evaluate the cost effectiveness of the systems based on exergy analysis. Exergoeconomic evaluation of both the systems revealed that the expander is the major contributor to the cost rate associated with both exergy destruction and the investment and operation of the system. This was deduced based on the value of total cost rate increase by the component, $\dot{Z}_k + \dot{C}_D$, obtained for the expander which is significantly higher than other components of the system in both cases.

Applying the exergoeconomic optimization procedure to the basic ORC system revealed that the cost effectiveness of the basic ORC system could not be significantly improved but the exergy destruction and the cost of exergy destruction was considerably reduced. This was majorly due to the fact that the scroll expander was assumed to perform with 90% isentropic efficiency under optimal conditions, a technological claim which has not yet been validated. On the other hand exergoeconomic optimization of the cogeneration system reduced the total cost of products by 2.6 ¢/kWh of exergy. It is to be noted that this reduction was achieved by reducing the refrigeration temperature at the expense of cooling capacity and by assuming that the isentropic efficiency of the expander can be up to 90%.

Experimental testing of the HSE18R prototype of the cogeneration system was performed at Salt Lake City, USA with the aim to evaluate the performance of the system and the expander. The maximum gross efficiency achieved by the power cycle of the system was 9.6%. The efficiency found from the simulation of the flow sheet model developed was 9.44%. The small difference in this value could be because the theoretical simulation of the flow sheet model was not a perfect reflection of the system in practice. Although the efficiency value obtained from simulation is lower, it is relatively comparable and thus validates the performance of the system during the experiment. The presence of pressure and temperature sensors at the inlet and outlet of the expander enabled the analysis of expander based on isentropic efficiency. Using a simple Matlab code and NIST Refprop database for thermophysical properties, the isentropic efficiency of the expander at all data points were calculated. The maximum isentropic efficiency achieved by the expander was 75% at a pressure ratio of 2.55.

The cogeneration system was tested with both the power and refrigeration cycle working in

synergy. Although the refrigeration part of the system was working it was not entirely ready for experimental testing which allowed for collection of only a few data points. Due to lack of enough sensors and standard testing conditions at the time of the experiment, the coefficient of performance (COP) calculated for the refrigeration cycle was based on assumptions. The COP obtained, though not accurate, was much lower than expected due to the continuous influx of heat into the refrigeration chamber from the open door. But it was concluded that the refrigeration cycle was working well and in synergy with the power cycle of the system.

Transcritical CO₂ cycle is seen as an attractive alternative for ORC based HSE systems as CO₂ as a working fluid is more environment friendly and has a closer fit of temperature curves in heat exchangers in the supercritical region, preventing pinch limitation. The net efficiency calculated by the cycle tempo model developed for transcritical CO₂ cycle calculated a net efficiency of 4.04% with a back work ratio of almost 50% emphasizing the need to operate the refrigerant pump in optimal design conditions. The HSE systems are a good candidate for waste heat recovery from the jacket cooling water of diesel engines in ships which is a huge potential as they are relatively untapped. OTEC application for HSE is not practical due to issues in scaling up and economic reasons but theoretically a feasible application.

9.2. Limitations of Research

The main limitation of this research work is the cost considerations during exergoeconomic analysis. While developing the cost balance equations for evaporator and preheater the specific cost of fuel exergy is assumed to be zero. This is because the cost per unit of exergy in the fuel stream varies widely depending on the application and infrastructure required to get access to the fuel exergy stream. Also, the operation hours of the systems are application dependent and the cost rate of investment and operation of a component, \dot{Z}_k , is calculated based on annual operation hours and varies with the operation hours considered for the application. Therefore, the cost balance equations when solved for specific applications will result in higher cost rates for the exergy streams. The other limitation is the sensitivity of the cost rate and specific cost values of exergy streams calculated to changes in economic parameters. Thus, the assumptions made and methodology used for economic analysis has to be stated clearly.

9.3. Future Recommendations

In future research, the exergoeconomic analysis performed on the systems should be expanded to include the concepts of advanced exergoeconomic analysis and exergoenvironmental analysis. Advanced exergoenvironmental analysis gives the information to effectively improve the system using iterative exergoeconomic procedure by pinpointing the location and measure of avoidable exergy destruction in a component. On the other hand exergoenvironmental analysis gives the information required to reduce the environmental impact of an energy system.

Advanced exergoeconomic analysis splits the exergy destruction into four categories as endogenous and exogenous exergy destruction, and avoidable and unavoidable exergy destruction. The endogenous and exogenous splitting of exergy destruction in a component estimates the exergy destruction caused by the component itself or by other components of the system. This information would help in effectively improving the overall performance of the system. Splitting the exergy destruction into avoidable and unavoidable parts provides the realistic measure of the potential to reduce the exergy destruction. Unavoidable part represents the exergy destruction rate that cannot be reduced due to technological limitations of the component being considered. The avoidable part represents the remaining part of exergy destruction that can be potentially

reduced.

Exergoenvironmental analysis helps in understanding the formation of environmental impact from a component level which is essential to improve the ecological performance of an energy conversion system. It rests on the notion that exergy should be the basis for assigning environmental impact to interaction between an energy system and its surroundings and to the sources of thermodynamic inefficiencies with it. The analysis consists of three steps, exergy analysis of the system and components, life cycle assessment of the components and streams, and exergoenvironmental costing. The exergoenvironmental costing assigns the environmental impact indicators obtained from the LCA to the exergy streams and exergoenvironmental variables are calculated to perform exergoenvironmental evaluation. Based on this evaluation the system could be improved for reduced environmental impact.

Experimentally validated mathematical models should be developed for the systems especially taking into consideration the geometrical changes made in the scroll expander to improve its performance. This would help in implementing rigorous optimization procedures based on exergoeconomic evaluation that would give more accurate results. This would also require economic modelling of the systems based on interaction between exergy efficiency and cost of components.

On a component level, the degree of super-heating of the vapour entering the scroll expander should be optimized to prevent thermodynamic losses in the scroll expander which performs lower at high degree of super heating. The super-heating should be just enough to prevent the working fluid from condensing during the expansion process while not compromising on the thermodynamic performance of the expander.

The quality of the research work conducted here could be further enriched and the limitations could be partially overcome by studying the systems for specific applications which would give more information regarding cost considerations for exergoeconomic evaluation, and annual operation hours of the system.

References

- Ataei, A., Safari, F., & Choi, J.-K. (2015). Thermodynamic performance analysis of different organic rankine cycles to generate power from renewable energy resources. American Journal of Renewable and Sustainable Energy, *1*(2), 31–38.
- Aydin, H. (2013). Performance analysis of a closed-cycle ocean thermal energy conversion system with solar preheating and superheating.
- Beckman, E. J. (2004). Supercritical and near-critical co₂ in green chemical synthesis and processing. The Journal of Supercritical Fluids, *28*(2), 121–191.
- Bejan, A., Tsatsaronis, G., & Moran, M. (1996). Thermal design and optimization.
- Bracco, R., Clemente, S., Micheli, D., & Reini, M. (2013). Experimental tests and modelization of a domestic-scale orc (organic rankine cycle). Energy, *58*, 107–116.
- Chang, J.-C., Hung, T.-C., He, Y.-L., & Zhang, W. (2015). Experimental study on low-temperature organic rankine cycle utilizing scroll type expander. Applied Energy, *155*, 150–159.
- Chen, H., Goswami, D. Y., Rahman, M. M., & Stefanakos, E. K. (2011). A supercritical rankine cycle using zeotropic mixture working fluids for the conversion of low-grade heat into power. Energy, *36*(1), 549–555.
- Chen, Y., Lundqvist, P., Johansson, A., & Platell, P. (2006). A comparative study of the carbon dioxide transcritical power cycle compared with an organic rankine cycle with r123 as working fluid in waste heat recovery. Applied Thermal Engineering, *26*(17), 2142–2147.
- Clark, E., & Wagner, S. (2017). The kigali amendment to the montreal protocol: Hfc phase-down. Retrieved from http://www.unep.fr/ozonaction/information/mmcfiles/7809-e-Factsheet_Kigali_Amendment_to_MP_2017.pdf
- Cziesla, F., & Tsatsaronis, G. (2002). Iterative exergoeconomic evaluation and improvement of thermal power plants using fuzzy inference systems. Energy Conversion and Management, *43*(9), 1537–1548.
- Damodaran, A. (2017). Cost of capital by sector (us). Retrieved from http://people.stern.nyu.edu/adamodar/New_Home_Page/datafile/wacc.htm
- Delgado-Torres, A. M., & García-Rodríguez, L. (2010). Analysis and optimization of the low-temperature solar organic rankine cycle (orc). Energy Conversion and Management, *51*(12), 2846–2856.
- Desideri, A., Gusev, S., Van den Broek, M., Lemort, V., & Quoilin, S. (2016). Experimental comparison of organic fluids for low temperature orc (organic rankine cycle) systems for waste heat recovery applications. Energy, *97*, 460–469.
- Devotta, S., Waghmare, A., Sawant, N., & Domkundwar, B. (2001). Alternatives to hfc-22 for air conditioners. Applied Thermal Engineering, *21*(6), 703–715.
- El-Sayed, Y., & Gaggioli, R. (1989). A critical review of second law costing methods: background and algebraic procedures. ASME J. Energy Resour. Technol, *111*, 1–7.
- Erlach, B., Serra, L., & Valero, A. (1999). Structural theory as standard for thermoeconomics. Energy Conversion and Management, *40*(15), 1627–1649.
- Evans, R., & Von Spakovsky, M. (1993). Engineering functional analysis part ii. Journal of Energy Resources Technology, *115*(2), 93–99.
- Evans, R. B. (1980). Thermoeconomic isolation and essergy analysis. Energy, *5*(8-9), 804–821.
- Frangopoulos, C. (1991, Jan). Intelligent functional approach; a method for analysis and optimal synthesis-design-operation of complex systems. International Journal of Energy-Environment-Economics; (United States), *1*:4.
- Frangopoulos, C. A. (1983). Thermoeconomic functional analysis: a method for optimal design or improvement of complex thermal systems (Unpublished doctoral dissertation). Georgia Institute of Technology.

- Frangopoulos, C. A. (1994). Application of the thermoeconomic functional approach to the cgam problem. *Energy*, *19*(3), 323–342.
- Gaggioli, R., & El-Sayed, Y. (1989). A critical review of second law costing methods: calculus procedures. *Journal of Energy Resources Technology*, *111*(1), 8–15.
- Garg, P., Karthik, G., Kumar, P., & Kumar, P. (2016, oct). Development of a generic tool to design scroll expanders for ORC applications. *Applied Thermal Engineering*, *109*, 878–888. doi: 10.1016/j.applthermaleng.2016.06.047
- Guo-Yan, Z., En, W., & Shan-Tung, T. (2008). Techno-economic study on compact heat exchangers. *International Journal of Energy Research*, *32*(12), 1119–1127.
- Harari, Y. N. (2014). *Sapiens: A brief history of humankind*. Random House.
- Iqbal, M. A., Ahmadi, M., Melhem, F., Rana, S., Akbarzadeh, A., & Date, A. (2017). Power generation from low grade heat using trilateral flash cycle. *Energy Procedia*, *110*, 492–497.
- IRENA. (2017). *Synergies between renewable energy and energy efficiency, a working paper based on remap*. Retrieved from <http://www.irena.org/remap/>
- Johnson, K. (2016, December 8). *Heat engines, systems for providing pressurized refrigerant, and related methods*. Google Patents. Retrieved from <https://google.com/patents/WO2016196144A1?c1=ru> (WO Patent App. PCT/US2016/034,178)
- Johnson, K., & Newman, C. (2015, December 24). *Organic rankine cycle decompression heat engine*. Google Patents. Retrieved from <https://www.google.com/patents/US20150369086> (US Patent App. 14/765,735)
- Kane, M., Larrain, D., Favrat, D., & Allani, Y. (2003). Small hybrid solar power system. *Energy*, *28*(14), 1427–1443.
- Karbassi, A., Abduli, M., & Abdollahzadeh, E. M. (2007). Sustainability of energy production and use in iran. *Energy Policy*, *35*(10), 5171–5180.
- Kim, S.-M., Oh, S.-D., Kwon, Y.-H., & Kwak, H.-Y. (1998). Exergoeconomic analysis of thermal systems. *Energy*, *23*(5), 393–406.
- Knoop, K., & Lechtenböhmer, S. (2017). The potential for energy efficiency in the eu member states—a comparison of studies. *Renewable and Sustainable Energy Reviews*, *68*, 1097–1105.
- Kwak, H.-Y., Byun, G.-T., Kwon, Y.-H., & Yang, H. (2004). Cost structure of cgam cogeneration system. *International journal of energy research*, *28*(13), 1145–1158.
- Kwak, H.-Y., Kim, D.-J., & Jeon, J.-S. (2003). Exergetic and thermoeconomic analyses of power plants. *Energy*, *28*(4), 343–360.
- Lazzaretto, A., & Tsatsaronis, G. (1999). On the calculation of efficiencies and costs in thermal systems. In *Proceedings of the asme advanced energy systems division* (Vol. 39, pp. 421–430).
- Lazzaretto, A., & Tsatsaronis, G. (2001). Comparison between speco and functional exergoeconomic approaches. In *Proceedings of the asme international mechanical engineering congress and exposition-imece-23656, november* (pp. 11–16).
- Lazzaretto, A., & Tsatsaronis, G. (2006). Speco: a systematic and general methodology for calculating efficiencies and costs in thermal systems. *Energy*, *31*(8), 1257–1289.
- Lei, B., Wang, J.-F., Wu, Y.-T., Ma, C.-F., Wang, W., Zhang, L., & Li, J.-Y. (2016). Experimental study and theoretical analysis of a roto-jet pump in small scale organic rankine cycles. *Energy Conversion and Management*, *111*, 198–204.
- Lemmon, E. W. (2003). Pseudo-pure fluid equations of state for the refrigerant blends r-410a, r-404a, r-507a, and r-407c. *International Journal of Thermophysics*, *24*(4), 991–1006.
- Lemort, V., Declaye, S., & Quoilin, S. (2012). Experimental characterization of a hermetic scroll expander for use in a micro-scale rankine cycle. *Proceedings of the Institution of Mechanical Engineers, Part A: Journal of Power and Energy*, *226*(1), 126–136.
- Lemort, V., Quoilin, S., Cuevas, C., & Lebrun, J. (2009). Testing and modeling a scroll expander integrated into an organic rankine cycle. *Applied Thermal Engineering*, *29*(14),

3094–3102.

- Leontaritis, A.-D., Pallis, P., Karellas, S., Papastergiou, A., Antoniou, N., Vourliotis, P., ... Dimopoulos, G. (2015). Experimental study on a low temperature orc unit for onboard waste heat recovery from marine diesel engines. *3rd Int. Semin. ORC Power Syst., Brussels*.
- Lozano, M., & Valero, A. (1993). Theory of the exergetic cost. *Energy*, *18*(9), 939–960.
- Lu, Y., Roskilly, A. P., Tang, K., Wang, Y., Jiang, L., Yuan, Y., & Wang, L. (2017, mar). Investigation and performance study of a dual-source chemisorption power generation cycle using scroll expander. *Applied Energy*. doi: 10.1016/j.apenergy.2017.02.068
- Ma, Z., Bao, H., & Roskilly, A. P. (2017, jan). Dynamic modelling and experimental validation of scroll expander for small scale power generation system. *Applied Energy*, *186*, 262–281. doi: 10.1016/j.apenergy.2016.08.025
- Mago, P., Srinivasan, K., Chamra, L., & Somayaji, C. (2008). An examination of exergy destruction in organic rankine cycles. *International Journal of Energy Research*, *32*(10), 926–938.
- Mathias, J. A., Johnston, J. R., Cao, J., Priedeman, D. K., & Christensen, R. N. (2009). Experimental testing of gerotor and scroll expanders used in, and energetic and exergetic modeling of, an organic rankine cycle. *Journal of Energy Resources Technology*, *131*(1), 012201.
- Meng, F., Zhang, H., Yang, F., Hou, X., Lei, B., Zhang, L., ... Shi, Z. (2017). Study of efficiency of a multistage centrifugal pump used in engine waste heat recovery application. *Applied Thermal Engineering*, *110*, 779–786.
- Oralli, E., Tarique, M. A., Zamfirescu, C., & Dincer, I. (2011, jun). A study on scroll compressor conversion into expander for rankine cycles. *International Journal of Low-Carbon Technologies*, *6*(3), 200–206. doi: 10.1093/ijlct/ctr008
- Parker, T., & Kiessling, A. (2016). Low-grade heat recycling for system synergies between waste heat and food production, a case study at the european spallation source. *Energy Science & Engineering*, *4*(2), 153–165.
- Peris, B., Navarro-Esbrí, J., Molés, F., González, M., & Mota-Babiloni, A. (2015). Experimental characterization of an orc (organic rankine cycle) for power and chp (combined heat and power) applications from low grade heat sources. *Energy*, *82*, 269–276.
- Quoilin, S., Lemort, V., & Lebrun, J. (2010). Experimental study and modeling of an organic rankine cycle using scroll expander. *Applied energy*, *87*(4), 1260–1268.
- Ramaraj, S., Yang, B., Braun, J. E., Groll, E. A., & Horton, W. T. (2014). Experimental analysis of oil flooded r410a scroll compressor. *International Journal of Refrigeration*, *46*, 185–195.
- Sakhrieh, A., Shreim, W., Fakhrudeen, H., Hasan, H., & Al-Salaymeh, A. (2016). Combined solar-geothermal power generation using organic rankine cycle. *JJMIE*, *10*(1).
- Salmi, W., Vanttola, J., Elg, M., Kuosa, M., & Lahdelma, R. (2017). Using waste heat of ship as energy source for an absorption refrigeration system. *Applied Thermal Engineering*, *115*, 501–516.
- Singh, D. V., & Pedersen, E. (2016). A review of waste heat recovery technologies for maritime applications. *Energy Conversion and Management*, *111*, 315–328.
- Song, P., Wei, M., Shi, L., Danish, S. N., & Ma, C. (2015). A review of scroll expanders for organic rankine cycle systems. *Applied Thermal Engineering*, *75*, 54–64.
- Span, R., & Wagner, W. (1996). A new equation of state for carbon dioxide covering the fluid region from the triple-point temperature to 1100 k at pressures up to 800 mpa. *Journal of physical and chemical reference data*, *25*(6), 1509–1596.
- Subbiah, M. (2012). The characteristics of brazed plate heat exchangers with different chevron angles. In *Heat exchangers - basics design applications*.
- Tchanche, B. F., Papadakis, G., Lambrinos, G., & Frangoudakis, A. (2009). Fluid selection for a low-temperature solar organic rankine cycle. *Applied Thermal Engineering*, *29*(11),

2468–2476.

- Tsatsaronis, G. (1996). Exergoeconomics: Is it only a new name? Chemical engineering & technology, *19*(2), 163–169.
- Tsatsaronis, G. (1999). Strengths and limitations of exergy analysis. In Thermodynamic optimization of complex energy systems (pp. 93–100). Springer.
- Tsatsaronis, G., & Czesla, F. (2001). Thermoeconomics. Encyclopedia of Physical Science and Technology.
- Tsatsaronis, G., & Czesla, F. (2004). Exergy and thermodynamic analysis.
- Tsatsaronis, G., Lin, L., & Pisa, J. (1993). Exergy costing in exergoeconomics. Journal of Energy Resources Technology, *115*(1), 9–16.
- Tsatsaronis, G., & Moran, M. J. (1997). Exergy-aided cost minimization. Energy Conversion and Management, *38*(15), 1535–1542.
- Tsatsaronis, G., & Park, M.-H. (2002). On avoidable and unavoidable exergy destructions and investment costs in thermal systems. Energy Conversion and Management, *43*(9), 1259–1270.
- UNEP. (2017). Status of ratification of the agreements on the protection of the stratospheric ozone layer. Retrieved from http://ozone.unep.org/sites/ozone/modules/unep/ozone_treaties/inc/datasheet.php
- USBLS. (2017). United states inflation rate. Retrieved from <https://tradingeconomics.com/united-states/inflation-cpi>
- Von Spakovsky, M., & Evans, R. (1993). Engineering functional analysis part i. Journal of Energy Resources Technology, *115*(2), 86–92.
- Wang, J., Zhao, L., & Wang, X. (2012). An experimental study on the recuperative low temperature solar rankine cycle using r245fa. Applied energy, *94*, 34–40.
- Wang, X., & Dai, Y. (2016). Exergoeconomic analysis of utilizing the transcritical co₂ cycle and the orc for a recompression supercritical co₂ cycle waste heat recovery: a comparative study. Applied Energy, *170*, 193–207.
- Xu, W., Zhang, J., Zhao, L., Deng, S., & Zhang, Y. (2017). Novel experimental research on the compression process in organic rankine cycle (orc). Energy Conversion and Management, *137*, 1–11.
- Yanagisawa, T., Fukuta, M., Ogi, Y., Hikichi, T., et al. (2001). Performance of an oil-free scroll-type air expander. In Proc. of the imeche conf. trans. on compressors and their systems (pp. 167–174).
- Zanelli, R., & Favrat, D. (1994). Experimental investigation of a hermetic scroll expander-generator. In 12th international compressor engineering conference (p. 459464).
- Zhang, J., Zhao, L., Wen, J., & Deng, S. (2016). An overview of 200 kw solar power plant based on organic rankine cycle. Energy Procedia, *88*, 356–362.

9.4. List of Acronyms

AHRI	Air-conditioning Heating and Refrigeration Institute
CC	Carrying Charges
CELF	Constant Escalation Levelization Factor
CHP	Combined Heat and Power
COP	Coefficient Of Performance
CRF	Capital Recovery Factor
EEA	Exergo-Economic Analysis
EEDI	Energy Efficient Design Index
EFA	Engineering Functional Analysis
GWP	Global Warming Potential
HEDC	Heat Engine Decompression Cycle
HSE	Heat Source Energy
HVAC	Heating Ventilation and Air Conditioning
IMO	International Maritime Organization
IRENA	International Renewable Energy Agency
LCA	Life Cycle Assessment
LIFO	Last In First Out
LMTD	Log Mean Temperature Difference
MOPSA	Modified Productive Structure Analysis
NIST	National Institute of Standards and Technology
NPSH	Net Positive Suction Head
ODP	Ocean Depleting Potential
OMC	Operation and Maintenance Cost
ORC	Organic Rankine Cycle
OTEC	Ocean Thermal Energy Conversion
POE	Polyolester Oil
RT	Refrigeration Tonnes
SMCR	Specified Maximum Continuous Rating
SPECO	Specific Exergy Costing
TEC	Theory of Exergy Cost
TRR	Total Revenue Requirement
UNEP	United Nations Environment Program
USA	United States of America

9.5. List of Symbols

\dot{E}	Rate of exergy flow in a stream
\dot{C}	Cost rate of exergy in a stream
ε	Exergetic Efficiency
$\dot{E}_{F,k}$	Fuel Exergy of k^{th} component
$\dot{E}_{P,k}$	Product exergy of k^{th} component
$\dot{E}_{D,k}$	Exergy destruction in k^{th} component
$\dot{C}_{F,k}$	Cost rate of fuel Exergy of k^{th} component
$\dot{C}_{P,k}$	Cost rate of product exergy of k^{th} component
$\dot{C}_{D,k}$	Cost rate of exergy destruction in k^{th} component
\dot{C}_{W_T}	Cost rate of turbine work output
\dot{C}_{W_P}	Cost rate of pump work
\dot{C}_{W_C}	Cost rate of compressor work
$c_{f,k}$	Average cost per unit of fuel exergy of k^{th} component
$c_{p,k}$	Average cost per unit of product exergy of k^{th} component
\dot{Z}_k^{CI}	Cost rate of capital investment in k^{th} component
\dot{Z}_k^{OM}	Cost rate of operation and maintenance for k^{th} component
\dot{Z}_k	Cost rate of total expenses for a component
r_k	relative cost difference
f_k	exergoeconomic factor
$Y_{D,k}$	Exergy destruction ratio based on total fuel exergy
$Y_{D,k}^*$	Exergy destruction ratio based on total exergy destruction
ρ	Density of fluid
α_v	Volumetric Expansivity
W_T	Turbine work
W_P	Pump work
W_C	Compressor Work

A. Modelling

ORC system with R410A

Input summary

```

Apparatus: NO=1, TYPE=2, APNAME='Reheater', POUT= 1.013, DELP=0,
            TOUT= 80
Apparatus: NO=2, TYPE=3, APNAME='Turbine', TUCODE=0, GDCODE= 1,
            ETHA=0.75
Apparatus: NO=3, TYPE=6, APNAME='Heat Exchgr.', DELP1=0.1, DELP2=0.2
Apparatus: NO=4, TYPE=4, APNAME='Condenser', EQCOD= 1, DELP1=0.2,
            DELT1= 5, DELP2=0.1, DELTH= 5, SATCOD=0
Apparatus: NO=5, TYPE=12, APNAME='Heat Exchgr.', POUT1= 42,
            DELP1=0.1, DELP2=0.2, DELTL= 5
Apparatus: NO=6, TYPE=8, APNAME='Pump', ETHA=0.9
Apparatus: NO=7, TYPE=8, APNAME='Pump', ETHA=0.8
Apparatus: NO=8, TYPE=8, APNAME='Pump', ETHA=0.8
Apparatus: NO=9, TYPE=10, APNAME='Sink/Source', POUT= 1.01325,
            DELP=0, TOUT= 15
Generator: NO=1, IGAPP=2, ETAGEN=0.95

Medium: Pipe No = 6, Type = REFFPROP: 'R410A'
Reference state: Liquid at normal boiling point (1 atm) (default)
Thermodynamic model: CSD equation of state (default)

Medium: Pipe No = 1, Type = 'WATERSTM'
Medium: Pipe No = 10, Type = 'WATERSTM'

Pipe: NO=3, XINL = 0
Pipe: NO=6, XOUTL = 1

Production Func.: Apparatus numbers:2, Power=0.04
Production Func.: Apparatus 5, Power = 0

Environment: Default environment like Baehr, but 15°C
Environment composition:
Specie = AR CO2 H2O N2 O2
Mole % = 0.91 0.03 1.68 76.78 20.6
Environment pressure: 1.01325 bar
Environment temperature: 15 °C
Heating values calculated at 1 atm, 25 °C
    
```

Figure A.1.: Input summary in cycle tempo of ORC with R410A

Cycle Tempo Schematic

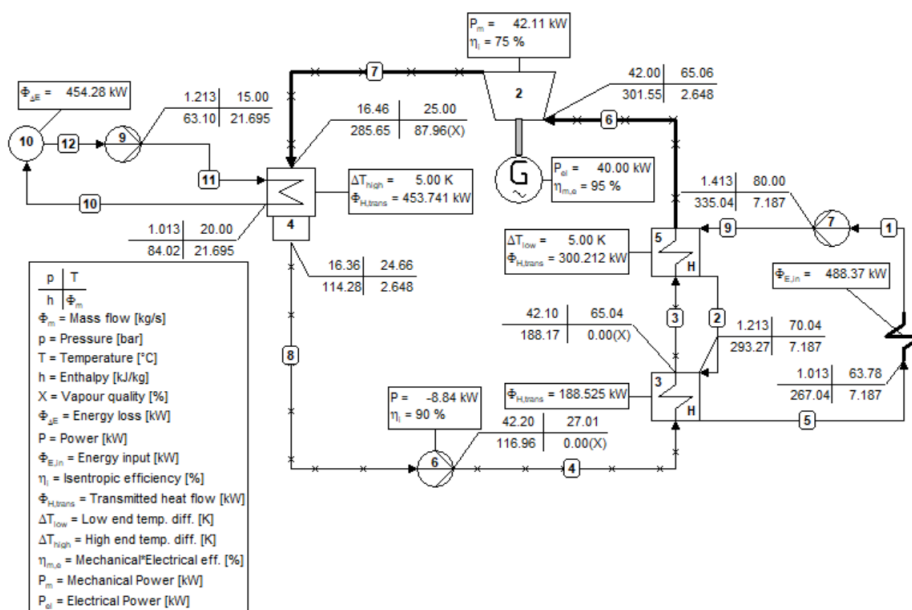


Figure A.2.: Cycle-Tempo schematic of ORC system with R410A

ORC system with internal heat exchanger

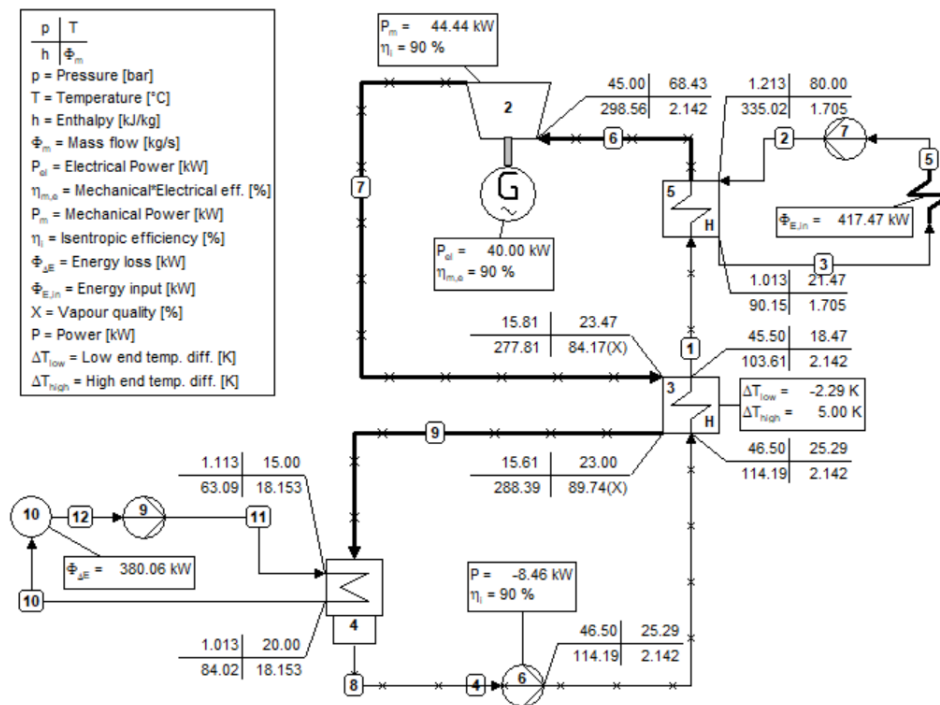


Figure A.3.: Cycle-Tempo schematic of ORC system with Internal heat exchanger

Cogeneration system with R410A

Input summary

```

Apparatus: NO=1, TYPE=8, APNAME='Pump', ETHAI=0.9
Apparatus: NO=2, TYPE=6, APNAME='Heat Exchgr.', DELP1=0.1, DELP2=0.2
Apparatus: NO=3, TYPE=12, APNAME='Heat Exchgr.', POUT1= 42,
DELP1=0.1, DELT1=0, DELP2=0.2, DELTL= 5
Apparatus: NO=4, TYPE=3, APNAME='Turbine', TUCODE=0, GDCODE= 1,
ETHAI=0.75
Apparatus: NO=5, TYPE=4, APNAME='Condenser', EEQCOD= 1, DELP1=0.1,
DELT1= 5, DELP2=0.2, DELTH= 5, SATCOD=0
Apparatus: NO=6, TYPE=10, APNAME='Sink/Source', DELH=0
Apparatus: NO=7, TYPE=12, APNAME='Heat Exchgr.', DELP1=0, DELP2=0,
TOUT2=0
Apparatus: NO=8, TYPE=29, APNAME='Compressor', ETHAI=0.75
Apparatus: NO=9, TYPE=8, APNAME='Pump', ETHAI=0.8
Apparatus: NO=10, TYPE=8, APNAME='Pump', ETHAI=0.8
Apparatus: NO=11, TYPE=9, APNAME='Node', DELP=0
Apparatus: NO=12, TYPE=9, APNAME='Node', DELP=0
Apparatus: NO=13, TYPE=2, APNAME='Reheater', POUT= 1.01325,
DELP=0, TOUT= 80
Apparatus: NO=14, TYPE=10, APNAME='Sink/Source', POUT= 1.01325,
DELP=0, TOUT= 15
Apparatus: NO=15, TYPE=10, APNAME='Sink/Source', POUT= 1.01325,
DELP=0, TOUT= 2
Apparatus: NO=16, TYPE=8, APNAME='Pump', ETHAI=0.8
Apparatus: NO=17, TYPE=10, APNAME='Dummy', DELP=0, TIN=-,
DELH=0, XIN= 1
Generator: NO=1, IGAPP=4, ETAGEN=0.95

Medium: Pipe No = 3, Type = REFPROP: 'R410A'
Reference state : Liquid at normal boiling point (1 atm) (default)
Thermodynamic model : CSD equation of state (default)

Medium: Pipe No = 17, Type = 'GASMX'
Specie = AR CO2 N2 O2
Mole % = 0.93 0.03 78.08 20.96

Medium: Pipe No = 6, Type = 'WATERSTM'
Medium: Pipe No = 9, Type = 'WATERSTM'

Pipe: NO=3, XOUTL= 1
Pipe: NO=15, DELP =0.1
    
```

Figure A.4.: Input summary in cycle tempo of cogeneration system with R410A

Cycle Tempo Schematic

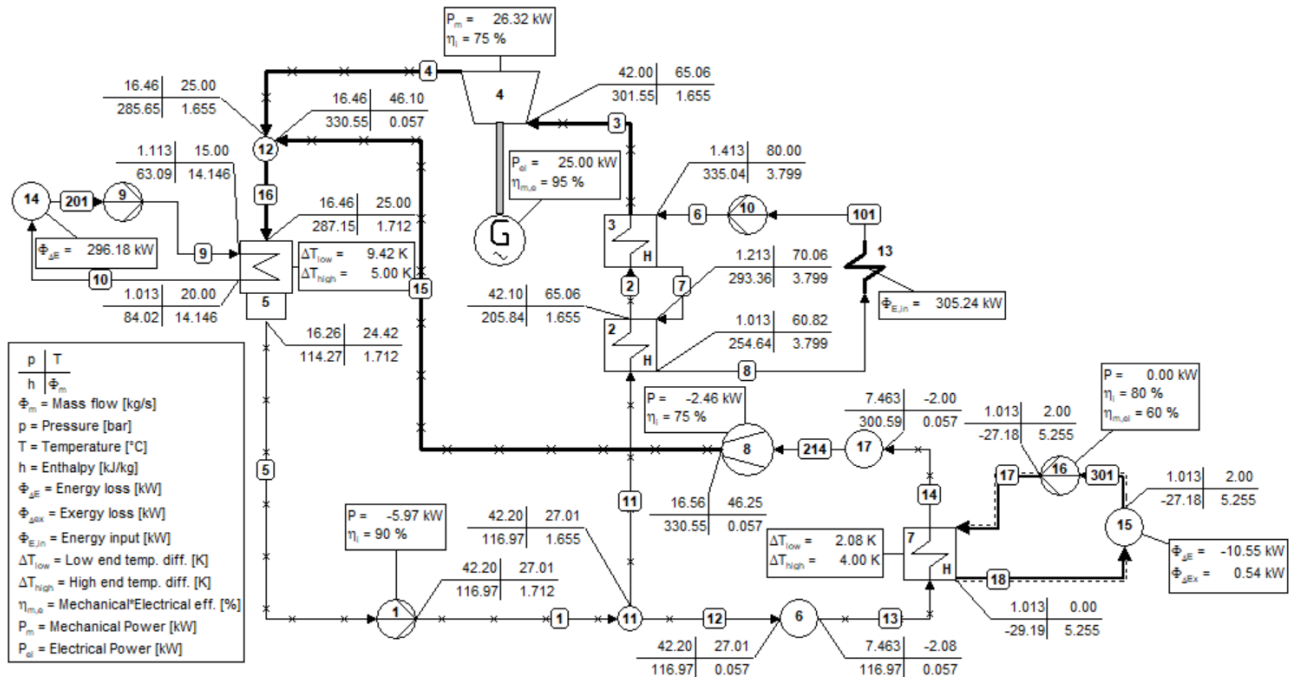


Figure A.5.: Cycle-Tempo schematic of Cogeneration system with R410A

Transcritical CO₂ Power cycle

Input summary

Apparatus: NO=1, TYPE=8, APNAME='Pump', ETHA=0.9
 Apparatus: NO=2, TYPE=6, APNAME='Heat Exchgr.', DELP1=0.5, DELP2=0.5, DELTL= 2
 Apparatus: NO=3, TYPE=12, APNAME='Heat Exchgr.', POUT1= 100, DELP1=0.5, DELP2=0.2, DELTH= 3, DELTH= 3
 Apparatus: NO=4, TYPE=3, APNAME='Turbine', TUCODE=0, GDCODE= 1, ETHA=0.75
 Apparatus: NO=5, TYPE=4, APNAME='Condenser', EEQCOD= 1, DELP1=0.2, DELT1= 5, DELP2=0.5, DELTH= 3, SATCOD=0
 Apparatus: NO=7, TYPE=8, APNAME='Pump', ETHA=0.8
 Apparatus: NO=9, TYPE=8, APNAME='Pump', ETHA=0.8
 Apparatus: NO=301, TYPE=2, APNAME='Reheater', POUT= 1.013, DELP=0, TOUT= 80
 Apparatus: NO=401, TYPE=10, APNAME='Sink/Source', POUT= 1.01325, DELP=0, TOUT= 15
 Generator: NO=1, IGAPP=4, ETAGEN=0.95
 Medium: Pipe No = 3, Library = RefProp, Fluid = CO2.FLD
 Medium: Pipe No = 7, Type = 'WATERSTM'
 Medium: Pipe No = 9, Type = 'WATERSTM'
 Pipe: NO=6, XINL =0
 Production Func.: Apparatus numbers:4, Power=0.04
 Production Func.: Apparatus 3, Power = 0
 Environment: Default environment like Baehr, but 15°C
 Environment composition:
 Specie = AR CO2 H2O N2 O2
 Mole % = 0.91 0.03 1.68 76.78 20.6
 Environment pressure: 1.01325 bar
 Environment temperature: 15 °C
 Heating values calculated at 1 atm, 25 °C

Figure A.6.: Input summary in cycle tempo for transcritical CO₂ power cycle

Cycle Tempo Schematic

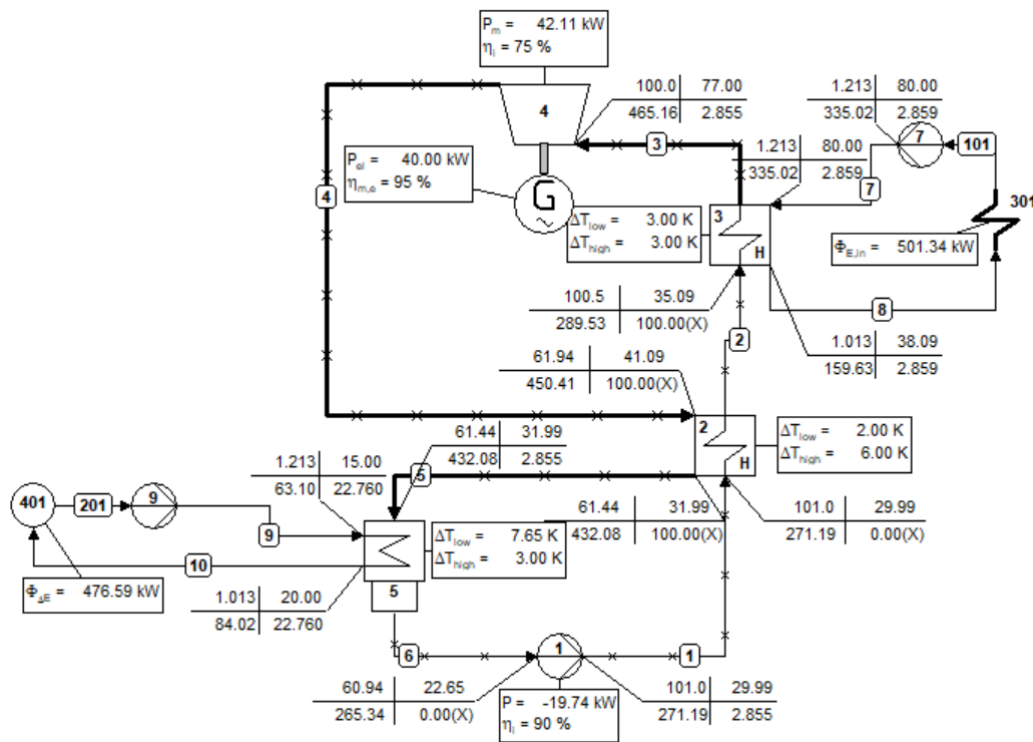


Figure A.7.: Cycle-Tempo schematic of transcritical CO₂ power cycle

Cycle tempo schematic for experimental comparison

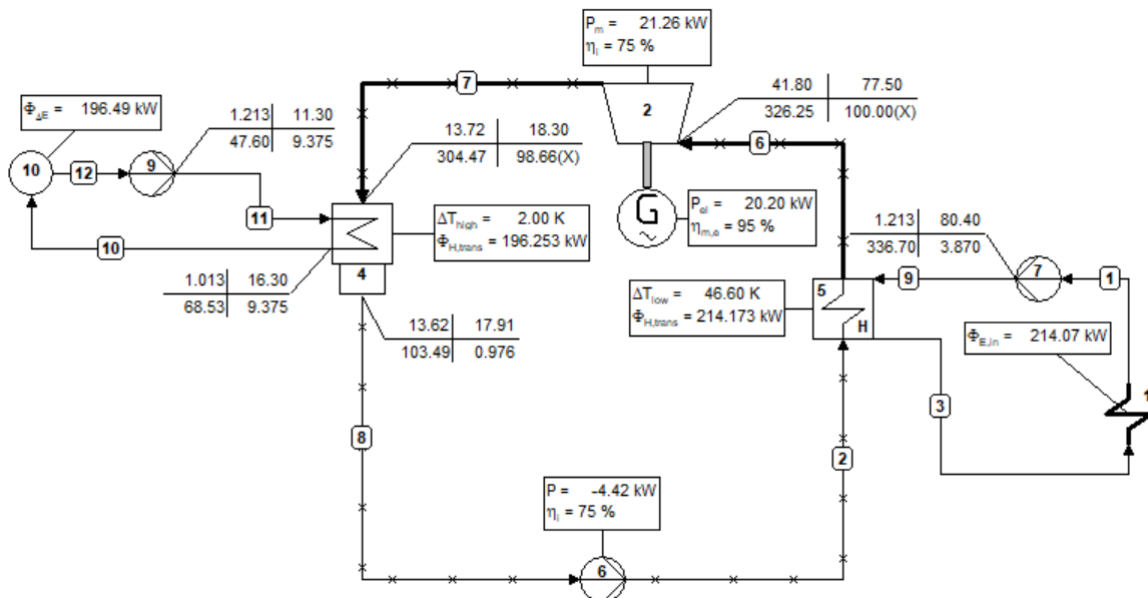


Figure A.8.: Cycle-Tempo schematic of the system simulated to compare with experimental result

B. Economic Analysis

Basic ORC system

Table B.1.: Economic Data for base case of the ORC system given in Section 3.1

Component	Cost (in \$)
Pump	5942.00
Preheater	1676.53
Evaporator	3727.10
Scroll Expander	12000.00
Condenser	6242.23
<i>Other System Equipment</i>	
Generator	3925.00
Motor	2000.00
Oil pump with electric motor	1058.00
Total Purchased equipment cost	36570.87
Sensors, flow meters and VFD drives	4963.00
PLC and Wiring	4025.00
Refrigerant tank and Piping	4864.00
Refrigerant and Oil	2200.00
Miscellaneous, Structure and Assembly	15000.00
Total Investment Cost	67622.87

Table B.2.: Effect of different scenarios on TRR of basic ORC system

Scenario	TCI [\$]	i_r [%]	e [%]	n [yrs]	TRR [\$/yr]
Base case	67622	2.75	1.7	20	7054
1	81147	2.75	1.7	20	8465
2	54098	2.75	1.7	20	5643
3	67622	6.04	1.7	20	8596
4	67622	7.72	3.36	20	10631
5	67622	2.75	2.7	20	7676
6	67622	2.75	3.36	20	8100
7	67622	2.75	1.7	10	11598
8	67622	2.75	1.7	15	8544

Cogeneration system

Table B.3.: Economic data for base case of cogeneration system given in Section 3.1

Component	Cost (in \$)
Pump	2942.00
Preheater	1442.32
Evaporator	2266.09
Scroll Expander	8000.00
Condenser	4524.29
Evaporator Coils and Expansion Valve	3000.00
Compressor	1059.36
<i>Other System Equipment</i>	
Generator	2625.00
Motor	1000.00
Oil pump with electric motor	568.00
Total Purchased Equipment cost	27427.06
Sensors, flow meters and VFD drives	4963.00
PLC and Wiring	4025.00
Refrigerant tank and Piping	3964.00
Refrigerant and Oil	1500.00
Miscellaneous, Structure and Assembly	8000.00
Total Investment Cost	49879.06

Table B.4.: Effect of different scenarios on TRR of cogeneration system

Scenario	TCI [\$]	i_r [%]	e [%]	n [yrs]	TRR [\$/yr]
Base case	49879	2.75	1.7	20	5203
1	59854	2.75	1.7	20	6244
2	39903	2.75	1.7	20	4162
3	49879	6.04	1.7	20	5532
4	49879	7.72	3.36	20	4889
5	49879	2.75	2.7	20	5662
6	49879	2.75	3.36	20	4762
7	49879	2.75	1.7	10	8555
8	49879	2.75	1.7	15	6302

C. Exergoeconomic Analysis

Basic ORC system

$$Eq1 : \dot{C}_1 = \dot{C}_{WP} + \dot{C}_5 + 0.1433$$

$$Eq2 : \dot{C}_2 = \dot{C}_1 + 0.0404$$

$$Eq3 : \dot{C}_3 = \dot{C}_2 + 0.0899$$

$$Eq4 : \dot{C}_{WT} = \dot{C}_3 - \dot{C}_4 + 0.2893$$

$$Eq5 : \dot{C}_{WP} = 0.2099 * \dot{C}_{WT}$$

$$Eq6 : \dot{C}_3 = 1.2497 * \dot{C}_4$$

$$Eq7 : \dot{C}_4 = 1.0837 * \dot{C}_5$$

Solving the above cost balance equations in Maple gives the cost rates of exergy streams in the system which is tabulated and given in Table C.1 below:

Table C.1.: Cost rates for all stream in the basic ORC system

Stream	C [\$/h]	c [\$/kWh]	E [kW]
1	1.39	0.0066	211.98
2	1.43	0.0061	233.08
3	1.52	0.0055	278.35
4	1.22	0.0055	222.74
5	1.12	0.0055	205.54
6	0	0.0000	192.39
7	0	0.0000	140.53
8	0	0.0000	111.63
9	0	0.0000	0.43
10	0.00	0.0000	3.90
CWp	0.12	0.0141	8.84
CWt	0.59	0.0141	42.11

Cogeneration System

The cost balance equations for the cogeneration system are given below.

$$Eq1 : \dot{C}_1 = \dot{C}_{WP} + \dot{C}_5 + 0.0698$$

$$Eq2 : \dot{C}_2 = \dot{C}_{11} + 0.0342$$

$$Eq3 : \dot{C}_3 = \dot{C}_2 + 0.0537$$

$$Eq4 : \dot{C}_{W_T} = \dot{C}_3 - \dot{C}_4 + 0.1897$$

$$Eq5 : \dot{C}_{18} = \dot{C}_{12} - \dot{C}_{14} + 0.0711$$

$$Eq6 : \dot{C}_{15} = \dot{C}_{W_C} + \dot{C}_{14} + 0.0251$$

$$Eq7 : \dot{C}_{W_P} = 0.226824 * \dot{C}_{W_T}$$

$$Eq8 : \dot{C}_{W_C} = 0.093465 * \dot{C}_{W_T}$$

$$Eq9 : \dot{C}_3 = 1.249713 * \dot{C}_4$$

$$Eq10 : \dot{C}_{16} = 0.037472 * \dot{C}_5$$

$$Eq11 : \dot{C}_{16} = \dot{C}_{15} + \dot{C}_4$$

$$Eq12 : \dot{C}_1 = \dot{C}_{11} + \dot{C}_{12}$$

$$Eq13 : \dot{C}_1 = 1.034722 * \dot{C}_{11}$$

$$Eq14 : \dot{C}_{12} = 1.260274 * \dot{C}_{14}$$

Solving the above equations in Maple gives the solution for each unknown i.e the cost rate of each exergy stream which is given in Table C.2.

Table C.2.: Cost rates for all streams in the cogeneration system

Stream	C [\$/h]	c [\$/kWh]	E[kW]
1	1.10	0.008	137.08
2	1.10	0.007	150.08
3	1.15	0.007	173.96
4	0.92	0.007	139.20
5	0.94	0.007	132.90
6	0	0.000	101.69
7	0	0.000	74.33
8	0	0.000	52.36
9	0	0.000	0.14
10	0	0.000	2.54
11	1.07	0.008	132.48
12	0.04	0.008	4.60
13	NA	NA	4.25
14	0.03	0.008	3.65
15	0.09	0.019	4.98
16	1.02	0.007	144.13
17	0.00	0.000	8.96
18	0.08	0.008	9.50
W _p	0.10	0.016	5.97
W _t	0.42	0.016	26.32
W _c	0.04	0.016	2.46

D. Exergoeconomic Optimization

Parametric study of decision variables

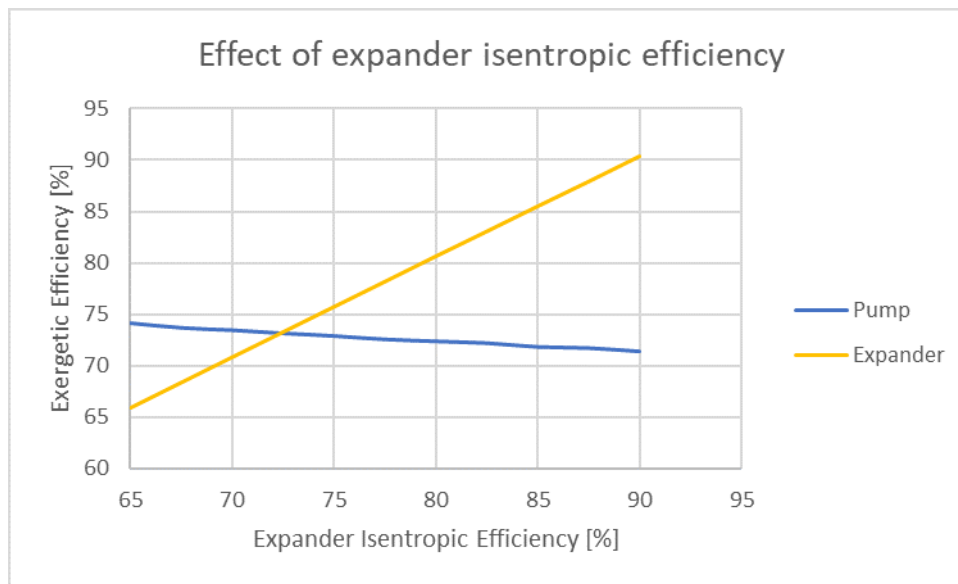


Figure D.1.: Effect of scroll isentropic efficiency

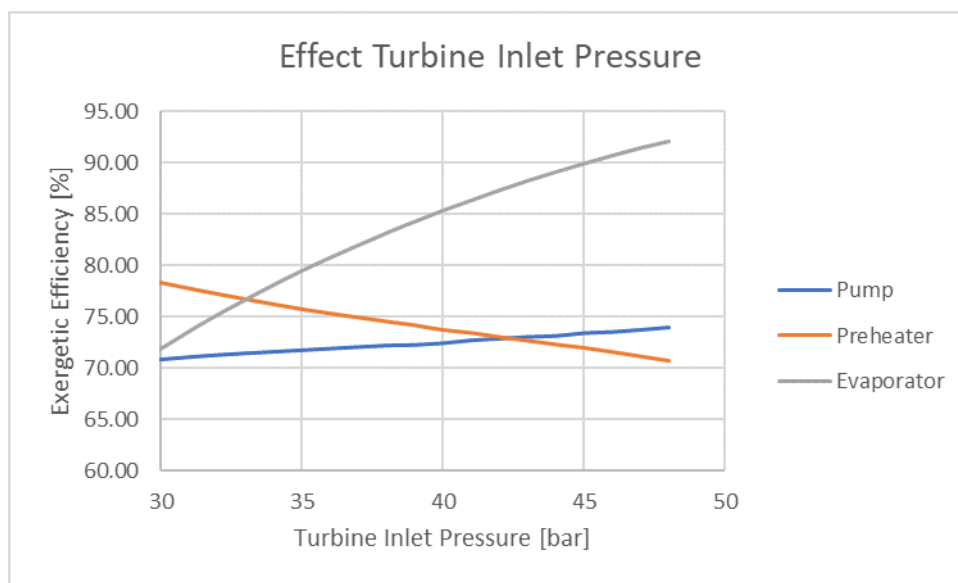


Figure D.2.: Effect of expander inlet pressure

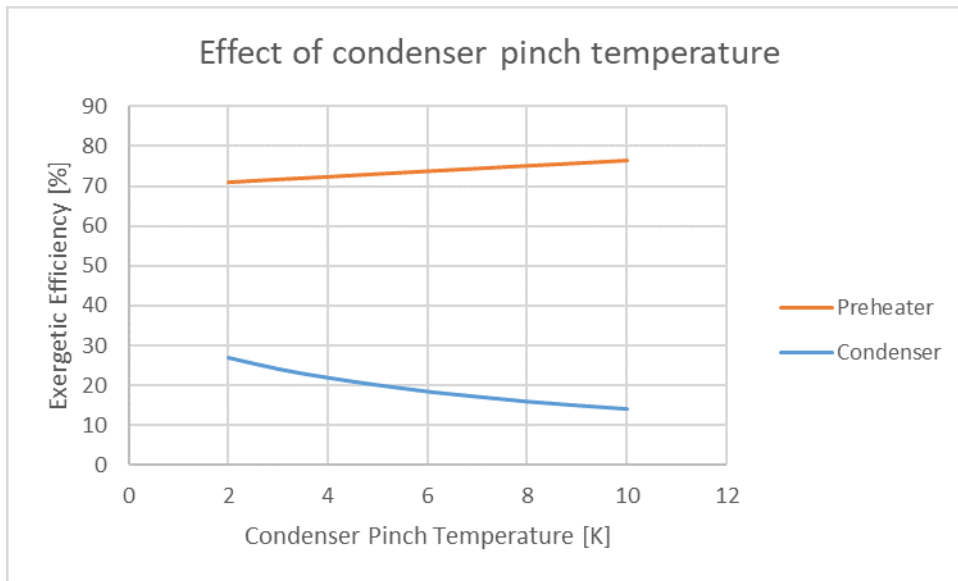


Figure D.3.: Effect of condenser pinch temperature

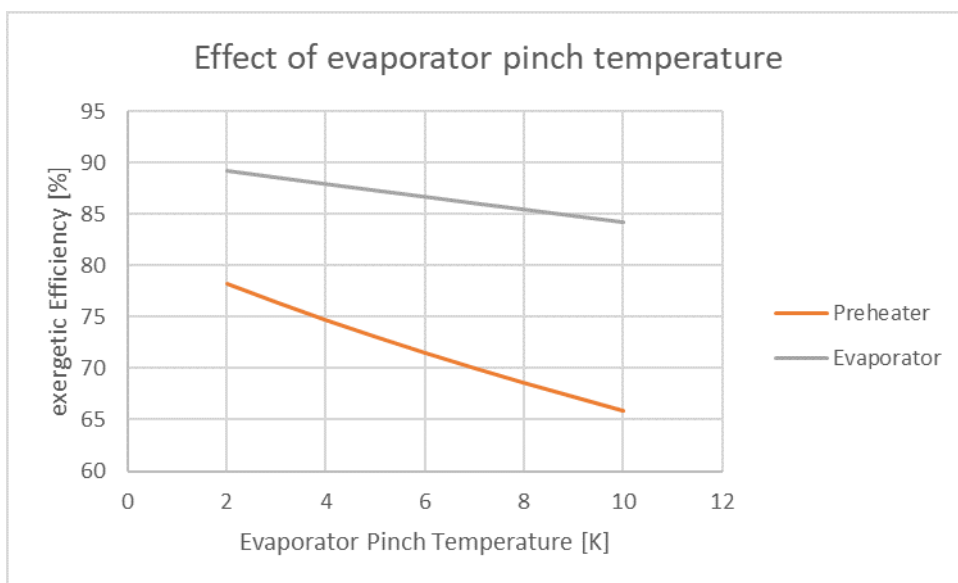


Figure D.4.: Effect of evaporator pinch temperature

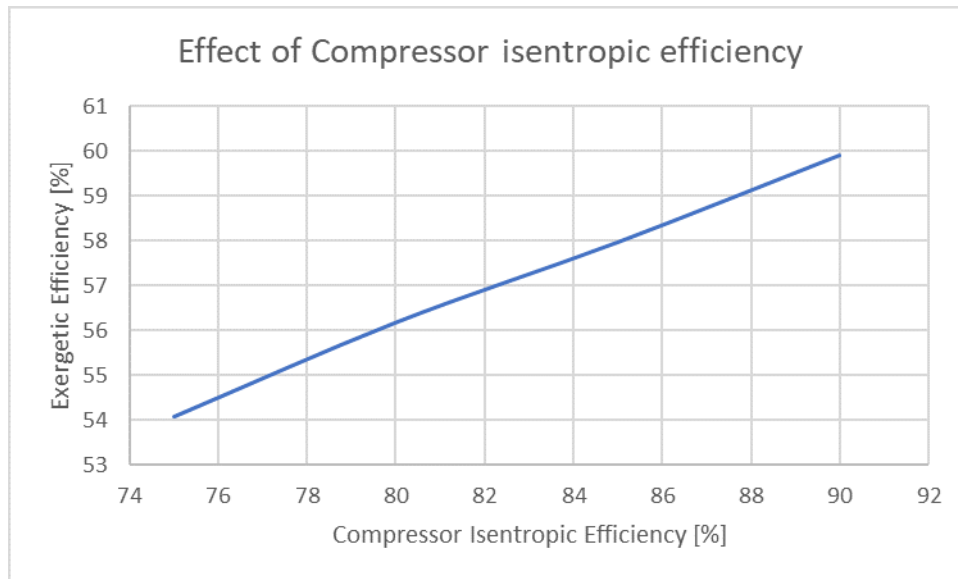


Figure D.5.: Effect of compressor isentropic efficiency

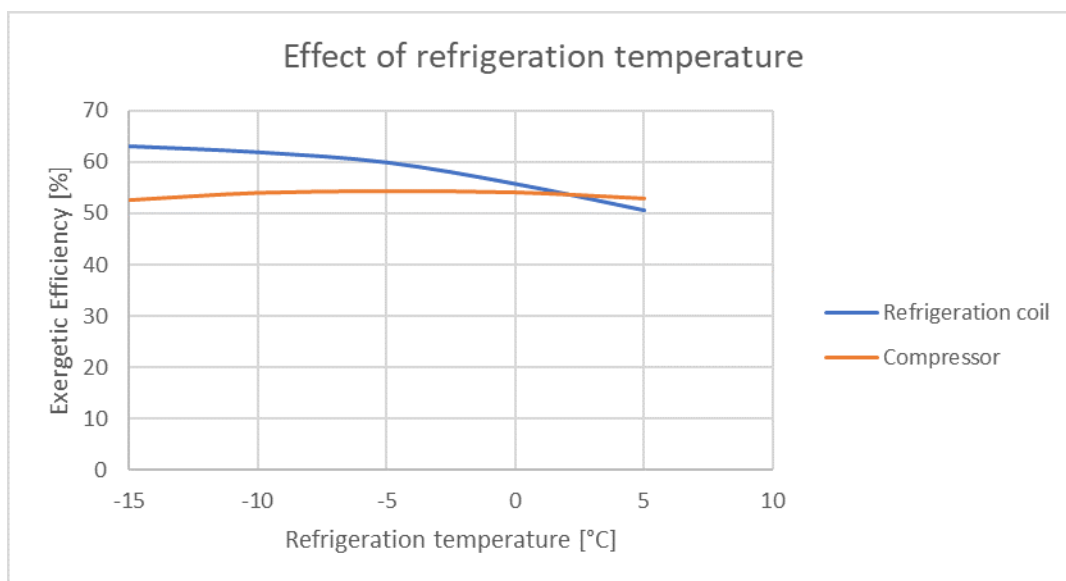


Figure D.6.: Effect of refrigeration temperature

Basic ORC System

Iteration 1

Table D.1.: First Iteration

Component	$c_{\{f\}}$ [\$/kWh]	$c_{\{p\}}$ [\$/kWh]	$C_{\{D\}}$ [\$/hr]	$Z_{\{k\}}$ [\$/hr]	$Z_{\{k\}} + C_{\{D\}}$ [\$/hr]	$r_{\{k\}}$	$f_{\{k\}}$
Pump C1	0.014	0.041	0.101	0.147	0.248	1.953	0.593
Preheater C2	0.000	0.002	0.015	0.035	0.050	0.423	0.703
Evaporator C3	0.000	0.002	0.011	0.082	0.093	0.129	0.886
Expander C4	0.006	0.014	0.140	0.298	0.438	1.509	0.680
Condenser C5	0.006	0.000	0.084	0.118	0.202	0.000	0.583

Iteration 2

Table D.2.: Second Iteration

Component	$c_{\{f\}}$ [\$/kWh]	$c_{\{p\}}$ [\$/kWh]	$C_{\{D\}}$ [\$/hr]	$Z_{\{k\}}$ [\$/hr]	$Z_{\{k\}} + C_{\{D\}}$ [\$/hr]	$r_{\{k\}}$	$f_{\{k\}}$
Pump C1	0.014	0.040	0.100	0.150	0.250	1.928	0.598
Preheater C2	0.000	0.001	0.014	0.036	0.050	0.405	0.711
Evaporator C3	0.000	0.002	0.010	0.086	0.095	0.113	0.899
Expander C4	0.006	0.014	0.097	0.302	0.399	1.426	0.757
Condenser C5	0.006	0.000	0.103	0.092	0.195	0.000	0.472

Iteration 3

Table D.3.: Third Iteration

Component	$c_{\{f\}}$ [\$/kWh]	$c_{\{p\}}$ [\$/kWh]	$C_{\{D\}}$ [\$/hr]	$Z_{\{k\}}$ [\$/hr]	$Z_{\{k\}} + C_{\{D\}}$ [\$/hr]	$r_{\{k\}}$	$f_{\{k\}}$
Pump C1	0.014	0.042	0.101	0.150	0.251	2.058	0.598
Preheater C2	0.000	0.002	0.014	0.034	0.048	0.405	0.712
Evaporator C3	0.000	0.002	0.009	0.082	0.092	0.113	0.899
Expander C4	0.006	0.014	0.060	0.304	0.364	1.335	0.834
Condenser C5	0.006	0.000	0.100	0.088	0.188	0.000	0.470

Iteration 4

Table D.4.: Fourth Iteration

Component	$c_{\{f\}}$ [\$/kWh]	$c_{\{p\}}$ [\$/kWh]	$C_{\{D\}}$ [\$/hr]	$Z_{\{k\}}$ [\$/hr]	$Z_{\{k\}} + C_{\{D\}}$ [\$/hr]	$r_{\{k\}}$	$f_{\{k\}}$
Pump C1	0.014	0.044	0.100	0.149	0.249	2.221	0.599
Preheater C2	0.000	0.002	0.014	0.033	0.046	0.423	0.703
Evaporator C3	0.000	0.002	0.010	0.076	0.086	0.129	0.886
Expander C4	0.006	0.014	0.061	0.301	0.362	1.318	0.832
Condenser C5	0.006	0.000	0.078	0.108	0.186	0.000	0.579

Cogeneration system

Iteration 1

Table D.5.: First Iteration

Component	$c_{\{f\}}$ [\$/kWh]	$c_{\{p\}}$ [\$/kWh]	$C_{\{D\}}$ [\$/hr]	$Z_{\{k\}}$ [\$/hr]	$Z_{\{k\}} + C_{\{D\}}$ [\$/hr]	$r_{\{k\}}$	$f_{\{k\}}$
Pump C1	0.016	0.039	0.071	0.072	0.143	1.479	0.502
Preheater C2	0.000	0.002	0.009	0.028	0.037	0.341	0.746
Evaporator C3	0.000	0.002	0.006	0.050	0.057	0.129	0.885
Expander C4	0.007	0.016	0.098	0.195	0.293	1.349	0.665
Condenser C5	0.007	0.000	0.070	0.084	0.154	0.000	0.547
Evaporator C7	0.008	0.153	0.072	0.073	0.145	17.826	0.504
Compressor C8	0.016	0.045	0.047	0.026	0.073	1.872	0.353

Iteration 2

Table D.6.: Second Iteration

Component	$c_{\{f\}}$ [\$/kWh]	$c_{\{p\}}$ [\$/kWh]	$C_{\{D\}}$ [\$/hr]	$Z_{\{k\}}$ [\$/hr]	$Z_{\{k\}} + C_{\{D\}}$ [\$/hr]	$r_{\{k\}}$	$f_{\{k\}}$
Pump C1	0.015	0.040	0.070	0.072	0.142	1.584	0.509
Preheater C2	0.000	0.002	0.009	0.027	0.036	0.340	0.746
Evaporator C3	0.000	0.002	0.006	0.048	0.054	0.129	0.886
Expander C4	0.007	0.015	0.068	0.197	0.265	1.263	0.742
Condenser C5	0.007	0.000	0.066	0.080	0.146	0.000	0.548
Evaporator C7	0.008	0.131	0.058	0.070	0.128	14.733	0.548
Compressor C8	0.015	0.044	0.043	0.026	0.069	1.875	0.379

Iteration 3

Table D.7.: Third Iteration

Component	$c_{-}\{f\}$ [\$/kWh]	$c_{-}\{p\}$ [\$/kWh]	$C_{-}\{D\}$ [\$/hr]	$Z_{-}\{k\}$ [\$/hr]	$Z_{-}\{k\} + C_{-}\{D\}$ [\$/hr]	$r_{-}\{k\}$	$f_{-}\{k\}$
Pump C1	0.015	0.041	0.069	0.073	0.142	1.696	0.514
Preheater C2	0.000	0.002	0.009	0.026	0.034	0.340	0.747
Evaporator C3	0.000	0.002	0.006	0.046	0.053	0.129	0.885
Expander C4	0.007	0.015	0.043	0.198	0.241	1.187	0.823
Condenser C5	0.007	0.000	0.063	0.077	0.140	0.000	0.549
Evaporator C7	0.009	0.123	0.050	0.067	0.118	13.396	0.572
Compressor C8	0.015	0.045	0.039	0.026	0.065	1.937	0.403

Iteration 4

Table D.8.: Fourth Iteration

Component	$c_{-}\{f\}$ [\$/kWh]	$c_{-}\{p\}$ [\$/kWh]	$C_{-}\{D\}$ [\$/hr]	$Z_{-}\{k\}$ [\$/hr]	$Z_{-}\{k\} + C_{-}\{D\}$ [\$/hr]	$r_{-}\{k\}$	$f_{-}\{k\}$
Pump C1	0.015	0.041	0.069	0.073	0.142	1.706	0.515
Preheater C2	0.000	0.002	0.009	0.026	0.035	0.340	0.746
Evaporator C3	0.000	0.002	0.006	0.047	0.053	0.129	0.886
Expander C4	0.007	0.015	0.043	0.199	0.241	1.192	0.824
Condenser C5	0.007	0.000	0.062	0.076	0.139	0.000	0.551
Evaporator C7	0.008	0.121	0.046	0.065	0.111	13.282	0.583
Compressor C8	0.015	0.047	0.040	0.026	0.067	2.085	0.394

E. Experimental Results

Matlab Code for Isentropic efficiency

```
%turbine isentropic efficiency calculation
clc
clear all

P_1 = xlsread('data.xlsx','N4:N23');
P_2 = xlsread('data.xlsx','O4:O23');
T_1 = xlsread('data.xlsx','L4:L23');
T_2 = xlsread('data.xlsx','M4:M23');
power = xlsread('data.xlsx','H4:H23');

for i = 1:1:20
P_1(i) = P_1(i)*100;
P_2(i) = P_2(i)*100;

H_1(i) = refpropm('H','T',T_1(i),'P',P_1(i),'R410A.mix');
S_1(i) = refpropm('S','T',T_1(i),'P',P_1(i),'R410A.mix');

H_2(i) = refpropm('H','T',T_2(i),'P',P_2(i),'R410A.mix');
H_2s(i) = refpropm('H','P',P_2(i),'S',S_1(i),'R410A.mix');

eff_isen(i) = ((H_2(i) - H_1(i))/(H_2s(i) - H_1(i)))*100;

end

display(eff_isen);
plot(power,eff_isen);
```